National Library of Canada
Bibliothèque nationale du Canada

Canadian Theses Service
Service des thèses canadiennes

Ottawa, Canada
K1A 0N4

NOTICE

The quality of this microform is heavily dependent upon the quality of the original thesis submitted for microfilming. Every effort has been made to ensure the highest quality of reproduction possible.

If pages are missing, contact the university which granted the degree.

Some pages may have indistinct print especially if the original pages were typed with a poor typewriter ribbon or if the university sent us an inferior photocopy.

Previously copyrighted materials (journal articles, published tests, etc.) are not filmed.

Reproduction in full or in part of this microform is governed by the Canadian Copyright Act, R.S.C. 1970, c. C-30.

AVIS

La qualité de cette microforme dépend grandement de la qualité de la thèse soumise au microfilmage. Nous avons tout fait pour assurer une qualité supérieure de reproduction.

S'il manque des pages, veuillez communiquer avec l'université qui a conféré le grade.

La qualité d'impression de certaines pages peut laisser à désirer, surtout si les pages originales ont été dactylographiées à l'aide d'un ruban usé ou si l'université nous a fait parvenir une photocopie de qualité inférieure.

Les documents qui font déjà l'objet d'un droit d'auteur (articles de revue, tests publiés, etc.) ne sont pas microfilmés.

La reproduction, même partielle, de cette microforme est soumise à la Loi canadienne sur le droit d'auteur, SRC 1970, c. C-30.

NL-339 (r. 88/04)

Canadä

THE UNIVERSITY OF ALBERTA

AN X-RAY DIFFRACTION STUDY OF SINTERING AND REDISPERSION OF $Pt/\gamma-Al_2O_3$ CATALYSTS

by

Ipin Guo

©

A THESIS

SUBMITTED TO THE FACULTY OF GRADUATE STUDIES AND RESEARCH
IN PARTIAL FULFILMENT OF THE REQUIREMENTS FOR THE DEGREE
OF MASTER OF SCIENCE

DEPARTMENT OF CHEMICAL ENGINEERING

EDMONTON, ALBERTA
FALL 1987

Permission has been granted to the National Library of Canada to microfilm this thesis and to lend or sell copies of the film.

The author (copyright owner) has reserved other publication rights, and neither the thesis nor extensive extracts from it may be printed or otherwise reproduced without his/her written permission.

L'autorisation a été accordée à la Bibliothèque nationale du Canada de microfilmer cette thèse et de prêter ou de vendre des exemplaires du film.

L'auteur (titulaire du droit d'auteur) se réserve les autres droits de publication; ni la thèse ni de longs extraits de celle-ci ne doivent être imprimés ou autrement reproduits sans son autorisation écrite.

ISBN 0-315-40918-5

THE UNIVERSITY OF ALBERTA

RELEASE FORM

NAME OF AUTHOR Ipin Guo

TITLE OF THESIS AN X-RAY DIFFRACTION STUDY OF SINTERING AND REDISPERSION OF $Pt/\gamma-Al_2O_3$ CATALYSTS

DEGREE FOR WHICH THESIS WAS PRESENTED MASTER OF SCIENCE

YEAR THIS DEGREE GRANTED FALL 1987

Permission is hereby granted to THE UNIVERSITY OF ALBERTA LIBRARY to reproduce single copies of this thesis and to lend or sell such copies for private, scholarly or scientific research purposes only.

The author reserves other publication rights, and neither the thesis nor extensive extracts from it may be printed or otherwise reproduced without the author's written permission.

(SIGNED) Ipin Guo

PERMANENT ADDRESS:

13908-110 Avenue
Edmonton, Alberta
T5M 2M5

DATED August 23 1987

THE UNIVERSITY OF ALBERTA

FACULTY OF GRADUATE STUDIES AND RESEARCH

The undersigned certify that they have read, and recommend to the Faculty of Graduate Studies and Research, for acceptance, a thesis entitled AN X-RAY DIFFRACTION STUDY OF SINTERING AND REDISPERSION OF Pt/γ-Al_2O_3 CATALYSTS submitted by Ipin Guo in partial fulfilment of the requirements for the degree of MASTER OF SCIENCE.

Sieghard Wanke
Supervisor

Reg Eadie

K T Chuang

Date August 21, 1987

ABSTRACT

The sintering and redispersion of Pt/γ-Al_2O_3 catalysts were studied by wide angle x-ray diffraction (XRD). The objectives of the study were to investigate the suitability of XRD for determining Pt crystallite sizes and size distributions, and to use the size information to elucidate the processes occurring during sintering and redispersion. Catalysts, containing 1 and 5 wt% Pt, were examined by XRD after treatment at 450 to 800°C in gas mixtures containing H_2, O_2, N_2, H_2O, He, HCl, CCl_4, C_2HCl_3 and Cl_2. Fourier analysis was used to determine Pt crystallite size distributions. Pt dispersions from XRD and H_2 adsorption were in good agreement; hence, XRD is a reliable method for characterization of supported Pt catalysts.

Significant changes in Pt crystallite sizes occurred during the various treatments. Treatment in O_2 at $\leq$700°C caused simultaneous sintering and redispersion which resulted in bimodal size distributions. Treatment in O_2 at 800°C caused severe sintering yielding average Pt crystallite sizes >10 nm. Treatment in He at 800°C also resulted in Pt sintering, but the average Pt crystallite sizes were <10 nm. Sintered Pt catalysts could be redispersed by treatment in Cl-containing atmospheres at $\leq$550°C. Cl_2, in N_2 or N_2-O_2, was more effective for regenerating sintered catalysts than gases containing HCl, C_2HCl_3 or CCl_4. The results agree with an atomic migration mechanism for sintering and redispersion.

ACKNOWLEDGMENTS

The author wishes to express his sincere thanks to Dr. S.E. Wanke for his supervision and direction of the research.

Ms. T.-T. Yu also deserves thanks, for she prepared the catalysts studied in this work and did most of the x-ray diffraction and chemisorption measurements. The author is indebted to Mr. W.C.S. Pick for developing the initial version of the computer software used for the analysis of XRD data. The author also wishes to express his gratitude to the staff of the DACS Centre for their help in the operation of the HP computer system.

Table of Contents

Chapter Page

1. INTRODUCTION 1

2. LITERATURE REVIEW 3

2.1 The Purpose of Sintering Studies 3

2.2 Sintering and Redispersion Studies 4

2.3 Characterization Methods for Sintering Studies 5

2.3.1 Chemisorption 5

2.3.2 Transmission Electron Microscopy 7

2.3.3 X-ray Diffraction 9

2.4 Other Catalysts Characterization Methods 12

3. X-RAY DIFFRACTION FOR CATALYST CHARACTERIZATION 13

3.1 Introduction to X-ray Diffraction 13

3.2 Instrumental Broadening 14

3.3 Line Broadening due to Crystal Imperfections 15

3.4 Line Broadening due to Crystallite Size 16

3.5 Estimation of β from Measured Line Breadths 18

3.6 Fourier Analysis of Line Profiles 20

4. EXPERIMENTAL METHODS AND RESULTS 22

4.1 Catalyst Preparation 22

4.2 Catalyst Treatment and Hydrogen Adsorption 24

4.3 X-ray Diffraction Measurements 29

4.3.1 x-ray equipment 29

4.3.2 XRD patterns for catalysts 30

4.3.3 XRD patterns for supports 37

4.3.4 XRD pattern for a standard sample 38

5. ANALYSIS OF XRD PATTERNS 42

5.1 Subtraction of the Support Pattern 42

5.2 Smoothing of XRD Line Profile 47
5.3 Correction for Instrumental Effects 56
5.4 Testing of Programs 61
5.5 Test for Strain Broadening 65
6. RESULTS AND DISCUSSION 70
6.1 Introduction 70
6.2 Average Pt Crystallite Sizes 70
6.3 Comparison of XRD and Chemisorption Results 76
6.4 Pt Crystallite Size Distributions 83
6.5 Processes Occurring during Sintering and Redispersion 93
6.5.1 Treatments in Oxygen 94
6.5.2 Treatment in Chlorine-Containing Atmospheres 96
6.5.3 Treatment in Helium 97
6.5.4 Processes Occurring during the Reduction Step 97
6.5.5 Summary of Sintering and Redispersion Processes 98
7. CONCLUSIONS AND RECOMMENDATIONS 100
8. REFERENCES 102
9. Appendix A. Programs and Documentation 106
10. Appendix B. Tabulation of Results 157

List of Tables

Table Page

4.1 Description of $Pt/\gamma-Al_2O_3$ catalysts and $\gamma-Al_2O_3$ supports 23

4.2 Treatment conditions and hydrogen adsorption uptakes for Catalyst GC1 [1.05% $Pt/\gamma-Al_2O_3$ (Alon)] 25

4.3 Treatment conditions and hydrogen adsorption uptakes for Catalysts GC2 [1.12% $Pt/\gamma-Al_2O_3$ (Kaiser KA-201)] 26

4.4 Treatment conditions and hydrogen adsorption uptakes for Catalyst GC3 [5.06% $Pt/\gamma-Al_2O_3$ (from Versal 850)] 27

4.5 Treatment conditions and hydrogen adsorption uptakes for Catalyst GC4 [5.06% $Pt/\gamma-Al_2O_3$ (from Versal 850)] 28

4.6 Treatment conditions for supports 38

5.1 Location of Pt and $\gamma-Al_2O_3$ diffraction lines 47

5.2 Comparison of input and calculated <D> values 63

6.1 Average crystallite sizes for Catalyst GC1 (1.05 wt% $Pt/\gamma-Al_2O_3$) 71

6.2 Average crystallite sizes for Catalyst GC2 (1.12 wt% $Pt/\gamma-Al_2O_3$) 72

6.3 Average crystallite sizes for Catalyst GC3 (5.06 wt% $Pt/\gamma-Al_2O_3$) 73

6.4 Average crystallite sizes for Catalyst GC4 (5.06 wt% $Pt/\gamma-Al_2O_3$) 73

6.5 Comparison of hydrogen chemisorption and XRD results for catalyst GC1 78

6.6 Comparison of hydrogen chemisorption and XRD results for catalyst GC2 79

6.7 Comparison of hydrogen chemisorption and XRD results for catalyst GC3 80

6.8 Comparison of hydrogen chemisorption and XRD results for catalyst GC4 80

List of Figures

Figure Page

4.1 Raw XRD Patterns for Catalyst GC1 31

4.2 Raw XRD Patterns for Catalyst GC2 32

4.3 Raw XRD Patterns for Catalyst GC2 (continued) 33

4.4 Raw XRD Patterns for Catalyst GC3 34

4.5 Raw XRD Patterns for Catalyst GC3 (continued) 35

4.6 Raw XRD Patterns for Catalyst GC4 36

4.7 Raw XRD Patterns for Supports 39

4.8 XRD Pattern for Standard Sample 41

5.1 Illustration of Support Subtraction for 1% Pt/γ-Al_2O_3 Catalysts 46

5.2 Subtracted XRD Patterns for Catalyst GC1 48

5.3 Subtracted XRD Patterns for Catalyst GC2 49

5.4 Subtracted XRD Patterns for Catalyst GC2 50

5.5 Subtracted XRD Patterns for Catalyst GC3 51

5.6 Subtracted XRD Patterns for Catalyst GC3 52

5.7 Subtracted XRD Patterns for Catalyst GC4 53

5.8 Typical Line Profiles for the Smoothing Function F_v 55

5.9 Illustration of Fitting Pt 111 Lines by the F_v Function 57

5.10 Results of Fourier Transform Analysis (F.T.A.) for Generated Pure Diffraction Profiles 64

5.11 Results of Fourier Transform Analysis (F.T.A.) for Generated Profiles with Different Values of V_i 66

5.12 Strain Analysis of 1% Pt Catalyst 68

5.13 Strain Analysis of 5% Pt Catalyst 69

Figure Page

6.1 Crystallite Size Distribution for Catalyst GC1 84

6.2 Crystallite Size Distribution for Catalyst GC2 87

6.3 Crystallite Size Distribution for Catalyst GC3 90

6.4 Crystallite Size Distribution for Catalyst GC4 92

NOMENCLATURE

The symbols used in this thesis are defined below. The number of the equation in which the symbol is first used is given in parenthesis; the units for each symbol is given in square brackets, and dimensionless expressions are indicated by [-].

Latin Symbols

a = dummy variable of integration (Eq. 3.11) [-]

A_i = area under Pt 111 line for Catalyst i (Eq. 6.1) [(c/s)·(°2θ)]

A_{MAX} = maximum area under Pt 111 line for Catalyst i (Eq. 6.1) [(c/s)·(°2θ)]

b = broadening due to instrumental effects (Eq. 3.4) [radians of 2θ]

B = measured breadth of X-ray profile (Eq. 3.4) [radians of 2θ]

B_i = parameters in fitting function (Eq. 5.4 & 5.5) [-]

B_{st} = broadening due to strain in crystallites (Eq. 3.4) [radians of 2θ]

C_a = constant (Eq. 5.10) [nm]

C_v = constant (Eq. 5.15) [nm]

d = distance between crystal planes (Eq. 3.1) [nm]

D_i = size of particle i (Eq. 2.1) [nm]

D_n = number average diameter (Eq. 2.1) [nm]

D_s = surface average diameter (Eq. 2.2) [nm]

D_v = volume average diameter (Eq. 2.3) [nm]

$\langle D \rangle$ = average crystallite size (Eq. 3.2) [nm]

$\langle D_a \rangle$ = area average crystallite size (Eq. 5.13) [nm]

$\langle D_v \rangle$ = volume average crystallite size (Eq. 5.17) [nm]

F_1 = Cauchy fitting function (Eq. 5.4) [c/s]

F_2 = Gaussian fitting function (Eq. 5.5) [c/s]

F_v = modified Voigt fitting function (Eq. 5.3) [c/s]

$f(s)$ = pure XRD line profile (Eq. 3.11) [c/s]

$F(j)$ = Fourier transform of f(s) (Eq. 3.13a) [c/s]

$g(s)$ = instrumental XRD line profile (Eq. 3.11) [c/s]

$G(j)$ = Fourier transform of g(s) (Eq. 3-13a) [c/s]

$h(s)$ = observed XRD line profile (Eq. 3.11) [c/s]

$H(j)$ = Fourier transform of h(s) (Eq. 3.13a) [c/s]

I = intensity of diffracted X-rays (Eq. 5.1) [c/s]

j = Fourier number (Eq. 3.11a) [-]

K = constant in Scherrer equation (Eq. 3.2) [-]

M = number of discrete sizes in distribution (Eq. 5.18) [-]

n = order of reflection (Eq. 3.1) [-]

n_i = number of particles with size D_i (Eq. 2.1) [-]

$P_a(D)$ = area weighted length distribution function (Eq. 5.10) [nm^{-1}]

$P_v(D)$ = volume weighted length distribution function (Eq. 5.15) [nm^{-1}]

s = dimensionless Bragg distance (Eq. 3.12) [-]

S = Pt surface area (Eq. 2.4) [m^2/g of catatalyst]

V_i = volume fraction of crystallites having size D_i (Eq. 5.18) [-]

X = fraction Pt detected by XRD (Eq. 6.1) [-]

y = mass fraction Pt in catalysts (Eq. 2.4) [-]

Greek Symbols

β = line breadth due to size broadening (Eq. 3.2) [radians]

β_i = integral line width (Eq. 3.3) [radians]

$\beta_{1/2}$ = width at half-height [radians]

Δ_H = baseline correction at high value of °2θ (Eq. 5.2) [c/s]

Δ_L = baseline correction at low value of °2θ (Eq. 5.2) [c/s]

θ = goniometer angle (Equation 3.1) [radians]

θ_H = high value of angle at which baseline correction is applied (Eq. 5.2) [°2θ]

θ_L = low value of angle at which baseline correction is applied (Eq. 5.2) [°2θ]

λ = X-ray wavelength (Eq. 3.1) [nm]

Φ = Pt dispersion (Eq. 6.3) [-]

Subscripts

catalyst = X-ray intensity for catalyst (Eq. 5.1)

high = upper limit (Eq. 6.4)

i = imaginary Fourier coefficients (Eq. 5.8)

low = lower limit (Eq. 6.3)

mn = minimum value of 2θ in Fourier analysis (Eq. 5.12)

mx = maximum value of 2θ in Fourier analysis (Eq. 5.12)

Pt,corr = corrected X-ray intensity for Pt (Eq. 5.2)

r = real Fourier coefficients (Eq. 5.8)

support = X-ray intensity for support (Eq. 5.1)

undet = XRD undetected Pt (Eq. 6.5)

1. INTRODUCTION

The commercialization of platinum reforming catalysts in 1949 (1) opened a new and exciting area for the use of noble metal catalysts i~~n the~~ upgrading of petroleum products. Mono- and multi-metallic supported catalysts have been extensively used by refiners all over the world to produce high octane gasoline. Platinum supported on high surface area γ-alumina is one of the important reforming catalysts.

During use, the activity and selectivity of reforming catalysts decreases as a result of poisoning and coking. Catalysts deactivated by coking and sulphur poisoning can be regenerated by burning off these compounds under controlled conditions. Another cause of catalyst deactivation is sintering. The term 'sintering', when used in conjunction with supported metal catalysts, refers to the loss of catalytic metal sites due to the agglomeration of metal. In fresh reforming catalyst, the metal, e.g. Pt, is present as small particles (≤ 1 nm in size), but use of the catalysts at elevated temperatures for prolonged periods results in increases in the average sizes of metal particles. This increase in size is accompanied by a loss in the numbers of active site (i.e. surface metal atoms; the total number of metal atoms does not change). The reverse of sintering, i.e. processes which result in decreases in metal particle sizes, is referred to as 'redispersion'.

The sintering and redispersion of supported metal catalysts have been studied extensively. A large amount of literature on the study of sintering - redispersion of supported catalysts has been published. Unfortunately, very few studies report changes in metal crystallite size distributions occurring as a result of sintering and redispersion treatments. Most sintering studies report changes in metal dispersion, i.e. changes in average metal particle sizes. However, changes in metal particle size distributions are needed in order to obtain an understanding of the sintering and redispersion mechanisms.

The objectives of the present work was to examine the suitability of wide-angle x-ray diffraction for the determination of Pt crystallite size distribution in Pt/γ-Al_2O_3 catalysts and to determine the effects of various sintering and redispersion treatments on Pt crystallite sizes. To achieve these objectives, XRD patterns were measured and analyzed for various Pt/γ-Al_2O_3 catalysts which had previously been characterized by hydrogen chemisorption. The software for analysis of XRD patterns developed by Pick (2) was upgraded during the current project.

2. LITERATURE REVIEW

2.1 The Purpose of Sintering Studies

In the early stages of commercialization of Pt/γ-Al_2O_3 reforming catalysts, many deactivation problems were faced. Reports on the deactivation of platinum supported on alumina by sintering started to appear soon after the commercial use of supported Pt catalysts for naphtha reforming (3). Numerous reviews dealing with the sintering of Pt/γ-Al_2O_3 and other supported catalysts have appeared in the last two decades (4-9).

Since metal-catalyzed reactions occur on the active sites of the metal surface, it is important to know the number of sites available for reaction. For most metal catalysts, the number of active sites is directly proportional to the number of metal atoms at the surface of the metal particles. The ratio of surface metal atoms to total metal atoms is referred to as the metal dispersion or simply 'dispersion'. For fresh catalysts the dispersion is often close to unity. Deactivation of catalysts by sintering results in decreases in dispersion, i.e. an increase in the average metal particle size. For some reactions the activity is not proportional to the number of metal surface atoms but depends on the size of the metal particles (10). Furthermore, sintering and redispersion rates appear to depend on the metal crystallite size distributions (4).

The objective of sintering and redispersion studies is to determine the mechanism(s) of the processes responsible for changes in metal particle sizes. Data on the changes in metal crystallite size distributions as a function of treatment conditions are required to achieve this objective.

2.2 Sintering and Redispersion Studies

The sintering of supported metal catalysts has been studied extensively for several decades, and several comprehensive reviews on the subject are available (4-9). It has been found that the main factors which influence sintering of supported metal catalysts are the type of metal, the sintering atmosphere and temperature, the nature of the support and the metal loading. Empirical, phenomenological and mechanistic models have been proposed for the sintering process (9); however, data on changes in metal particle size distribution are required to discriminate among the various models. Such data are not available.

Systematic studies of redispersion are much less abundant than sintering studies. Recent efforts in redispersion have largely dealt with the chemical states of the metal on the support during redispersion in various atmospheres (11-14). These studies elucidate the chemical process occurring during redispersion and sintering, but they do not yield information on the rates of sintering. Preliminary data on the effects of atmospheres on redispersion of supported Pt catalysts have recently been published

(15), but these data do not include changes in Pt size distribution since hydrogen chemisorption was the main tool used for determine Pt dispersions.

The various experimental techniques used for characterization of supported metal catalysts are discussed in the next section.

2.3 Characterization Methods for Sintering Studies

The characterization techniques employed for sintering and redispersion studies must yield directly or indirectly information about metal particle sizes since sintering and redispersion are concerned with changes in these sizes. Chemisorption, transmission electron microscopy and x-ray diffraction are the most commonly used methods for obtaining metal particle size information. The application of these methods to sintering studies has been reviewed previously. An excellent review of the methods commonly used for the characterization of supported metal catalysts has appeared recently (16); hence, only a brief account of the techniques and the information obtained by these techniques will be presented.

2.3.1 Chemisorption

Chemisorption is commonly used for determining the metal dispersion of supported metal catalysts from measurements of the amount of gas, such as hydrogen or carbon monoxide, adsorbed by catalyst under well-defined conditions.

To convert the amount of gas adsorbed to a metal dispersion requires an assumption regarding the adsorption stoichiometry. To convert the metal dispersion to an average metal particle size requires knowledge about the shape of the metal particles (17). There exists considerable evidence that the 'normal' adsorption stoichiometry for hydrogen on Pt at room temperature is about one hydrogen atom per surface metal atom (18). The adsorption stoichiometry for carbon monoxide on Pt is somewhat more variable (19,20). Hence, hydrogen adsorption can be used to monitor changes in Pt dispersion or average Pt particle size, as a function of treatment conditions. However, chemisorption does not provide any information on Pt particle size distribution.

Although hydrogen adsorption measurements are very reproducible (21), the hydrogen adsorption stoichiometry may be a function of pretreatment conditions, e.g. hydrogen adsorption uptakes may be suppressed greatly by high temperature reduction. This suppression in hydrogen adsorption has been attributed to support-metal complex formation (22), and so-called 'strong metal support interaction' (SMSI). Tauster and co-workers (23), who coined the term SMSI, attributed this effect to the reducibility of the support. Recent results, however, have shown that severe suppression of hydrogen adsorption uptakes as a result of reduction at high temperature also occur for Pt on 'irreducible' supports such as alumina and magnesia (24).

2.3.2 Transmission Electron Microscopy

Pt particles smaller than 1.0 nm can be detected and measured by transmission electron microscopy (TEM) (25). Measurement of a large number of Pt particles should, in principle, allow the determination of Pt particle size distribution, and many metal crystallite size distribution have been reported for supported metal catalysts from TEM investigations (22,26). Various average metal particle sizes can readily be calculated from the particle size distributions (27). The different average particle size commonly calculated are the number average size (D_n), the surface average size (D_s) and the volume average size (D_v). The different sizes are given by the following equations:

$$D_n = \frac{\Sigma\, n_i \cdot D_i}{\Sigma\, n_i} \qquad [2.1]$$

$$D_s = \frac{\Sigma\, n_i \cdot D_i^3}{\Sigma\, n_i \cdot D_i^2} \qquad [2.2]$$

$$D_v = \frac{\Sigma\, n_i \cdot D_i^4}{\Sigma\, n_i \cdot D_i^3} \qquad [2.3]$$

where D_i = particle diameter

n_i = number of particles with size D_i.

In catalysis the surface average size, D_s, is of interest since the surface area of the metal can readily be calculated from D_s by (4):

$$S \simeq 2.9\, y/D_s \qquad [2.4]$$

where S = Pt surface area in m^2/g of catalyst
y = mass fraction of Pt in catalyst
D_s = surface average Pt particle size in nm

Although TEM can detect small metal particles on supports, the reliability of measured particle size distribution for conventional supported metal catalysts, i.e. metal supported on porous, high-surface area carriers, is questionable. The difficulties encountered in TEM characterization include interference by the support, difficulty in obtaining representative sampling (9,16) and problems with reliable detection and size determination of Pt particles ≤ 2.0 nm in size (25,28). The difficulties of obtaining representative samples for conventional supported metal catalysts, in which the metal is usually distributed unevenly over the support surface, is illustrated by considering a typical catalyst which has a total surface area of 200 m^2/g. TEM micrographs with a magnification of at least 100,000 are required for detection of metal particles in the nanometer range; therefore, over one billion (10^9) micrographs are required to examine the surface of 0.005 gram of catalyst. Typically fewer than 10 micrographs are taken per catalyst sample! Another way of illustrating the problem of obtaining representative sampling by TEM is given by von Heimendahl (29); he stated that the total quantity of all materials examined by TEM in the world prior to 1979 is less than 1.0 cubic millimeter.

These limitations make TEM a qualitative or at best a semi-quantitative tool for the characterization of supported metal catalysts. However, the information obtained from TEM (range of metal particle sizes and nature of size distribution - unimodal or bimodal) is very useful as supporting evidence for properties obtained by other characterization methods.

2.3.3 X-ray Diffraction

Wide-angle x-ray diffraction (XRD) has been used for many years in catalyst characterization studies (30). XRD in these early studies was mainly used to obtain average crystallite sizes by the Scherrer equation (31), or to determine qualitatively whether the catalysts contained XRD detectable metal. XRD is still used for qualitative determination of metal detectability, especially in SMSI studies, although quantitative determinations of XRD detectable metal were done over a decade ago (32). Many of the previous XRD studies have used catalysts with fairly high metal loadings (≥2 wt% metal) because lower metal loading did not yield detectable metal diffraction lines.

The qualitative determination of whether a supported metal catalyst contains XRD detectable metal and the quantitative determination of an average size of XRD detected metal are useful for defining the state of the metal on the support. Older studies (6,22,32,33) claim that XRD detectability of metal crystallites is limited to metal crystallites greater than about 3 to 5 nm in size, but with current x-ray diffractometers and detectors the lower limit of detectability has been decreased to 2.0 nm or less (18,30,34). In addition to obtaining average crystallite size, XRD can also be used to obtain information about the crystallite size distribution.

The theory for calculating crystallite size distribution from XRD line shapes has been available for many years (35), but XRD (wide angle) has not been used extensively for determining metal crystallite size distribution for supported metal catalysts. Fourier analysis of XRD lines is required to obtain crystallite size information and high quality XRD patterns (i.e. good signal to noise ratios) are needed to perform this analysis. Pick (2) reviewed the use of XRD for determination of metal crystallite size distributions. The results reviewed by Pick (2) show that crystallite size distribution can be obtained for supported metal catalysts, but very slow scans (e.g. counting for 500 seconds per step) are needed to get line profiles of sufficient quality for Fourier analysis (36). However, care has to be taken in the data treatment and in the interpretation of the results (2). The Fourier analysis of XRD line shapes will be discussed later in the thesis.

Two common misconceptions should be pointed out: first, the sizes determined by XRD are not 'crystallite' sizes; they are the height of (hkl) planes responsible for the XRD line from which the height of the 'size' was calculated.

Hence, not only the size, but also the shape, of the metal crystallites influence XRD determined size. Usually the term 'crystallite size' is used instead of length in the [hkl] direction. In this thesis, crystallite size for Pt refers to the height of the 111 stacking, since the 111 Pt line was used for most of the analysis. The results of Moraweck et al. (37), who investigated a supported NiO by XRD and TEM, clearly show that significant difference in dimensions can be present along different crystal axes.

The second misconception is that the metal crystallite sizes obtained by different methods (e.g. by Scherrer equation, Fourier analysis, TEM or chemisorption) should be equal (38). Each method determines different average crystallite sizes (see Equation 2.1 to 2.3) and care has to be taken when comparing average sizes for catalysts with broad crystallite size distributions. Furthermore, different methods detect different amounts of metal, e.g. chemisorption 'sees' all the metal surface, and XRD only detects metal crystallites greater than about 2 nm. Hence, the average size calculated from chemisorption uptakes are based on all surface metal particles while the average sizes calculated from XRD are based only on the metal detected by XRD. Very little attention has been given in the past to quantifying the fraction of XRD detected metal.

2.4 Other Catalysts Characterization Methods

Metal crystallite size information can also be obtained by small angle x-ray scattering (SAXS) and by magnetization studies. SAXS is a well known technique for particle, not necessarily crystallite, size determinations (30). The application of SAXS to supported metal catalysts is complicated by the support interference since many supports, such as alumina, are composed of porous agglomerates of submicron particles. This support interference can be eliminated experimentally by compressing the catalyst at very high pressures in order to collapse the pores (39) or by using pore maskants which have electron densities similar to that of the support (40). Recent advances in data analysis for SAXS have made it possible to calculate metal particle sizes without experimental correction or elimination of the support interference (41,42). These improvement in analysis techniques make SAXS a useful tool for determining particle size information in support metal catalysts.

For certain catalysts, such as supported nickel magnetization studies yield information on the nickel particle size (43). The individual nickel particles, when placed in a magnetic field, behave like paramagnetic atoms with very large magnetic moments. Nickel particle size information can be obtained from data of magnetization current. This technique is useful for characterization of supported nickel, but it cannot be used for supported platinum.

3. X-RAY DIFFRACTION FOR CATALYST CHARACTERIZATION

3.1 Introduction to X-ray Diffraction

X-ray diffraction is a well established technique for the characterization of materials. The basic theory and uses of XRD are discussed in numerous books (e.g, 31,35,44,45). The basic principle of XRD will not be reviewed here; however some equations required later and the factors affecting the determination of metal crystallite sizes will be discussed briefly.

A crystalline material will diffract (reflect) x-rays when a monochromatic x-ray beam strikes a crystal at a certain angle. The conditions at which constructive (in-phase) scattering occurs is given by the Bragg equation:

$$n\,\lambda = 2d\cdot\sin\theta \qquad [3.1]$$

where λ = the wave-length of the x-rays

d = the distance between two (hkl) planes in the crystal

θ = the angle between the incident x-ray beam and the (hkl) planes

n = an integer which is the order of the reflection (e.g. n=1 for the 111 plane; n=2 for the 222 plane)

According to the Bragg equation the various x-ray reflections only occur at those values of θ which satisfy

Equation (3.1). At other angles no diffraction x-ray beam is observed due to destructive interference, i.e. a XRD pattern, according to Bragg's law, consist of lines at those values of θ which satisfy Equation (3.1). However, measured XRD patterns do not consist of sharp lines, at distinct values of θ, but consist of curves (referred to as broadened lines) with maxima at values of θ close to those given by the Bragg equation. The broadening of the x-ray lines is due to several factors. A brief discussion of these factors which affect the analysis of XRD patterns of supported metal catalysts is given below.

3.2 Instrumental Broadening

To obtain sharp XRD lines requires monochromatic and parallel x-ray beams, i.e. all the x-rays have the same wavelength (λ) and strike the sample at the same angle θ. X-ray tubes do not produce monochromatic x-rays and even the use of filters and monochromators fails to produce truly monochromatic x-rays. Divergence slits are used to obtain beams of nearly parallel x-rays. However, infinitesimally small slits are needed to obtain truly parallel x-ray beams, but such beams would have infinitesimal intensities. Divergence slits with finite sizes are used to obtain x-ray beams with reasonable intensities; this, however, results in slightly non-parallel x-rays.

The non-monochromatic and non-parallel nature of the x-ray beam striking a crystalline sample results in line broadening, i.e. the diffracted x-ray intensity is non-zero at values of θ slightly removed from θ_{Bragg}. Other instrumental factors, such as alignment of the diffractometer, flatness of the specimen surface, x-ray absorption by the specimen and size of receiving slits, cause broadening of the diffracted x-ray lines. The combined influence of all of these effects on the shape of the diffracted x-ray line is referred to as 'instrumental broadening'.

Many but not all of the factors contributing to instrumental broadening can quantitatively be accounted for by theory (35). In practice, instrumental broadening is determined experimentally by measuring the x-ray line shape (line profile) for a well-defined sample for which the major line broadening is due to instrumental broadening. Such a well-defined sample has to consist of well-annealed crystals which are larger than 300 nm in size (35). The methods used to correct measured line profiles for instrumental broadening will be described in Section 5.3.

3.3 Line Broadening due to Crystal Imperfections

The nature of the sample being examined by XRD also contributes to the broadening of the diffracted x-ray lines. The Bragg law assumes that crystals are perfect, but real crystals usually contain imperfections such as faults, dislocations and strains (31). These crystal imperfections all contribute to the shape and breadth of the diffraction lines. The contributions to the line width due to crystal imperfections are often referred to as 'strain broadening'. A priori correction for strain broadening is not possible since the degree of crystalline disorder in samples is not known. Often strain broadening is neglected in XRD studies of supported metal catalysts (46), since it is assumed that the small crystals are annealed by high temperature treatments. However, the presence of strong-metal support interactions or epitaxial crystalline growth may invalidate this assumption. Empirical corrections for strain broadening have also been proposed (47).

However, strain broadening can be separated from other types of broadening by analyzing several XRD lines for the same sample. This is not always possible for supported metal catalysts because only the most intense line can be measured reliably (46). The methods of testing for the presence of strain broadening are discussed in Sections 3.5 and 5.5.

3.4 Line Broadening due to Crystallite Size

Another factor which causes broadening of XRD lines is the size of the crystal. It is the crystal size effect on the shape of the XRD lines which makes XRD useful for the characterization of supported metal catalysts. Small crystals cause line broadening because the destructive interference of x-rays diffracted from small crystals is incomplete near the Bragg angles. Average crystallite sizes can be estimated from XRD line broadening due to crystal size from the Scherrer equation (31,35). The Scherrer equation is:

$$\langle D \rangle = \frac{K\,\lambda}{\beta \cos\theta} \qquad [3.2]$$

where $\langle D \rangle$ = the average crystal size

K = a constant which is close to unity, but depends on the definition of β and the shape of the crystallites

λ = wave length of the x-rays

θ = Bragg angle

β = the breadth of the XRD line in radians due to size effects

Two common methods for defining the line breadth β are in use: one, the width of the line at half the maximum intensity is used ($\beta_{1/2}$); or two, the integral width, β_i, is used. The integral width is defined as:

$$\beta_i = \frac{\text{area under XRD line}}{\text{maximum intensity of the line}} \qquad [3.3]$$

It should be pointed out that $\beta_{1/2}$ and β_i are not the experimentally measured line breadth, but are only the contribution of the size broadening to the total broadening, i.e. the measured line widths have to be corrected for instrumental and strain broadening in order to obtain $\beta_{1/2}$ and β_i. Furthermore, the average size, $\langle D \rangle$, obtained by the

Scherrer equation is not a well defined average, but is approximately equal to a volume weighted average (see Equation 3.2). However, different values of K have to be used for $\beta_{1/2}$ and β_i. For $\beta_{1/2}$, $K \simeq 0.9$, while for β_i, $K \simeq 1.0$ (16,35).

Simple methods for obtaining β from measured line widths are presented in the next section.

3.5 Estimation of β from Measured Line Breadths

The experimentally measured line breadths are due to instrumental broadening, strain broadening and size broadening, i.e.:

$$B = f(b,\ B_{st}, \beta) \qquad [3.4]$$

where B = experimentally measured line breadth

b = line breadth due to instrumental broadening

B_{st} = line breadth due to strain broadening

β = line breadth due to size broadening

According to Langford (48), the strain and size effects can be separated because strain and size broadening have different θ dependences. If the line profile is approximated by a Cauchy (Lorentzian) distribution, then the following relationship applies:

$$B \cdot \cos\theta = \beta + B_{st} \cdot \sin\theta \qquad [3.5]$$

If the line profile is approximated by a Gaussian distribution, then Equation 3.6 is valid.

$$B^2 \cdot \cos^2\theta = \beta^2 + B_{st}^2 \cdot \sin^2\theta \qquad [3.6]$$

Hence, plots of B versus $\sin\theta$ and B^2 versus $\sin^2\theta$ yields values of β and B_{st} for the two limiting shapes (Cauchy and Gaussian) of the line profiles. Note, values of B for two or more values of θ, i.e. more than a single XRD line, are required to separate size and strain broadening.

Various simple methods have been proposed for correcting for instrumental broadening. The original method proposed by Scherrer (35) was to assume that instrumental and size broadening are additive, i.e.:

$$B = b + \beta \qquad [3.7]$$

or

$$\beta = B - b \qquad [3.8]$$

This type of correction is applicable for Cauchy profiles (48).

For Gaussian profiles the correction is (48):

$$B^2 = b^2 + \beta^2 \qquad [3.9]$$

or

$$\beta = (B^2 - b^2)^{1/2} \qquad [3.10]$$

These methods of obtaining β are approximate since they not only neglect strain broadening but also assume the shapes of the line profiles. Experience has shown the corrections according to Equation 3.10 are superior to corrections by Equation 3.8 (35).

The values of <D>, obtained by calculating β from Equation 3.10 and substituting β into Equation 3.2, may not be correct in an absolute sense, but this simple method is valuable for comparing crystallite size for different catalysts of the same composition. More involved methods, such as the Fourier transform method discussed in the next section, are required to obtain more accurate crystallite sizes and crystallite size distributions.

3.6 Fourier Analysis of Line Profiles

Fourier transform analysis of XRD lines is useful because the experimentally observed line profile, h(s), is the convolution of the instrumental profile, g(s), and the size-broadened profile, f(s) (49,50). [The strain broadening and other effects which contribute to the line shape will be neglected in this discussion]. Hence, h(s) is given by:

$$h(s) = \int_{-\infty}^{\infty} g(a)\, f(s-a)\, da \qquad [3.11]$$

or

$$h(s) = \int_{-\infty}^{\infty} f(a)\, g(s-a)\, da \qquad [3.11a]$$

where s is a dimensionless Bragg angle given by:

$$s = n \left[2d \sin\theta/\lambda - 1 \right] \qquad [3.12]$$

Taking the Fourier transform of Equation 3.11 reduces the convolution integral to the following product of functions:

$$\text{Fourier transform of } h(s) = H(j) = G(j)\cdot F(j) \qquad [3.13a]$$

or

$$F(j) = H(j)/G(j) \qquad [3.13b]$$

Hence, the Fourier transform of the profile due to broadening can be obtained from the machine profile measured with a 'standard' sample, and the measured profile for a catalyst sample. More details regarding the specific method of XRD data analysis are given in Chapter 5. Reviews of the Fourier transform method of analyzing XRD profiles should be consulted for detailed descriptions of the method (16,35,44,45).

4. EXPERIMENTAL METHODS AND RESULTS

All the catalysts examined in the current study were $Pt/\gamma-Al_2O_3$ prepared in the laboratory. The catalyst preparations, catalysts treatments and hydrogen adsorption studies were done by Ms. T.-T. Yu (a former research associate in the Department of Chemical Engineering). The XRD measurements were carried out by the author and Ms. Yu, and the analysis of the XRD data was done solely by the author. A brief description of the catalyst preparation and treatment procedures, although not done by the author, are presented for the sake of completeness.

4.1 Catalyst Preparation

The four $Pt/\gamma-Al_2O_3$ catalysts described in Table 4.1 were examined in the current work. The catalysts were prepared by impregnation of $\gamma-Al_2O_3$ with an acetone solution of $Pt(C_5H_7O_2)_2$ (Cat. GC1) or aqueous solutions of H_2PtCl_6 (Cat. GC2, GC3, and GC4). The impregnation procedures have been described previously (51,52). The Pt contents of the catalysts were determined by neutron activation analysis.

Catalysts with different Pt loadings and different $\gamma-Al_2O_3$ supports were used in this study in order to determine the sensitivity of XRD for characterization of $Pt/\gamma-Al_2O_3$ catalysts.

Table 4.1 Description of Pt/γ-Al_2O_3 catalysts and γ-Al_2O_3 supports

CATALYST NUMBER	SUPPORT NUMBER	PLATINUM PRECURSOR	Pt CONTENT (wt%)	COMMENTS
GC1	GS1	$Pt(C_5H_7O_2)_2$	1.05	directly reduced[1]
GC2	GS2	H_2PtCl_6	1.12	calcined before reduction[2]
GC3	GS3	H_2PtCl_6	5.06	directly reduced[1]
GC4	GS3	H_2PtCl_6	5.06	calcined before reduction[2]
			SURFACE AREA (m^2/g)	
-	GS1	-	100	Alon from Cabot Corp.
-	GS2	-	260	KA-201 from Kaiser
-	GS3	-	240	from Versal 850[3]

[1] Catalyst reduced in flowing H_2 directly after impregnation and drying.

[2] Catalyst calcined in flowing O_2 at 200°C for 2h, and at 500°C for 1h before reduction in flowing H_2 at 500°C for 1h.

[3] Versal 850, a boehmite obtained from Kaiser Corp., was coverted to γ-Al_2O_3 by heating in air at 550°C for 24h.

4.2 Catalyst Treatment and Hydrogen Adsorption

The treatments and hydrogen adsorption measurements were carried out in a previously described flow apparatus (15). The treatment procedure consisted of placing 0.5 to 2.0 g of a catalyst sample into a quartz U-tube, heating the sample to the desired temperature in flowing N_2, replacing the N_2 with the desired treatment gas, and treating the catalysts in the desired atmosphere for the desired length of time. All treatment were done in flowing gases. Treatment gases containing CCl_4, C_2HCl_3 and HCl were obtained by bubbling N_2 (or O_2) through solutions of these compounds and mixing the resulting saturated streams with O_2 and/or N_2 to obtain the desired composition. Mixtures containing Cl_2 were obtained by adding N_2 and O_2 in the desired amounts to a 3.25 mol% Cl_2 in N_2 mixture. The N_2 (Matheson grade, 99.9995%), He (UHP grade), O_2 (UHP grade) and the Cl_2-N_2 mixture were purchased from Matheson. The H_2 was generated in the laboratory with a Matheson (Model 8320) H_2 generator.

After the treatment, the catalysts were reduced in flowing H_2 at 500°C for 1 h and degassed in flowing N_2 at 500°C for 2 h. Hydrogen adsorption uptakes were measured at room temperature by the dynamic flow method (21). The treatments and hydrogen adsorption measurements were done in the same apparatus without removing the catalyst from the U-tube between treatments and adsorption measurements.

The treatment conditions and H_2 adsorption uptakes for the four catalysts are described in Tables 4.2 to 4.5. The

Table 4.2 Treatment conditions and hydrogen adsorption uptakes for Catalyst GC1 [1.05% Pt/γ-Al_2O_3 (Alon)]

	TREATMENT CONDITIONS[a]									HYDROGEN
RUN	Composition of Treatment Atmosphere (mol%)							Temp.	Time	UPTAKES
	H_2	O_2	N_2	CCl_4	C_2HCl_3	HCl	H_2O	(°C)	(h)	(H/Pt)
GC1-1	100							500	1	0.44
GC1-2		6.7	93	0.3			0.04	510	1	0.42
GC1-3		100						550	1	0.53
GC1-4		17	83		0.1		0.1	510	1	0.47
GC1-5		100						550	1	0.55
GC1-6		13	87			0.05	0.03	510	1	0.41
GC1-7		100						550	1	0.35
GC1-8		24	76			0.08	0.04	510	1	0.25
GC1-9		24	76			0.4	0.03	520	1	0.58
GC1-10		24	76			0.4	0.03	520	1	0.82

[a] Treatments done sequentially on the same sample.

Table 4.3 Treatment conditions and hydrogen adsorption uptakes for Catalyst GC2 [1.12% Pt/γ-Al_2O_3 (Kaiser KA-201)]

RUN	TREATMENT CONDITIONS[a] Composition of Treatment Atmosphere (mol%) H_2	He	O_2	N_2	Cl_2	HCl	H_2O	Temp. (°C)	Time (h)	HYDROGEN UPTAKES (H/Pt)
GC2-1	100							500	1	0.86
GC2-2		100						800	16	0.08
GC2-3				99.6		0.4	0.03	520	1	0.41
GC2-4			16	84		0.4	0.02	520	1	0.76
GC2-5				99.6		0.4	0.03	520	2	0.74
GC2-6		100						800	16	0.19
GC2-7			100					700	1	0.20
GC2-8			24	76		0.4	0.03	520	1	n.m.[b]
GC2-9			24	76		0.4	0.03	520	2	0.94
GC2-10		100						800	16	0.23
GC2-11			100					700	1	0.19
GC2-12			100					800	1	0.04
GC2-13				96.75	3.25			450	1.3	0.61

[a] Treatments done sequentially on the same sample.

[b] n.m. = not measured.

Table 4.4 Treatment conditions and hydrogen adsorption uptakes for Catalyst GC3 [5.06% Pt/γ-Al_2O_3 (from Versal 850)]

RUN	TREATMENT CONDITIONS[a] Composition of Treatment Atmosphere (mol%)								HYDROGEN UPTAKES
	H_2	O_2	N_2	Cl_2	HCl	H_2O	Temp. (°C)	Time (h)	(H/Pt)
GC3-1	fresh (as reduced after impregnation)								n.m.[b]
GC3-2	100						500	1	0.49
GC3-3		100					700	1	0.15
GC3-4		24	76		0.4	0.03	520	1	0.18
GC3-5		24	76		0.4	0.03	520	16	0.37
GC3-6		20	80	0.06			520	4.5	0.40
GC3-7		20	80	0.06			520	16	0.52
GC3-8			96.75	3.25			450	1	0.94
GC3-9		100					800	1	0.11
GC3-10			96.75	3.25			450	1	0.96

[a] Runs GC3-1 to GC3-3 were done sequentially on the same sample. After Run GC3-3, the treated sample was divided into two portions; Runs GC3-4 to GC3-7 were done sequentially on one portion and Runs GC3-8 to GC3-10 were done sequentially on the other portion.

[b] n.m. = not measured.

Table 4.5 Treatment conditions and hydrogen adsorption uptakes for Catalyst GC4 [5.06% Pt/γ-Al_2O_3 (from Versal 850)]

	TREATMENT CONDITIONS[a]							HYDROGEN
RUN	Composition of Treatment Atmosphere (mol%)					Temp. (°C)	Time (h)	UPTAKES (H/Pt)
	H_2	He	O_2	N_2	Cl_2			
GC4-1	fresh (as reduced after impregnation and calcination)							n.m.[b]
GC4-2	100					500	1	0.53
GC4-3		100				800	16	0.17
GC4-4			20	80	0.06	520	1	0.22
GC4-5			20	80	0.06	520	4	0.42
GC4-6			20	80	0.06	520	4	0.54

[a] Treatments done sequentially on the same sample.

[b] n.m. = not measured.

H_2 adsorption results are expressed in terms of H/Pt ratios, where H is the number of H atoms adsorbed by the sample and Pt is the number of Pt atoms in the sample.

4.3 X-ray Diffraction Measurements

4.3.1 x-ray equipment

A Philips x-ray diffractometer system was used to measure the XRD profiles. The diffraction system consisted of a Philips PW1730/10 x-ray generator, a Philips PW1050/70 vertical goniometer, a Philips PW2233/20 Copper x-ray tube, an AMRAY Model E3-202 GVW7794 graphite monochromator and a Philips PW1965/60 proportional x-ray detector. A 1° divergence (incident) slit and a 0.1° receiving slit were used for all the measurements.

Treated catalyst samples were placed into the cylindrical cavity of a custom-made stainless steel specimen holder. The specimen holder consisted of a stainless steel block (5 mm thick) with a 19 mm diameter and 2 mm deep cylindrical cavity. The samples were carefully placed into the cavity to ensure approximately equal density throughout the packed sample. The surface of the specimen was smoothed by gently pressing and rotating a glass slide over the surface of the sample. The sample holder containing the catalyst was easily handled and the surface of the specimen remained smooth throughout the handling and measurement of the XRD patterns.

All XRD measurements were done in the step-scan mode with a step size of 0.02 °2θ and counting for 100 s per step. The majority of the XRD scans were collected over a range of 36 to 44 °2θ since the most intense Pt line (the 111 line) is located at 39.8 °2θ. It took about 12 h to obtain one XRD pattern for the 36 to 44 °2θ range. The output signal of the diffractometer, i.e. angle-intensity pairs, were sent directly to the HP-1000 minicomputer located in the Data Acquisition and Control (DACS) centre of the Department of Chemical Engineering. The data were stored on disc and also copied to magnetic tape for backup protection. All plotting and data analysis were done with the facilities of DACS centre.

4.3.2 XRD patterns for catalysts

The 'raw' XRD patterns for the catalysts after the various treatments are shown in Figures 4.1 to 4.6. The patterns are off-set for clarity, but otherwise they are point-by-point plots of the data as measured. The intensities of these plots cannot be compared directly because two different Cu tubes were used (one tube burned out during the course of these measurements). All the results except those for samples GC3-4 to -7, GC3-10 and GC4-3 to -6 were obtained with the old tube. The XRD intensity from the new tube was 3.11 times greater than that from the old tube. This factor was used to adjust the intensities of XRD patterns when comparing patterns obtained with the old and new Cu tubes.

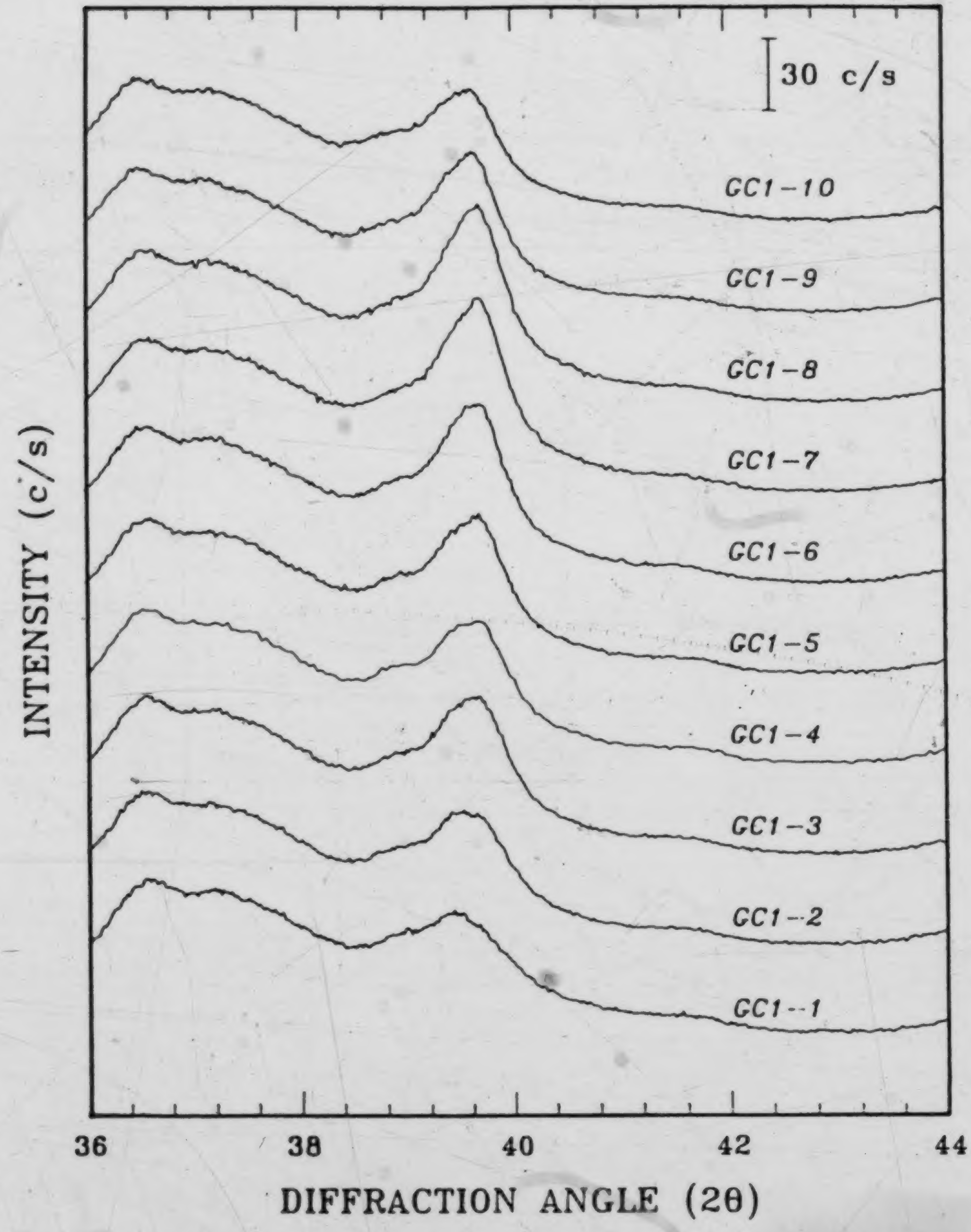

Figure 4.1 Raw XRD Patterns for Catalyst GC1
(See Table 4.2 for description of treatments)

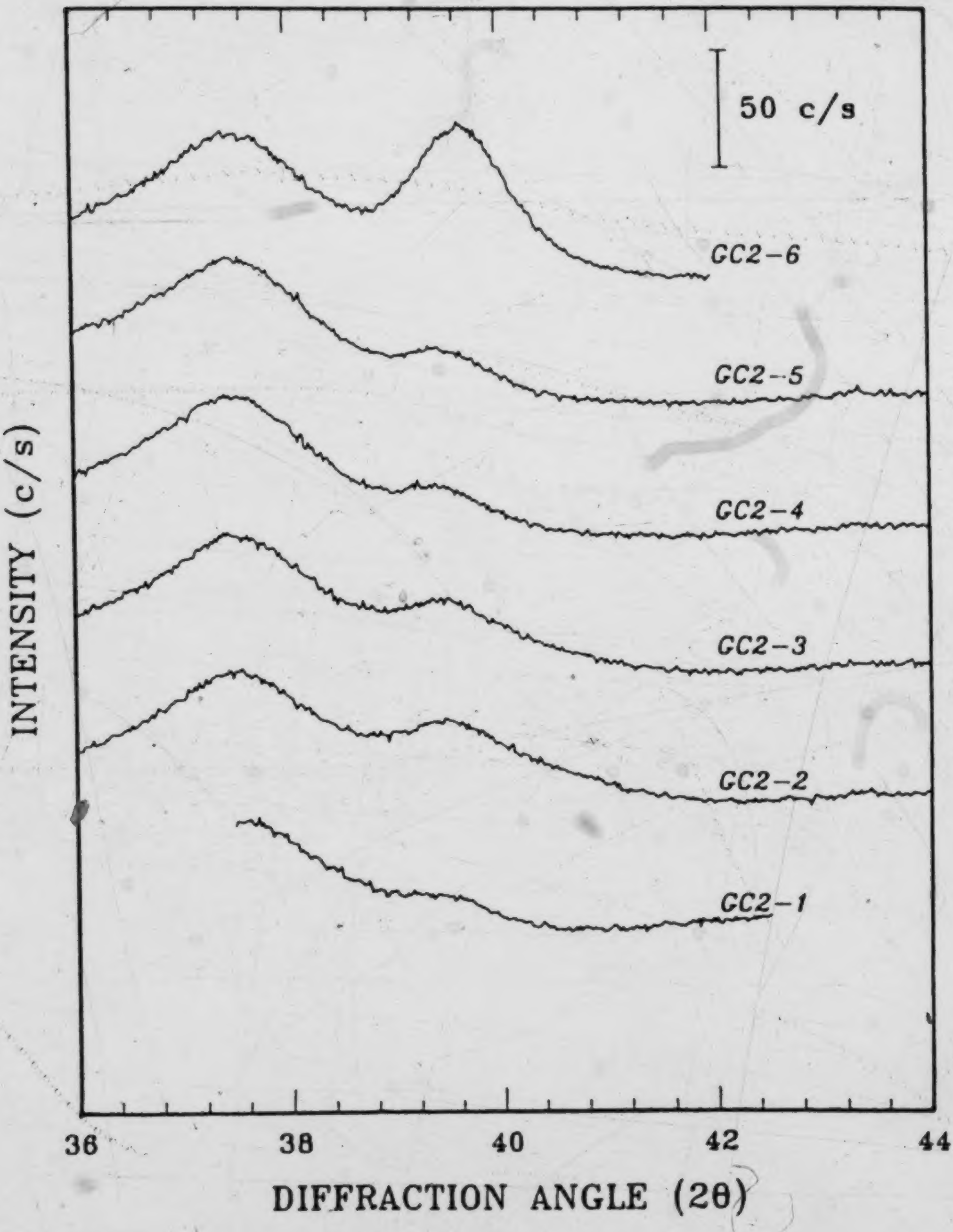

Figure 4.2 Raw XRD Patterns for Catalyst GC2
(See Table 4.3 for description of treatments)

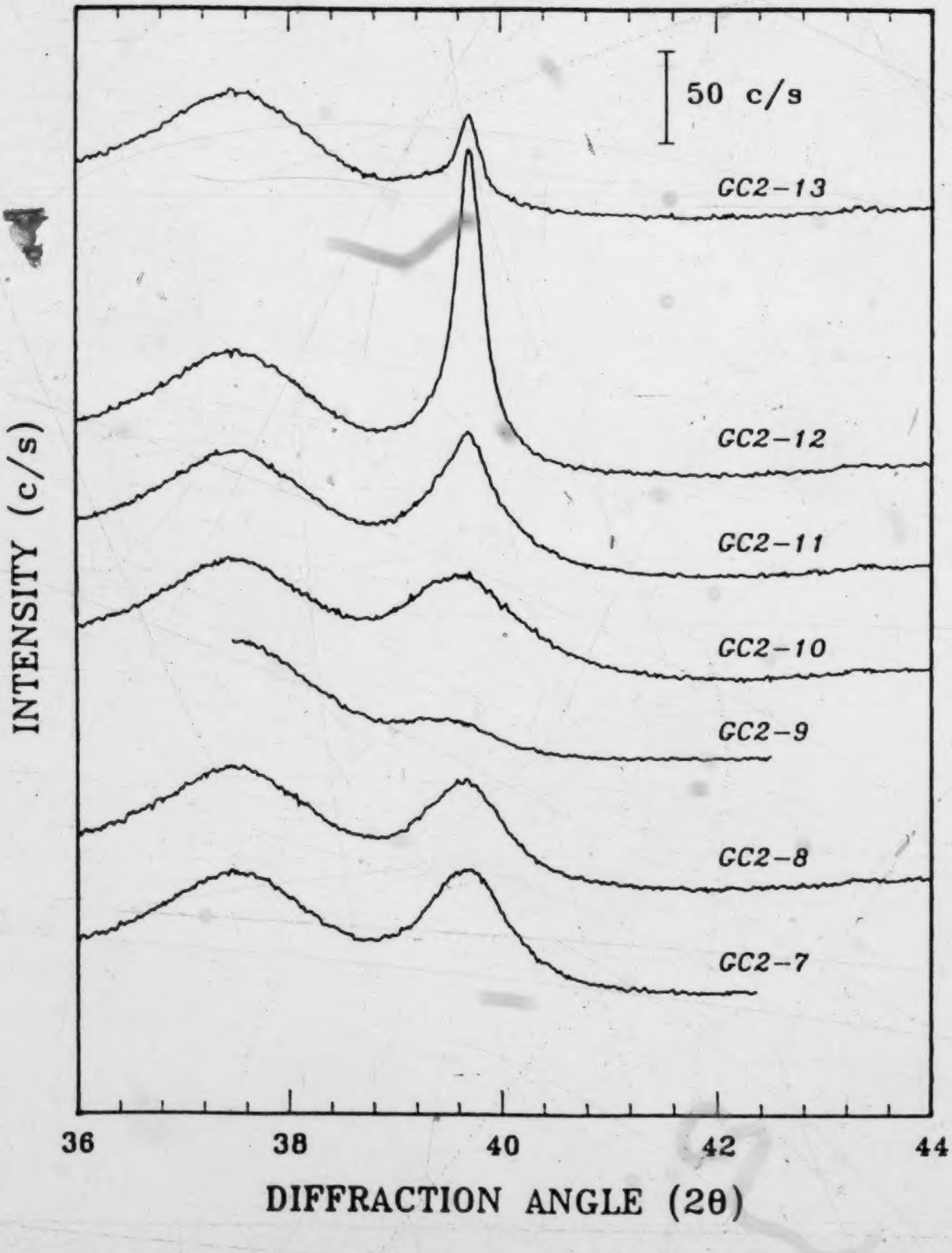

Figure 4.3 Raw XRD Patterns for GC2(continued)
(See Table 4.3 for description of treatments)

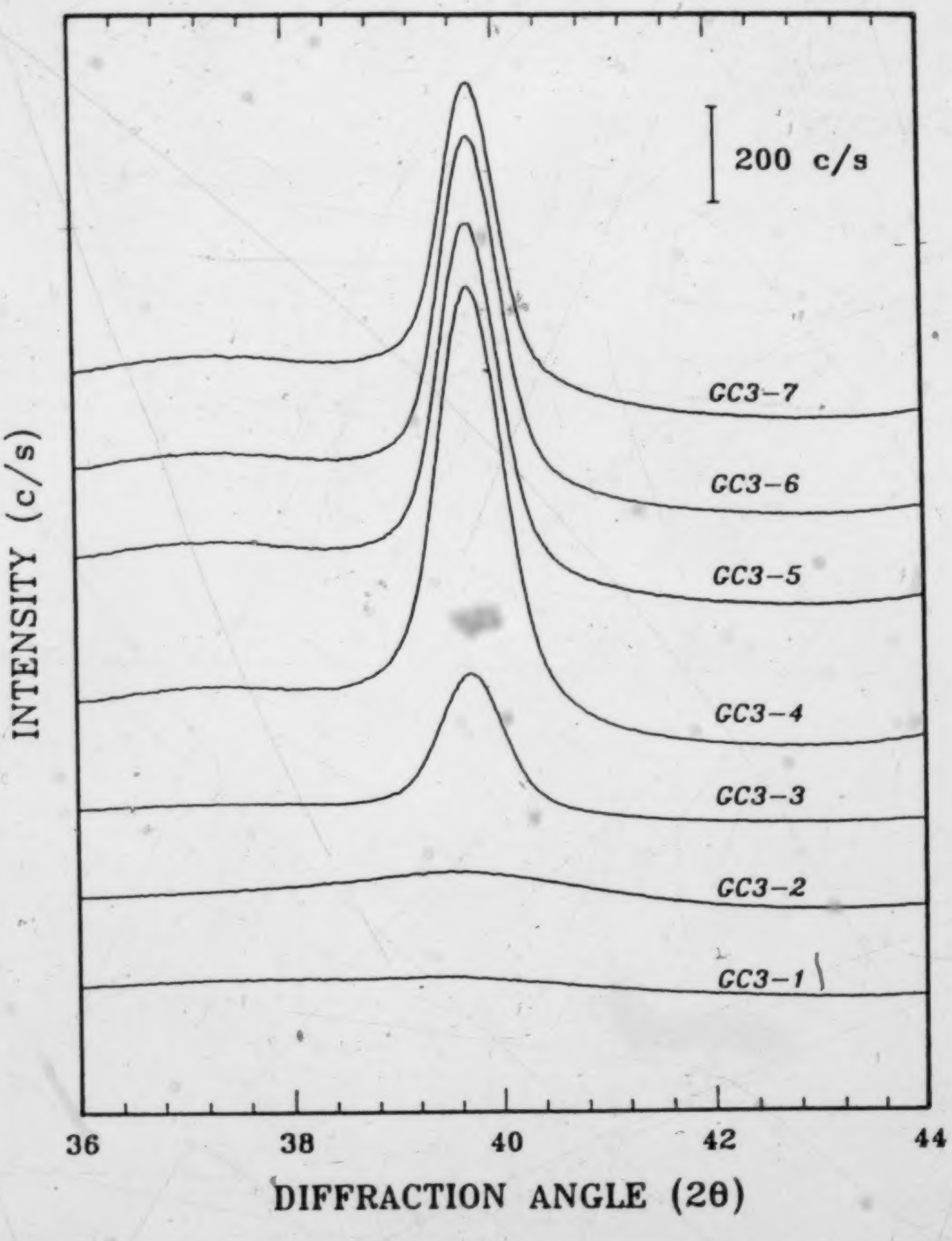

Figure 4.4 Raw XRD Patterns for Catalyst GC3
(See Table 4.4 for description of treatments)

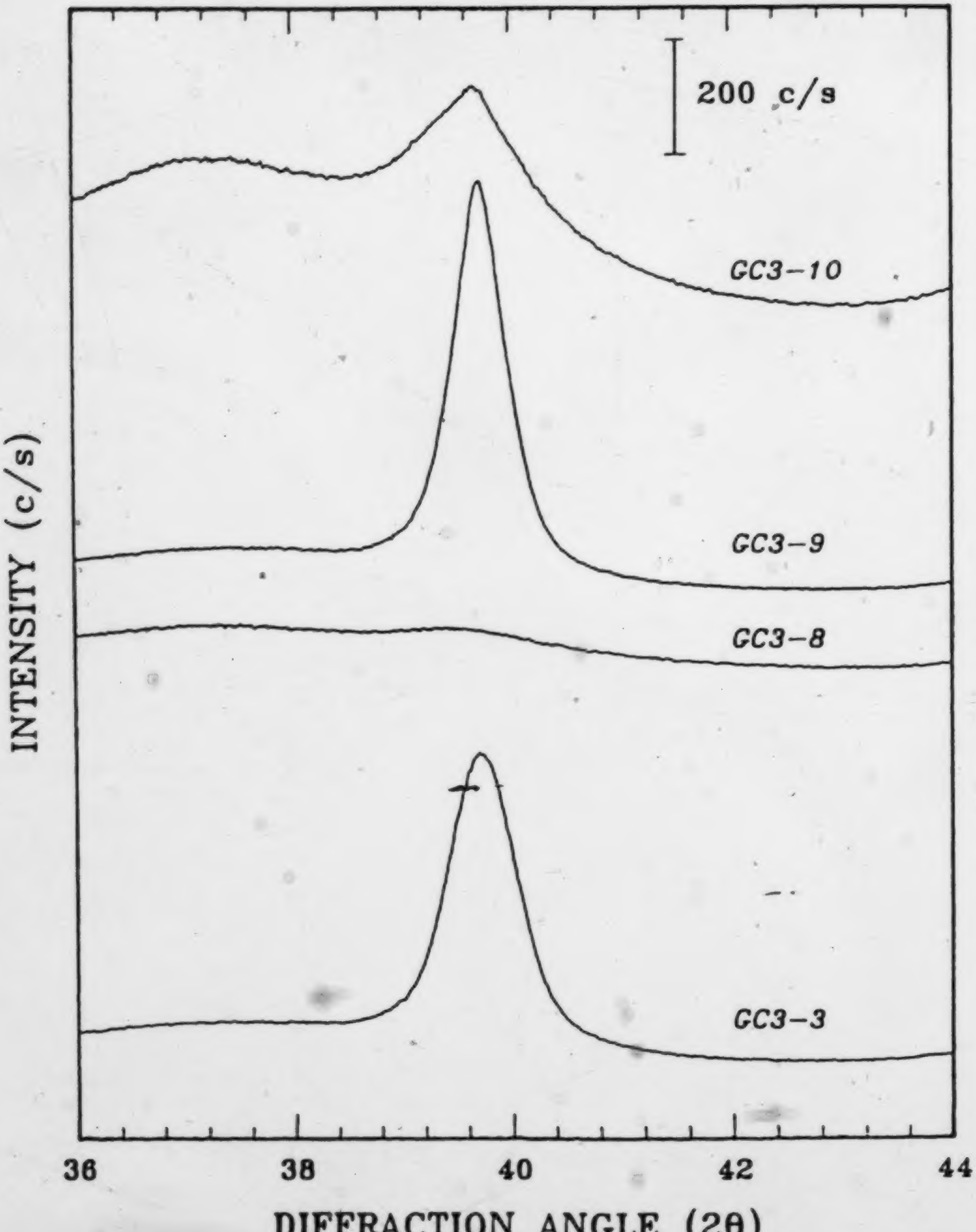

Figure 4.5 Raw XRD Patterns for GC3(continued)
(See Table 4.4 for description of treatments)

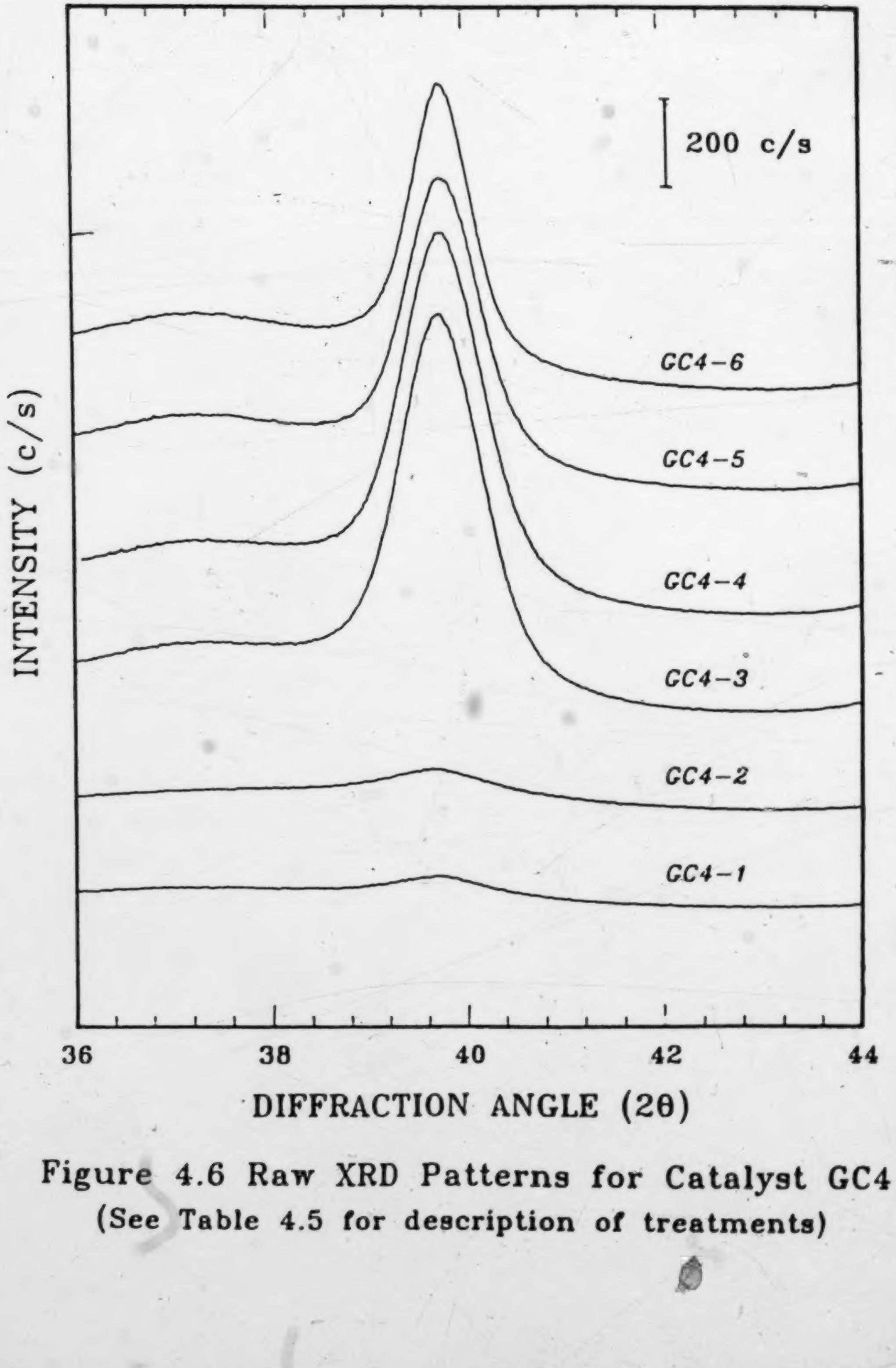

Figure 4.6 Raw XRD Patterns for Catalyst GC4
(See Table 4.5 for description of treatments)

4.3.3 XRD patterns for supports

In order to obtain the XRD pattern for the platinum in supported Pt catalysts, it is necessary to correct for the XRD pattern of the support. This requires measurement of the XRD patterns for the supports. The severe treatments of the catalyst samples may results in changes in the XRD patterns of the supports. For this reason support XRD patterns were measured after various thermal treatments. The treatments of the supports are described in Table 4.6 and the as-measured XRD patterns are shown in Figure 4.7.

Only one pattern is shown for Alon (Support GS1) since previous studies (51) showed the thermal treatments of Alon only result in minor changes in the XRD pattern. The results for supports GS2 and GS3, in Figure 4.7, show the changes as a result of thermal treatments are also small.

The change in diffracted x-ray intensity as a result of changing the x-ray tube is also illustrated in Figure 4.7. Runs GS3-1 and -2 were done with the old tube and Runs GS3-3 and -4 were done with the new tube. The average ratio of the intensities of old to new tubes is 0.322 with a standard deviation of 0.007.

It should be pointed out that storage of samples treated at elevated temperature resulted in small changes in the support component of the XRD patterns. The method of correction for these changes is described in Chapter 5.

Table 4.6 Treatment conditions for supports

RUN	TREATMENT CONDITIONS[a]
GS1-1	Fresh support
GS2-1	Fresh support
[illegible]-2	$H_2(100)^b$; 700°C, 72h
GS2-3	$HCl(0.4), H_2O(0.03), O_2(24), N_2(76)$; 520°C; 1h
GS2-4	$H_2(100)$; 800°C; 16h
GS3-1	Fresh support(after decomposition of boehmite)
GS3-2	He(100); 800°C; 16h
GS3-3	He(100); 800°C; 16h (repeat of GS3-2 with new x-ray tube)
GS3-4	$Cl_2(0.15), O_2(19), N_2(81)$; 520°C, 1h

[a] Treatments GS2-2 to GS2-4 done sequentially on same sample

[a] Treatments GS3-4 and GS3-5 done sequentially on same sample

[b] Values in brackets are the compositions of the treatment atmosphere in mol%.

4.3.4 XRD pattern for a standard sample

In order to correct the measured XRD patterns for instrumental broadening (see Chapter 3), a XRD pattern is required in which the only cause of line broadening is instrumental broadening. The sample chosen as the standard sample was a physical mixture of Pt black and silicalite (silicalite is a pentasil zeolite manufactured by Union Carbide). Silicalite, rather than γ-Al_2O_3, was chosen for the standard sample because silicalite gives low background

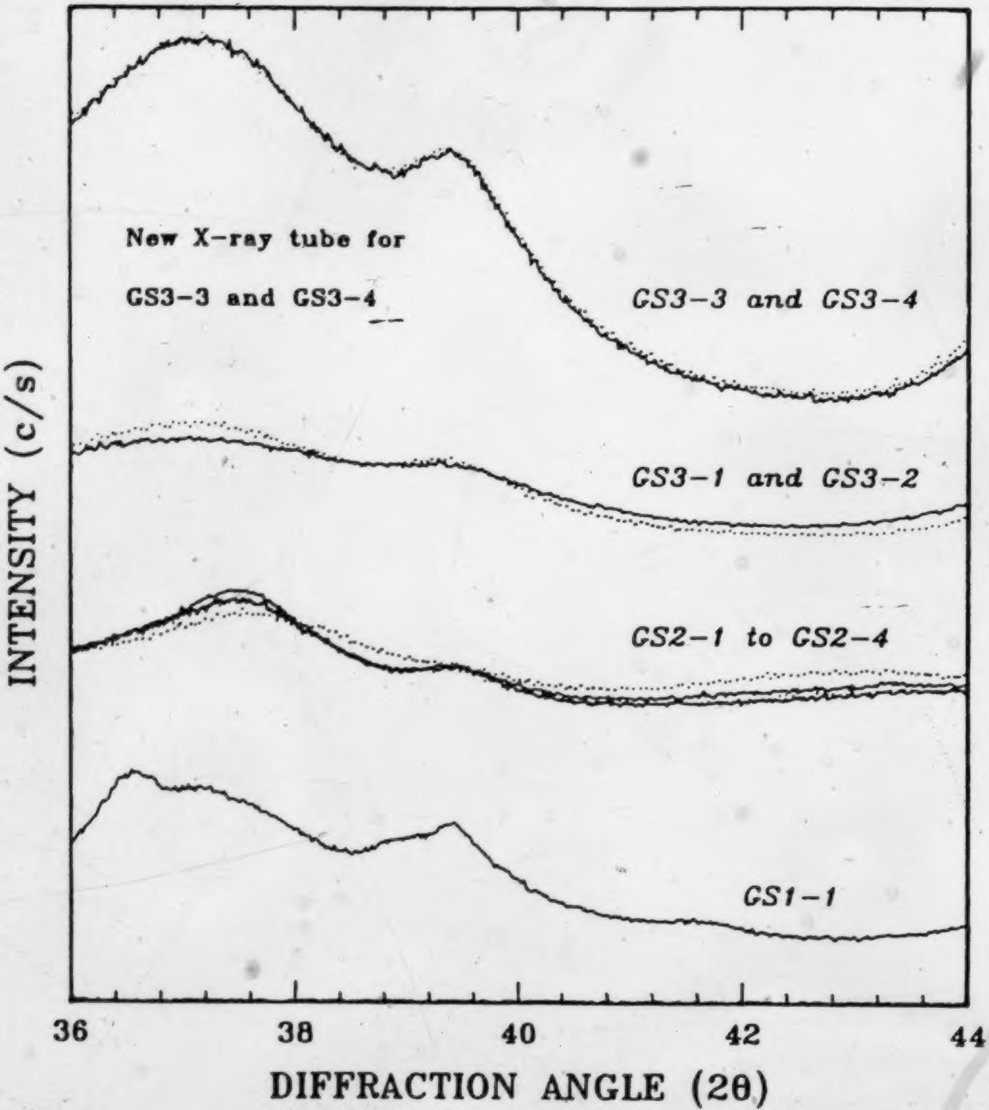

Figure 4.7 Raw XRD patterns for Supports
(See Table 4.6 for description of treatments)

Patterns GS2-1 to GS2-4 are offset 100 c/s from the origin
Patterns GS3-1 to GS3-4 are offset 200 c/s from the origin

intensities of x-rays, and has no diffraction lines that interfere with the Pt 111 line.

The Pt black was well mixed with the silicalite powder. This physical mixture was heated in flowing H_2 at 150°C for 4 h, and at 500°C for 1 h, followed by treatment in flowing N_2 at 500°C for 2 h. This treatment was carried out to anneal and sinter the Pt black. Examination of the sintered and annealed mixture by transmission electron microscopy showed that most of the Pt was present as particles larger than 300 nm. The XRD pattern for this sample is shown in Figure 4.8. This pattern was used to correct all the other XRD patterns for instrumental broadening using the procedures described in Chapter 5.

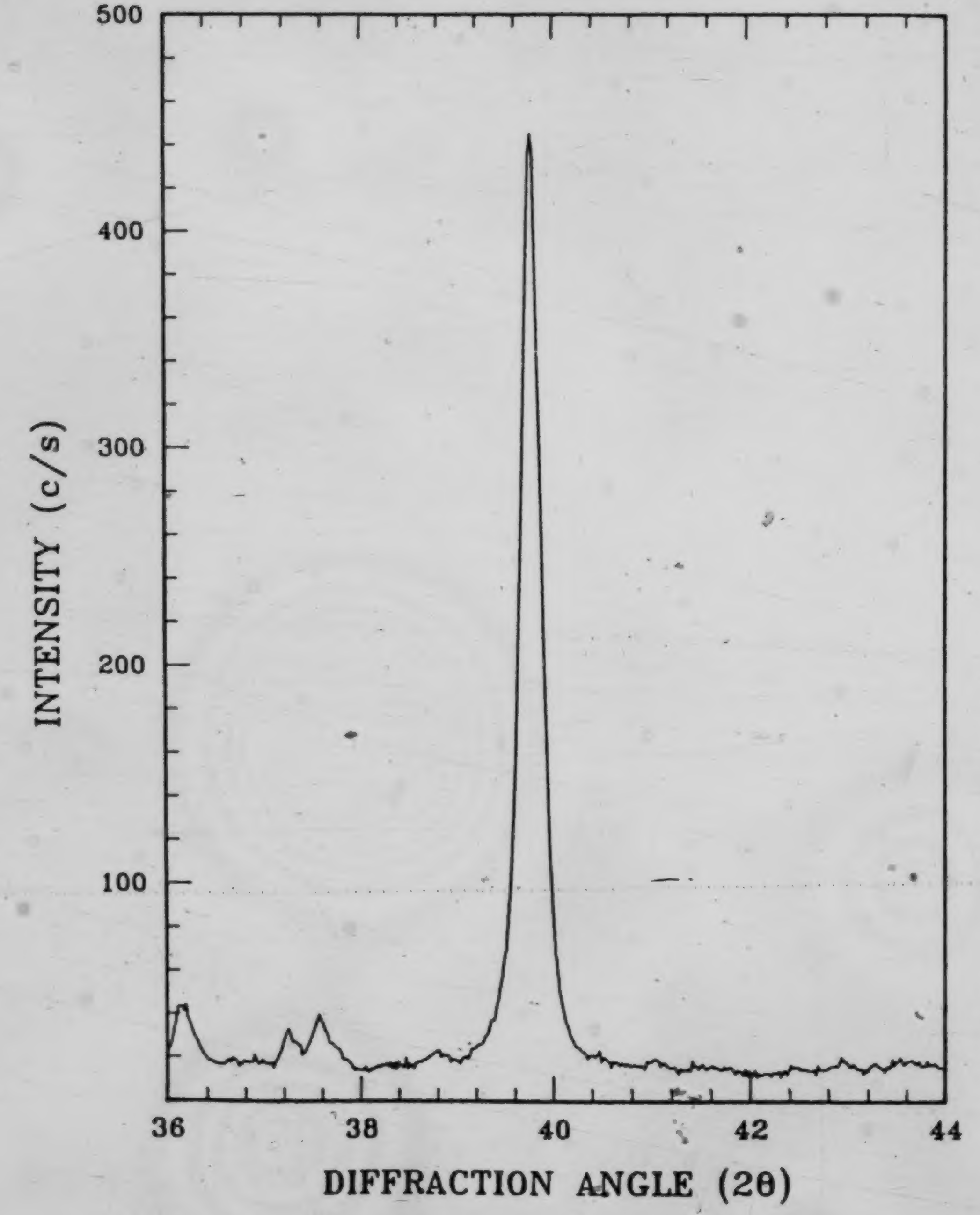

Figure 4.8 XRD Pattern for Standard Sample (Annealed mixture of Pt black and silicalite)

5. ANALYSIS OF XRD PATTERNS

The general principles involved in obtaining crystallite size information from XRD line broadening were described in Chapter 3. In the current chapter the specific methods used in the present investigation are presented. The main steps involved in converting XRD patterns of supported metal catalysts to metal crystallite sizes are elimination of support contribution to the XRD patterns, smoothing of the line profile of the metal, correcting for instrumental effects and checking for the presence of strain broadening. The individual steps are described in the following sections. The computations were carried out on the HP-1000 minicomputers in the DACS centre and the programs used are listed in Appendix A.

5.1 Subtraction of the Support Pattern

The support contribution was removed from the measured profile for the supported metal catalyst by a weighted point-by-point subtraction of the support pattern (see Figure 4.7) from the pattern of the supported metal catalyst (see Figures 4.1 to 4.6). The intensity I_{Pt} of the x-rays due to diffraction at a given value of 2θ by the Pt is then given by:

$$I_{Pt} = I_{Catalyst} - [S.F.] \cdot I_{Support} \qquad [5.1]$$

The 'Scaling Factor', S.F., is required to compensate for the decreased amount of support that the x-rays 'see' due to the presence of the Pt, i.e. the x-rays do not penetrate the sample as deeply if Pt is present in the sample. A scaling factor of 0.95 (2) was used for catalysts GC1 and GC2, and a scaling factor of 0.90 was used for catalysts GC3 and GC4. Values of I_{Pt} were calculated according to Equation 5.1 at each measured value of 2θ (e.g. $0.02°2\theta$ steps).

Values of I_{Pt} should be close to zero at values of 2θ reasonably far removed from the centroid of a Bragg diffraction line for the metal (e.g. at $2\theta = 2\theta_{Bragg} \pm 4°$). However, values of I_{Pt} in the 'tails' of the line profiles calculated according to Equation 5.1 usually deviated slightly from zero. The deviations were not large (averaging less than ±5 c/s), but subsequent data fitting and analysis required that these 'tails' of the XRD line approach zero intensity. Several reasons, such as slightly incorrect values of the scaling factors, contribution to background x-ray intensity due to highly dispersed Pt and variations in support profiles, can account for the variations in the tails.

The x-ray intensities for the Pt, i.e. I_{Pt}, obtained by Equation 5.1 were corrected for deviations from zero intensities in the tails of the line profile by a linear base-line correction. The correction method consisted of determining I_{Pt} in the tails of the line profiles (i.e. about 4° 2θ away from the peak maximum) and then shifting the base line at both ends of the pattern so that the intensity in the tails was approximately equal to zero. The corrected intensity as a function of 2θ is then given by:

$$I_{Pt,corr.} = I_{Pt} - \Delta_L - [(\Delta_H - \Delta_L)\cdot(2\theta - 2\theta_L)]/[2\theta_H - 2\theta_L] \qquad [5.2]$$

where $2\theta_L$ = low value of 2θ at which baseline shift is determined, i.e. the value of 2θ somewhere in the low angle tail

$2\theta_H$ = high value of 2θ at which baseline shift is determined, i.e. the value of 2θ somewhere in the high angle tail

Δ_L = baseline shift at $2\theta_L$

Δ_H = baseline shift at $2\theta_H$

The values of Δ_L and Δ_H were obtained by examining a plot of I_{Pt} as a function of 2θ on the computer monitor and estimating the shift in intensity required to reduce the intensities in the tails of the line profile to zero. A corrected value of the x-ray intensity was calculated at each measured value of 2θ, e.g. at 0.02 °2θ intervals. The interactive program XRMD, listed in Appendix A, was used to calculate the subtracted profiles.

Most of XRD patterns analyzed in this work spanned a range of 2θ from 36 to 44°, i.e. the pattern contained the Pt 111 line which has a maximum intensity at 39.8 °2θ. For the patterns the values of $2\theta_L$ and $2\theta_H$ of 36 and 44°, respectively were used. However, two patterns, with wider ranges of 2θ (30 to 90 °) were examined. The values of $2\theta_L$ and $2\theta_H$ for these two cases were 30 and 90°, respectively.

In Figure 5.1 the results of a support subtraction are illustrated. The raw XRD patterns for the catalyst and the support are shown in the top part of the figure (the intensities are offset from zero for clarity). The subtracted pattern is shown in the bottom part of the figure. Examination of the subtracted pattern show that the above described method results in excellent removal of the support contributions from the XRD profile of the supported metal catalysts. Excellent removal of the support line occurs even in the regions where there is severe interference by the support, i.e. the 400 and 440 lines of γ-Al_2O_3 in the vicinities of the Pt 200 and 220 lines (see Figure 5.1). A tabulation of the Pt and γ-Al_2O_3 diffraction lines in the 30 to 90 °2θ range is given in Table 5.1.

The subtracted XRD patterns for the other catalyst samples are shown in Figures 5.2 to 5.7. The patterns in these figures are offset for clarity; the intensity for each subtracted pattern at 36 °2θ is approximately equal to zero. The baseline corrections that were used for each sample are listed in Appendix B. In the subsequent analysis only the subtracted patterns will be used since these patterns contain the information related to Pt crystallite sizes.

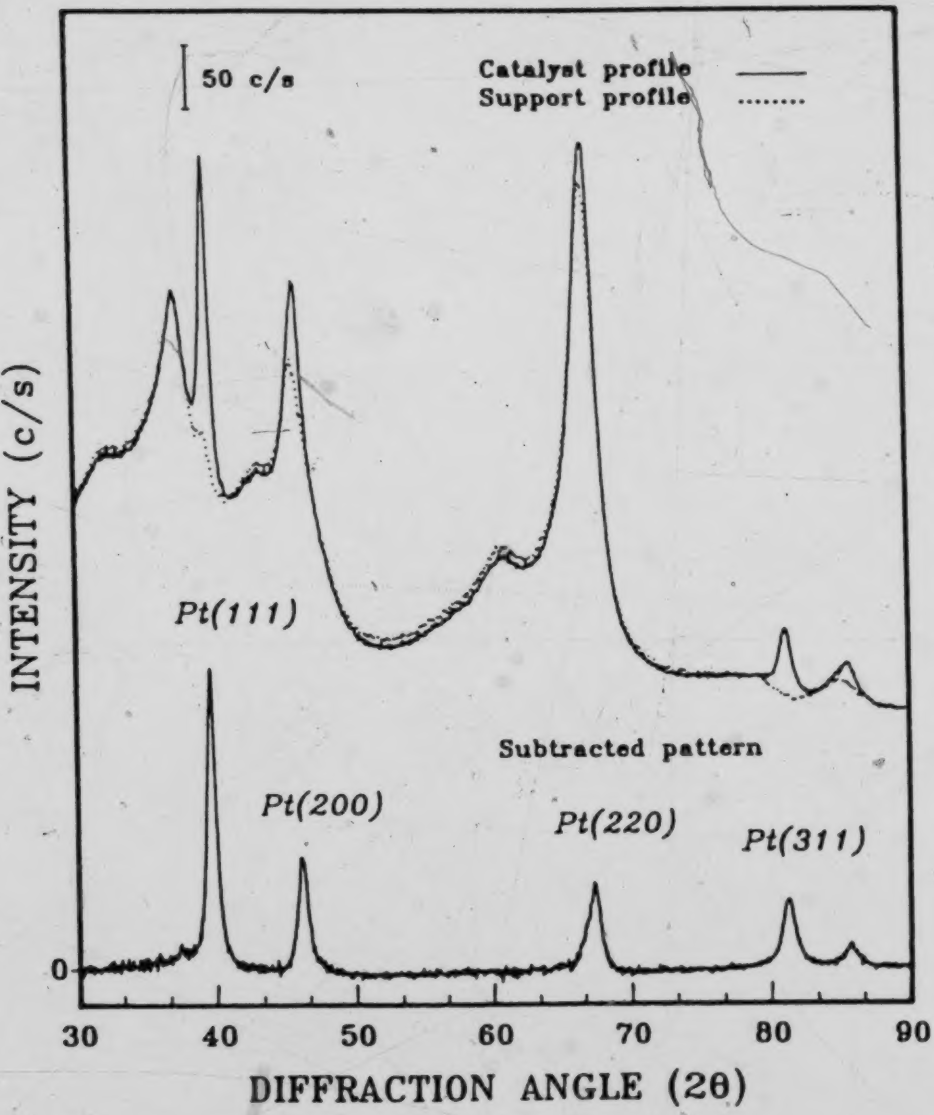

Figure 5.1 Illustration of Support Subtraction for 1% Pt/γ-Al_2O_3 Catalyst

($2\theta_L=30$, $2\theta_H=90$, $\Delta_L=4.0$ c/s, $\Delta_H=-1.0$ c/s, S.F.=0.95)

Table 5.1 Location of Pt and γ-Al_2O_3 diffraction lines

Index of plane (hkl)	Lattice Spacing d (nm)	°2θ for Cu Radiation	Approximate Relative Intensity
Platinum			
111	0.2265	39.80	100
200	0.1962	46.27	50
220	0.1387	67.53	30
311	0.1183	81.36	30
222	0.1133	87.80	10
γ-Al_2O_3			
220	0.280	32.0	20
311	0.239	37.6	80
222	0.228	39.5	50
400	0.198	45.8	100
511	0.152	61.0	30
440	0.140	66.8	100
444	0.114	85.1	20

5.2 Smoothing of XRD Line Profile

Examination of the subtracted patterns (Figure 5.2 to 5.7) shows that the patterns contain noise, i.e. fluctuation in intensity in adjacent 2θ values. The level of noise is too high for direct Fourier analysis of the subtracted profiles. The signal to noise ratio could be improved by increasing the counting times at each step. However, the counting time of 100 s per step used in this work already requires over 11 h for the measurement of one XRD pattern,

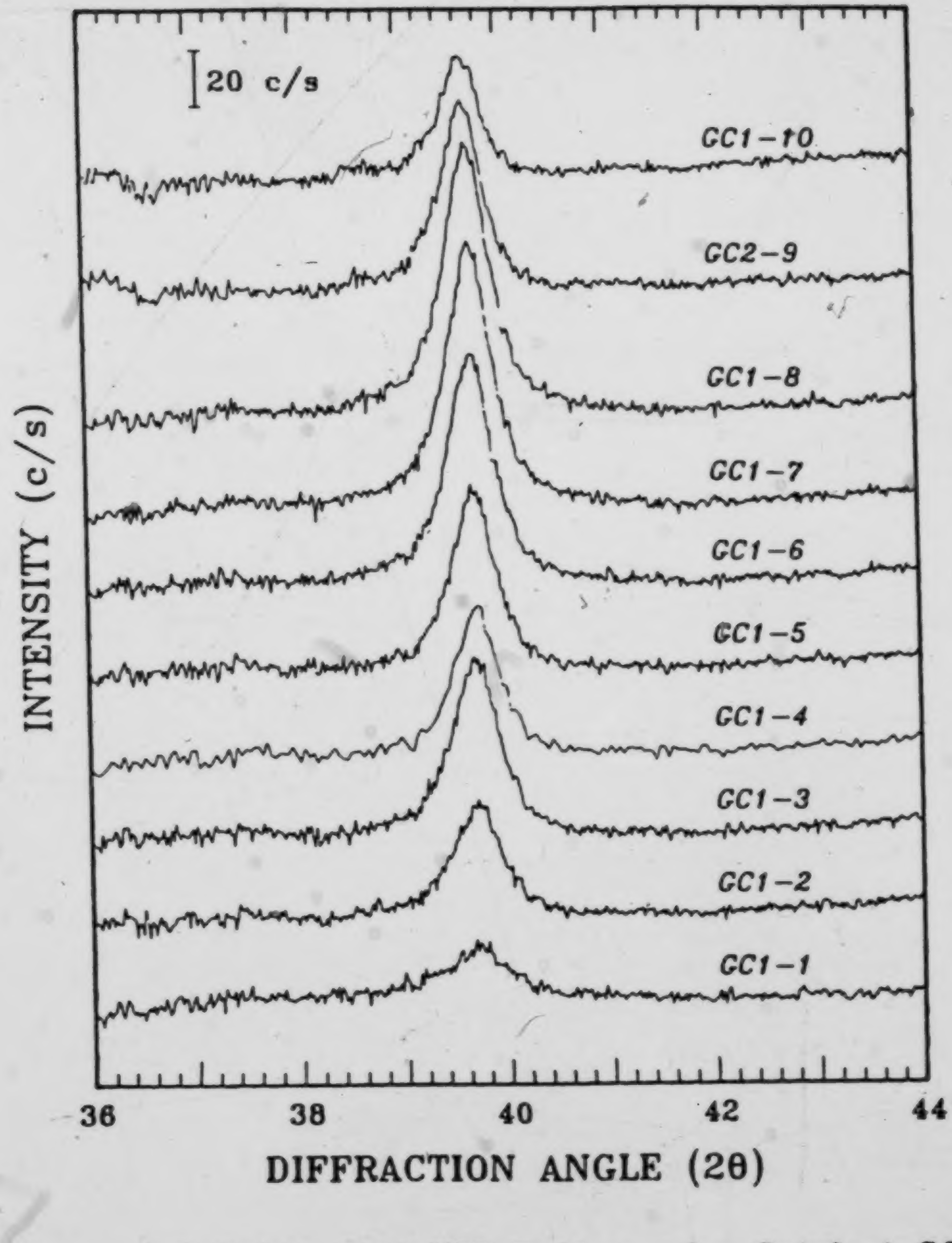

Figure 5.2 Subtracted XRD Patterns for Catalyst GC1

(See Table 4.2)

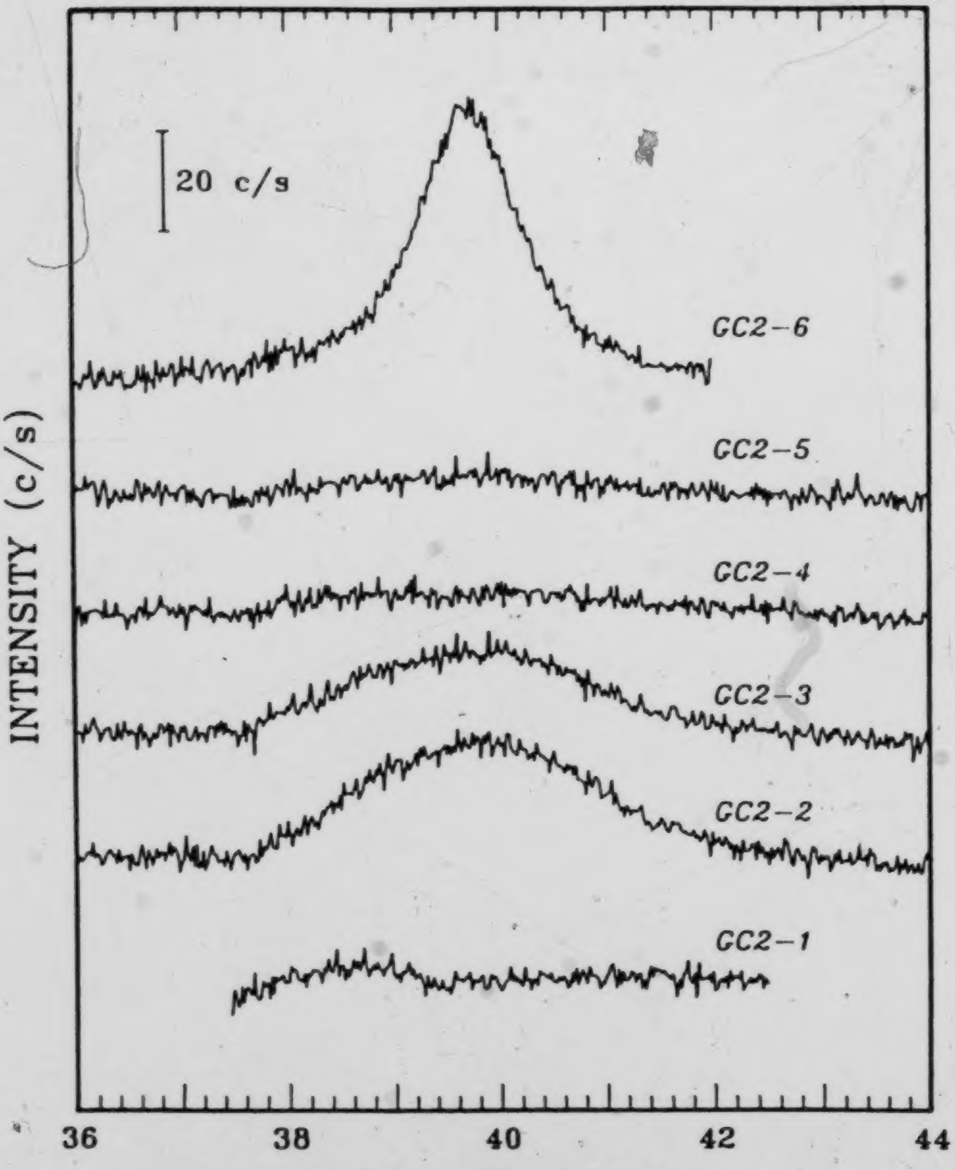

Figure 5.3 Subtracted XRD Patterns for Catalyst GC2

(See Table 4.3)

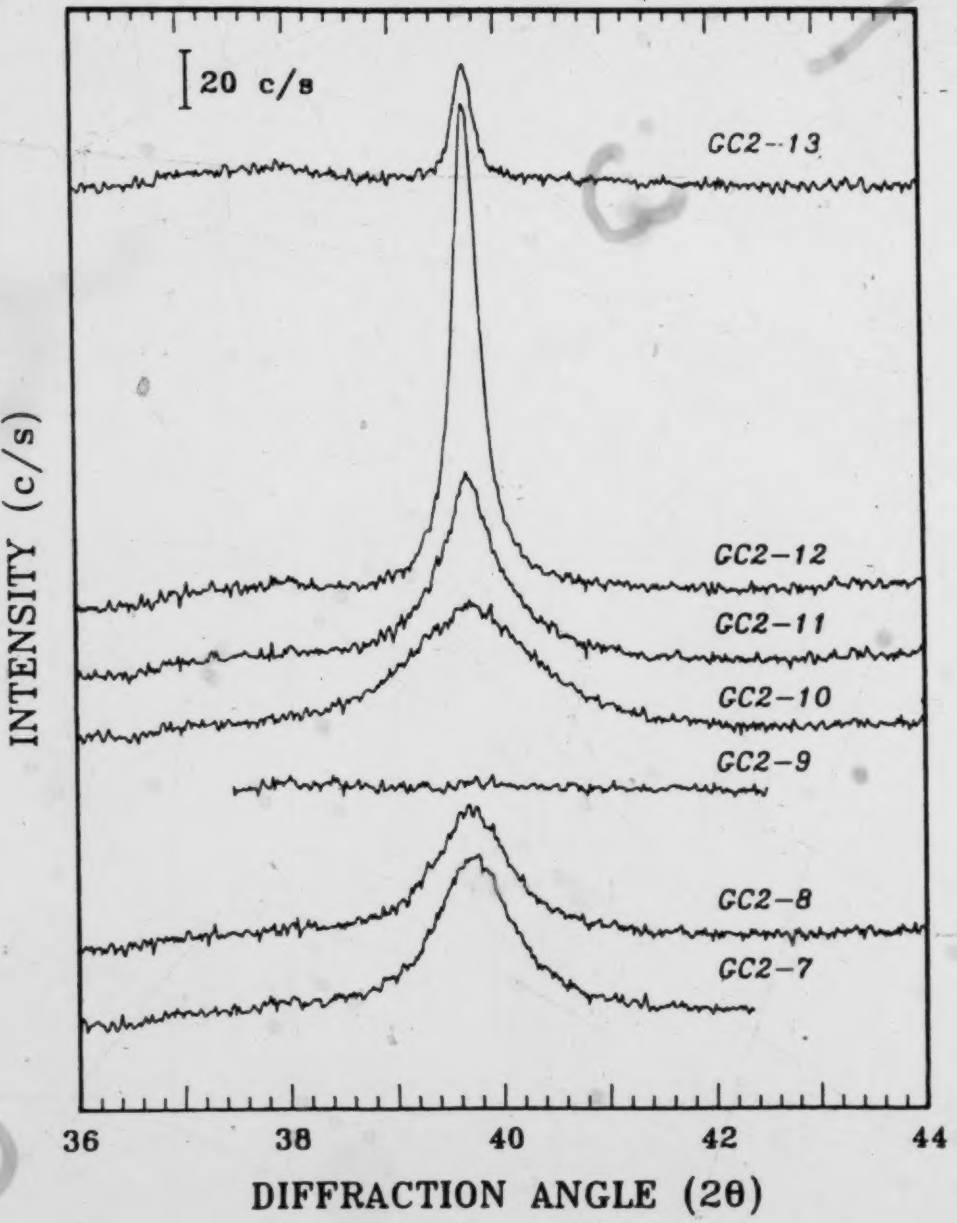

Figure 5.4 Subtracted XRD Patterns for Catalyst GC2

(See Table 4.3)

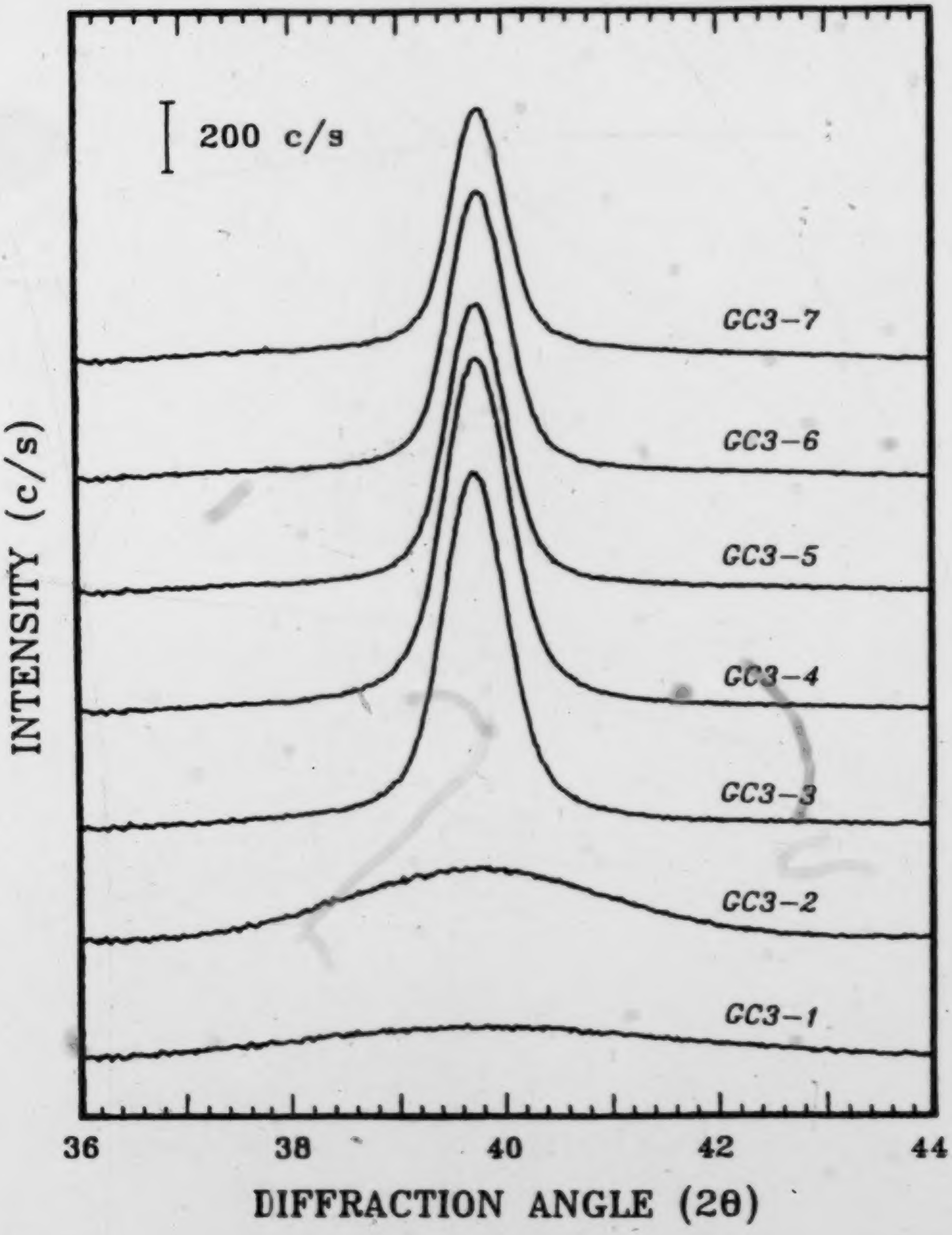

Figure 5.5 Subtracted XRD Patterns for Catalyst GC3

(See Table 4.4)

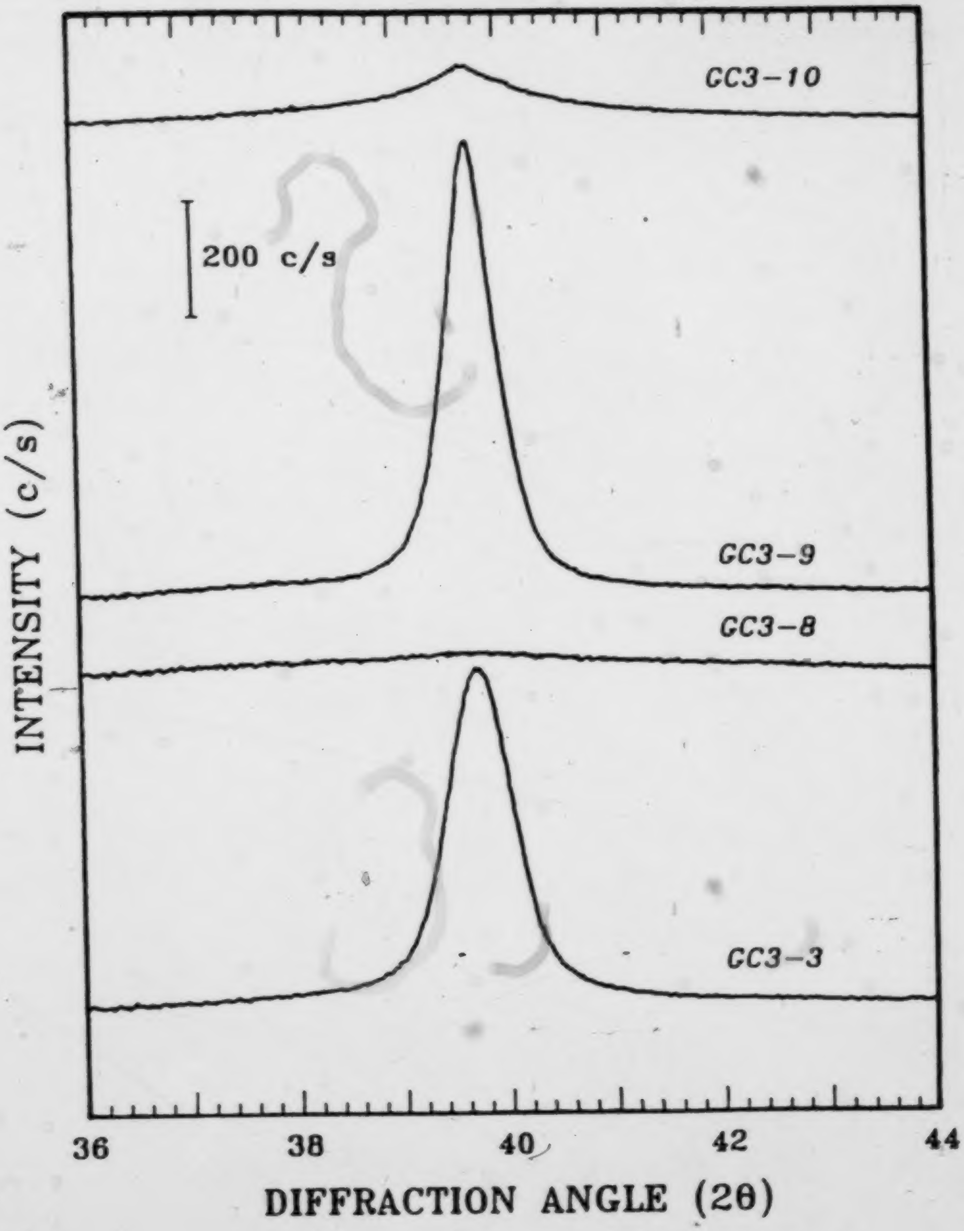

Figure 5.6 Subtracted XRD Patterns for Catalyst GC3

(See Table 4.4)

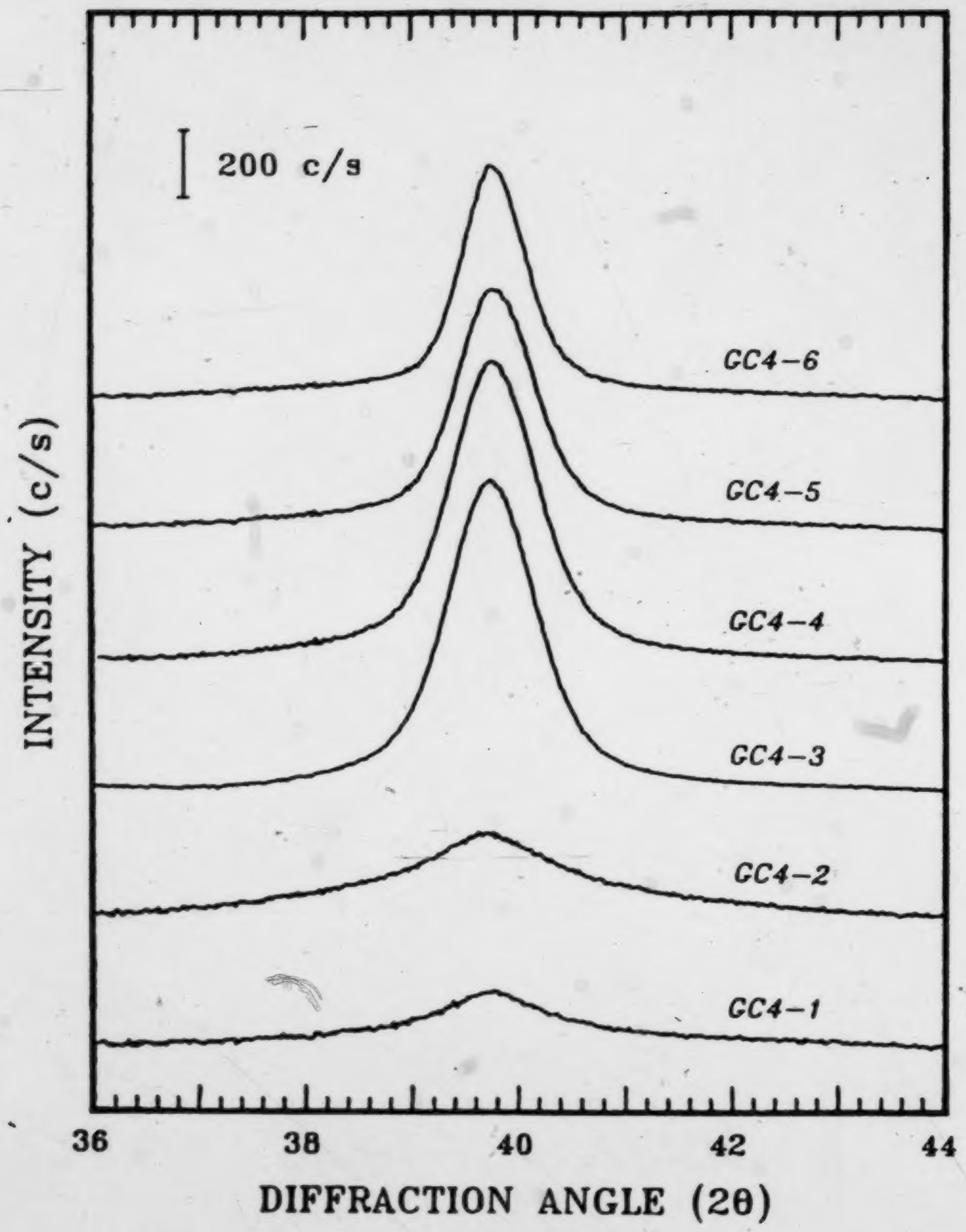

Figure 5.7 Subtracted XRD Patterns for Catalyst GC4

(See Table 4.5)

and much larger counting times would be required to obtain XRD patterns with sufficiently low noise for direct Fourier analysis. The usual method for the elimination of noise is to fit the XRD profile with an analytic function, i.e. smoothing of data (35).

Various functions have been proposed for fitting XRD line profiles, and these have been reviewed by Pick (2). In this work we use the modified Voigt function, recommended and used by Pick, for fitting the XRD line profiles. This modified Voigt function, a combination of the Gaussian and Cauchy distribution functions, is given by:

$$F_v = F_1(2\theta) + F_2(2\theta) \qquad [5.3]$$

where

$$F_1(2\theta) = \frac{B_1}{[1 + u \cdot B_2 \cdot (2\theta - B_3)^2]^{B_4}} \qquad [5.4]$$

$$F_2(2\theta) = B_5 \cdot \{\exp[-u \cdot B_6(2\theta - B_3)^2]\}^{B_7} \qquad [5.5]$$

The B_i's and u are adjustable parameters, B_3 is the value of 2θ at which the intensity is a maximum and u is a parameter to account for asymmetric profiles, i.e. $u = 1.0$ for $2\theta < B_3$ and $u = B_8$ for $2\theta > B_3$ (for symmetric profiles B_8 is equal to unity).

The behavior of the function F_v (Equation 5.3) is illustrated in Figure 5.8. The three shapes shown in Figure 5.8 correspond to the general line profiles observed for the Pt 111 line, i.e. sharp lines (solid line), broad lines

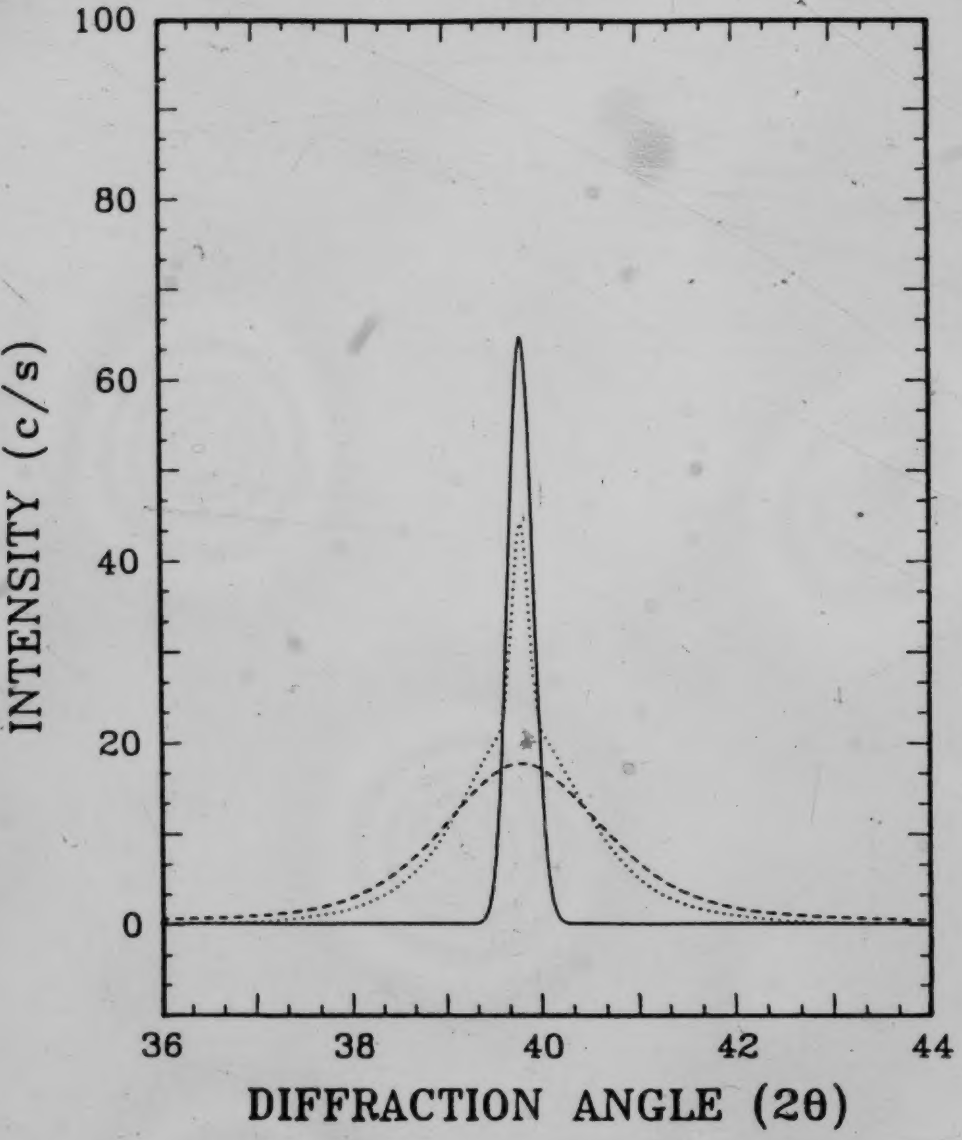

Figure 5.8 Typical Line Profiles for the Smoothing Function F_V

(dashed line) and a superimposed sharp and broad line (dotted line). Hence, the function F_v appears to have the general properties required for fitting (smoothing) the Pt 111 line profiles.

The degree of fit obtainable with F_v was tested for three Pt 111 lines with different shapes. The fit obtained is illustrated in Figure 5.9. The results in Figure 5.9 show that F_v is an excellent smoothing function for Pt 111 lines with different shapes. The eight adjustable parameters in F_v, i.e. B_1 to B_8, were estimated by non-linear regression using the BSOLVE algorithm (53). Details of the parameter estimation method and listing of programs for determining the parameters for fitting XRD lines have been presented by Pick (2).

All the Pt 111 lines shown in Figures 5.2 to 5.7 were fit to the function F_v; the parameters B_1 to B_8 for the various catalyst samples are given in Appendix B. The smoothed (fitted) values of intensity (F_v) as a function of 2θ were used in the subsequent Fourier analysis.

5.3 Correction for Instrumental Effects

As discussed in Chapter 3, Fourier analysis allows the separation of the various factors which contribute to the line broadening (see Equation 3.13). Discrete Fourier transforms, i.e. real and imaginary Fourier coefficients, were calculated from the smoothed Pt line profiles for each catalyst sample and for the standard sample. The smoothed

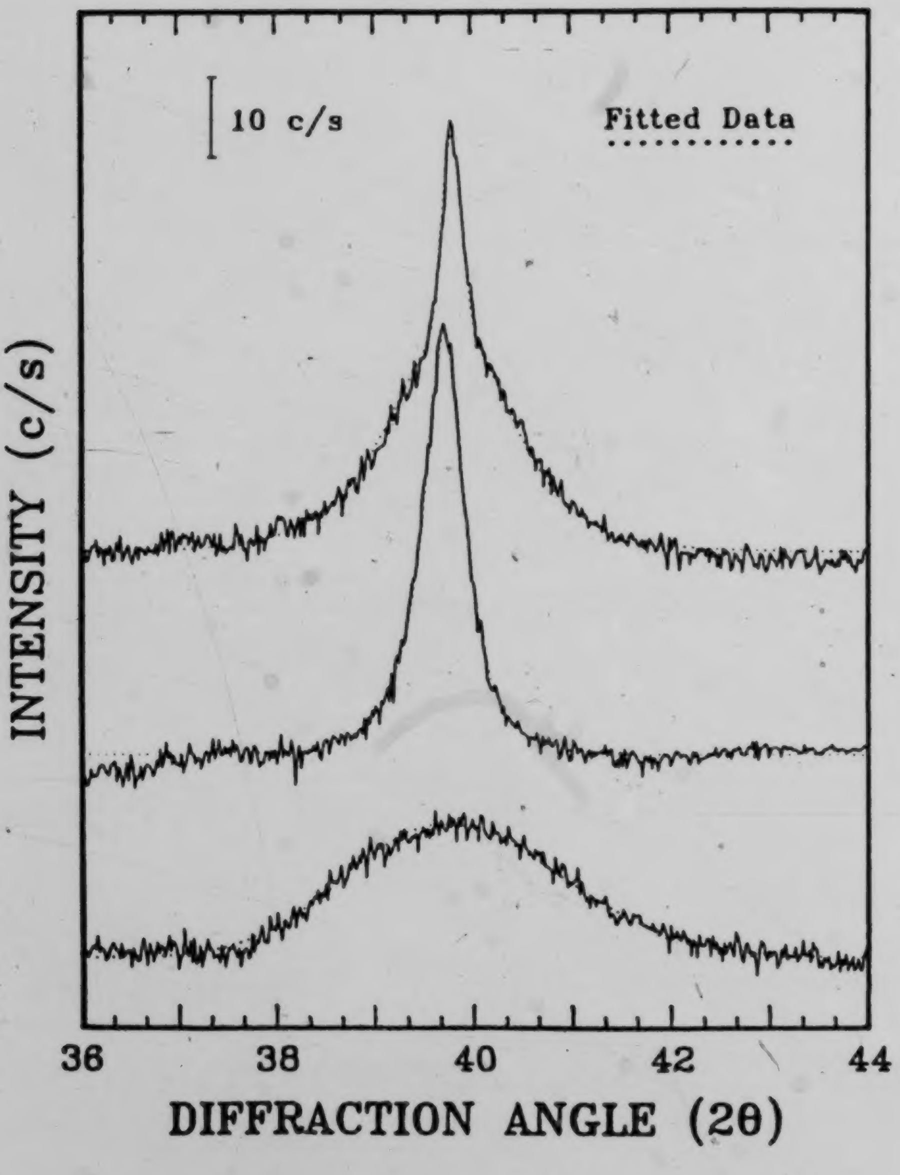

Figure 5.9 Illustration of Fitting Pt(111) Lines by the F_V Functions

profile for the samples becomes h(s) and the smoothed profile for the standard sample becomes g(s) (see Equation 3.11). The discrete Fourier coefficients for these profiles were calculated according to the following equations(34):

$$H_r(j) = \frac{1}{N} \sum_s h(s) \cdot \cos(2\pi sj/N) \qquad [5.6]$$

$$H_i(j) = \frac{1}{N} \sum_s h(s) \cdot \sin(2\pi sj/N) \qquad [5.7]$$

$H_r(j)$ and $H_i(j)$ are the real and imaginary values of the Fourier coefficients of h(s). The Fourier coefficient for g(s), i.e. $G_r(j)$ and $G_i(j)$ were calculated in a similar manner by replacing h(s) with g(s) in Equations 5.6 and 5.7. Values of j from 0 to 119, i.e. 120 Fourier coefficients, were used, and the functions h(s) and g(s) were divided into 240 equal increments, i.e. the summation was carried over 241 steps in s.

The values of $H_r(j)$, $H_i(j)$, $G_r(j)$ and $G_i(j)$ were used to calculate the Fourier coefficient for the 'pure' line profile f(s), i.e. the line profile from which instrumental broadening effects have been removed. The Fourier coefficients for f(s), according to Equation 3.13b, are given by:

$$F_r(j) = \frac{H_r(j) \cdot G_r(j) + H_i(j) \cdot G_i(j)}{G_r(j)^2 + G_i(j)^2} \qquad [5.8]$$

and

$$F_i(j) = \frac{H_i(j) \cdot G_r(j) - H_r(j) \cdot G_i(j)}{G_r(j)^2 + G_i(j)^2} \qquad [5.9]$$

The pure line profile, f(s), can be generated from $F_r(j)$ and $F_i(j)$ values; however, f(s) is not needed to obtain crystallite sizes since average crystallite sizes and size distributions can be calculated directly from $F_r(j)$ values (16,35,44).

The surface area weighted size distribution is given by:

$$P_a(D) = \frac{1}{C_a} \frac{d^2F_r(j)}{dj^2} \qquad [5.10]$$

where C_a is a normalizing constant which yields:

$$\int P_a(D)\, dD = 1.0 \qquad [5.11]$$

and D is a length defined as

$$D = j \cdot \lambda / [2(\sin\theta_{mx} - \sin\theta_{mn})] \qquad [5.12]$$

θ_{mx} and θ_{mn} are the maximum and minimum values of θ used in the Fourier analysis and λ is the wavelength of the x-rays. For θ_{mx} equal to 22° and θ_{mn} equal to 18°, the value of D/j is 1.145 nm. The surface area weighted average crystallite size for the size distribution $P_a(D)$ is given by:

$$\langle D_a \rangle = \frac{\Sigma\, D \cdot P_a(D)}{\Sigma\, P_a(D)} \qquad [5.13]$$

The summation is carried out over all values of j; used to calculate $P_a(D)$. For values of j greater than 40, i.e. for D ≥45 nm, the values of $P_a(D)$ approach zero; hence, only the first 40 or fewer Fourier coefficients were needed for the current analyses.

The second derivatives, required for evaluation of $P_s(D)$, (Equation 5.10), were calculated by the following difference formula:

$$\frac{d^2F_r(j)}{d^2j} = [F_r(j-2)-F_r(j-1)-F_r(j)+F_r(j+1)]/2 \qquad [5.14]$$

The average size, $\langle D_s \rangle$, given by Equation 5.13 is similar to the average size D_s given by Equation 2.2. Volume weighted crystallite size distribution can also be calculated from the Fourier coefficients, i.e.:

$$P_v(D) = \frac{j}{C_v}\,\frac{d^2F_r(j)}{dj^2} \qquad [5.15]$$

where C_v is a normalizing constant which yields:

$$\int P_v(D)\ dD = 1.0 \qquad [5.16]$$

The corresponding volume weighted crystallite size, similar to D_v defined by Equation 2.3, is:

$$\langle D_v \rangle = \frac{\Sigma\, D \cdot P_v(D)}{\Sigma\, P_v(D)} \qquad [5.17]$$

All the calculations required to obtain the crystallite size distribution and average crystallite sizes, from the smoothed F_v function were done using the computer program YXPRO and the associated subroutines. The calculations and corresponding computer programs are lengthy and involved, and it is not possible to ensure that all the programs are error free. Hence, the empirical method of testing the programs was used.

5.4 Testing of Programs

Testing of the computer program YXPRO was done by generating a pure diffraction profiles for the Pt 111 line for cases with different Pt size distributions, and using these generated pure profiles as the input profiles for YXPRO. If YXPRO accurately reproduces the essential features of the various Pt size distributions used to generate the pure profiles, then the Pt size distributions obtained with YXPRO for pure profiles with unknown size distributions have a high degree of reliability.

Pure diffraction lines, i.e. intensity as a function of s, were generated according to Equation 5.18 derived by Delhez et al. (47), namely:

$$I(s) = \sum_{i=1}^{M} \frac{V_i}{D_i} \frac{\sin^2(\pi D_i s/d)}{\sin^2(\pi s)} \qquad [5.18]$$

where $s = (2d \cdot \sin\theta/\lambda) - 1$

d = distance between Pt (111) planes = 0.2265 nm

M = number of discrete crystallite sizes in distribution

D_i = size of crystallites

V_i = mass fraction of crystallites with size D_i

Pure profiles were generated for the following cases: one, all particles in sample of same size, i.e. $M = 1.0$; two, various particles sizes ($M = 2$ to 7) and each size having the same mass fraction, i.e. $V_i = 1/M$; and three, distributions containing particles of two sizes with varying values of V_i. The program XPURE was used for the calculations.

The results for Case 1, for particle sizes from 1 to 50 nm, are summarized in Table 5.2. Also included in Table 5.2 for comparison are values of $\langle D \rangle_i$ and $\langle D \rangle_{1/2}$ calculated from the Scherrer equation (Equation 3.2). All the sizes calculated by the various methods are very close to the size used to generated the pure profile. The errors in the average size calculated from YXPRO, i.e. $\langle D_a \rangle$ and $\langle D_v \rangle$, were less than 3% with the exception of the 1.0 nm case. The Scherrer equation also yielded accurate crystallite sizes for unisized crystallites.

The results for Case 2 are shown in Figure 5.10. All the distributions used to generate the pure profiles had a volume average crystallite size $\langle D_v \rangle$, of 20 nm. The values of $\langle D_v \rangle$ obtained from the Fourier analysis, using YXPRO, were very close to 20 nm (see Figure 5.10). The input sizes were at discrete values of D_i, e.g. 5, 10, 20 nm, but the calculated size distributions were spread around these input values. This is expected since the calculation of crystallite sizes required numerical differentiation (see Equation 5.10 and 5.15). The maxima in the calculated size distributions correspond very well to the input sizes. The areas under the different peaks in each calculated size distributions are about equal. This is in agreement with the input size distribution since V_i was the same for all the D_i's in a given distribution.

Table 5.2 Comparison of input and calculated <D> values

Runs	Input (nm)	$D_{1/2}$[1] (nm)	D_i[2] (nm)	$\langle D_a \rangle$[3] (nm)	$\langle D_v \rangle$[4] (nm)	Error[5] (%)
GENE1	1.00	0.99	1.02	1.07	1.12	12.0
GENE3	3.00	3.34	3.25	3.05	3.07	2.3[illegible]
GENE5	5.00	5.18	5.18	5.12	5.17	3.40
GENE10	10.00	10.14	10.17	10.07	10.17	1.17
GENE20	20.00	20.33	20.25	20.17	20.31	1.55
GENE30	30.00	30.34	30.32	30.24	30.28	0.93
GENE50	50.00	50.78	50.67	50.15	50.24	0.44

[1] $D_{1/2}$ represents crystallite size based on half width, Equation 3.2

[2] D_i represents crystallite size based on integral width, Equation 3.2

[3] D_a is the Fourier area weighted crystallite size based on Equation 5.13

[4] D_v is the Fourier volume weighted crystallite size based on Equation 5.17

[5] Error is calculated by $[(\langle D \rangle_v - \text{Input})/\text{Input}] * 100\%$

Variations in V_i were examined in the final case. Two distributions, each containing only 10 and 30 nm (D_1 = 10 nm and D_2 = 30 nm) crystallites, were used to generate pure profiles. The first profile was generated with $V_1 = 0.75$ and $V_2 = 0.25$, and the second profile was generated with V_1

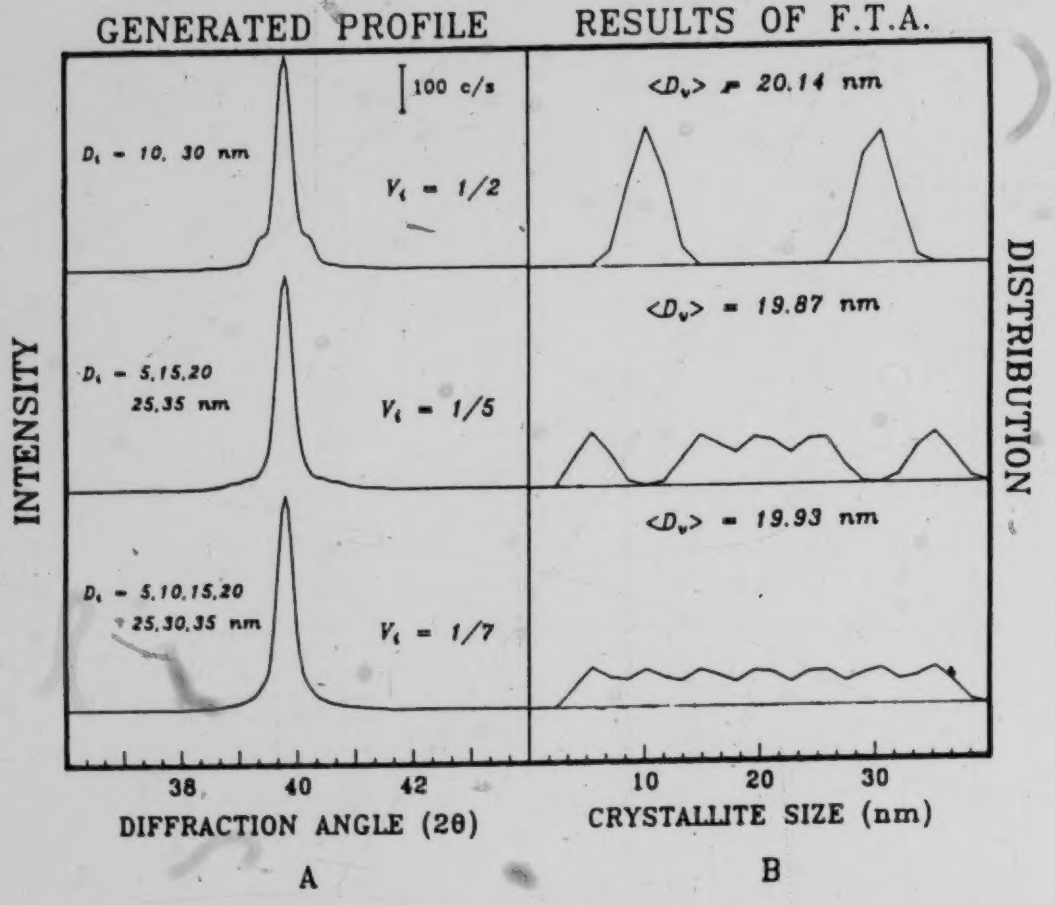

Figure 5.10 Results of Fourier Transform Analysis (F.T.A.) for Generated Pure Diffraction Profiles

= 0.25 and V_2 = 0.75. The $<D_v>$ values for these two distributions are 15 and 25 nm, respectively. The generated profiles and the results of the Fourier analysis for these two distributions are shown in Figure 5.11. The results in this figure show that not only are the average sizes regenerated accurately but the relative abundance of each crystallite size is also reproduced accurately.

The above testing of the YXPRO program demonstrated that accurate average Pt crystallite sizes and reliable crystallite size distribution are obtained from pure diffraction profiles by the previously described methods and computational procedures employed in the computer programs. It is now necessary to demonstrate that the broadening of the pure diffraction profiles obtained from the measured XRD patterns for supported metal catalysts is mainly due to size broadening.

5.5 Test for Strain Broadening

In chapter 3 the method for separating size and strain broadening were described and Equation 3.5 and 3.6 can be used to determine whether strain broadening is significant. However, several diffraction lines for the same sample are required to use Equation 3.5 and 3.6. Hence, diffraction patterns for two catalyst samples, [1 wt% Pt and 5 wt% Pt (Catalyst GC3) after treatment in O_2 at 700°C] were measured from 30 to 90 °2θ. All five Pt lines, [111, 200, 220, 311 and 222], were readily detected in both samples (see Figure

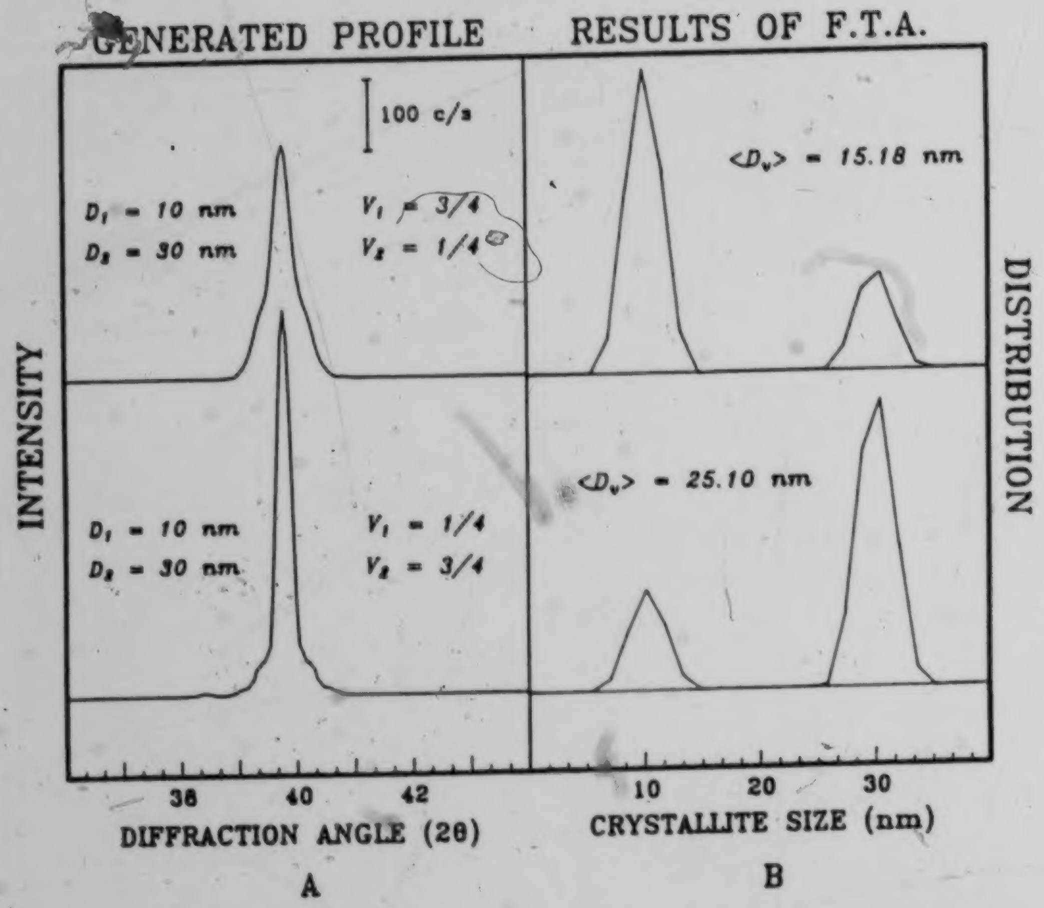

Figure 5.11 Results of Fourier Transform Analysis (F.T.A.) for Generated Profiles with Different Values of V_1

5.1 for 1% Pt catalyst). The 1 wt% catalyst was similar to Catalyst GC2 (i.e. 1 wt% Pt on Support GS2), but a fresh preparation had to be used since fresh samples of GC1 and GC2 were no longer available. The breadth of each of the five lines was determined for Cauchy and Gaussian line profiles. The values of B are plotted as a function of θ according to Equation 3.5 and 3.6. In the absence of strain broadening, the lines should have zero slope. The plots in Figures 5.12 and 5.13 do not have zero slopes, but the deviations from zero are small. The deviations from zero slope are within the experimental error of determining B. Hence, it is concluded that strain broadening was not significant for the catalysts examined in this work, and strain broadening was neglected in all the crystallite size analysis presented in Chapter 6. Sashital et al. (34) also concluded from x-ray studies that strain broadening was not significant for Pt/SiO$_2$ catalysts.

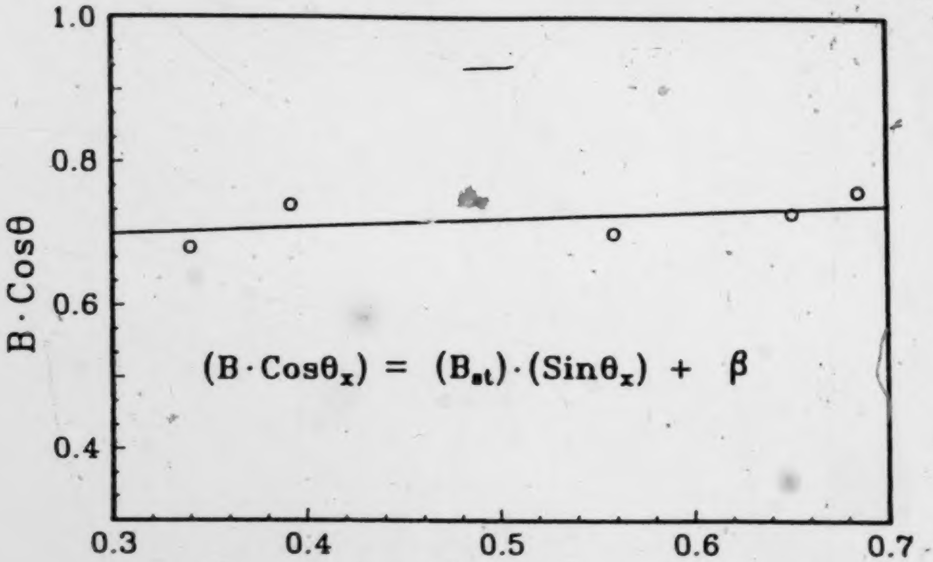

A) Cauchy Form

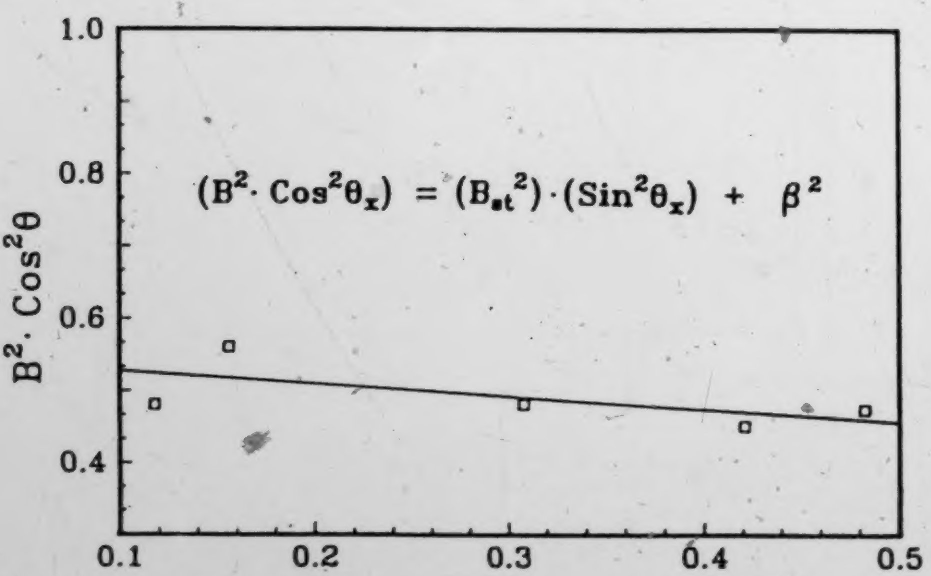

B) Gaussian Form

Figure 5.12 Strain Analysis of 1% Pt Catalyst

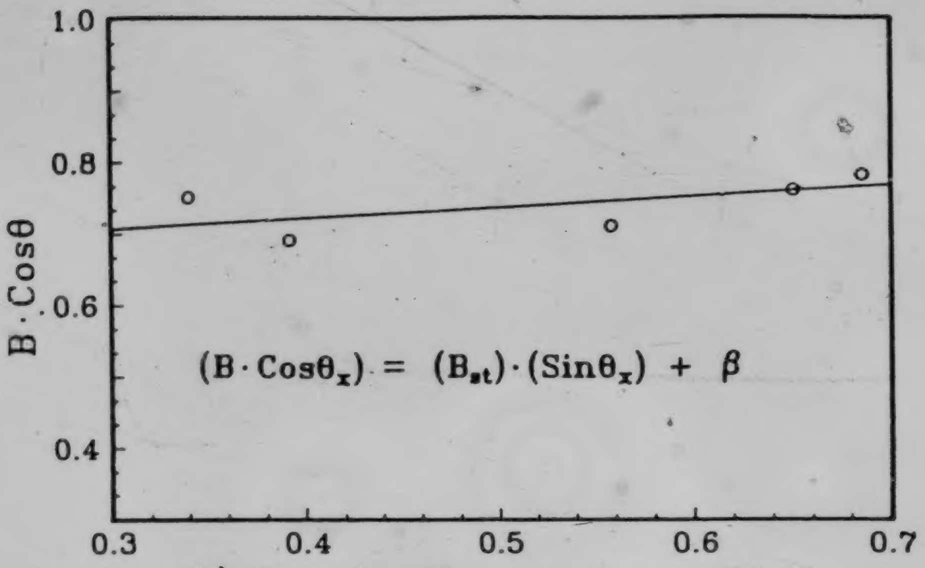

A) Cauchy Form

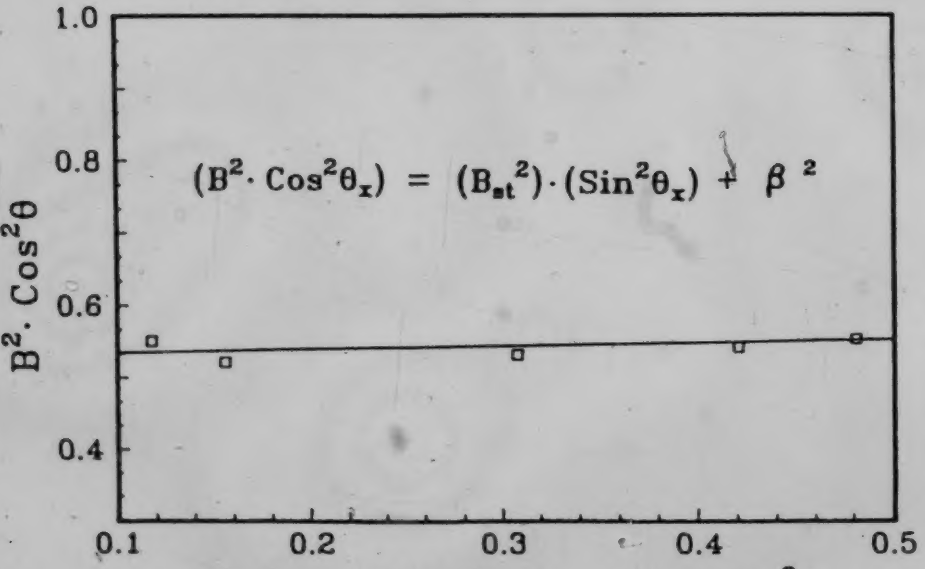

B) Gaussian Form

Figure 5.13 Strain Analysis of 5% Pt Catalyst

6. RESULTS AND DISCUSSION

6.1 Introduction

One of the main objectives of this work was to demonstrate that XRD can be used to obtain Pt crystallite size information for Pt on a support (γ-Al_2O_3) which causes significant interference with the Pt diffraction lines. It has been demonstrated in the previous chapter that pure Pt 111 lines can be obtained by appropriate subtraction and subsequent smoothing of the line profiles. Another objective was the determination of changes in Pt crystallite sizes as a function of various thermal treatments.

In this chapter the calculated Pt crystallite sizes and size distributions for the various catalyst samples described in Tables 4.2 to 4.5 are presented and discussed. X-ray diffraction results are also compared with hydrogen chemisorption results.

6.2 Average Pt Crystallite Sizes

In Chapter 3 the determination of average crystallite sizes by the Scherrer equation (Equation 3.2) was described. In Tables 6.1 to 6.4, the Pt crystallite sizes based on the width at half-height, $<D_{1/2}>$, and the integral width, $<D_i>$, are tabulated for all the catalyst samples examined. Values of K in Equation 3.2 equal to 0.90 and 1.0 were used to calculate $<D_{1/2}>$ and $<D_i>$, respectively. The area average

Table 6.1 Average crystallite sizes for Catalyst GC1 (1.05 wt% $Pt/\gamma\text{-}Al_2O_3$)

Runs	$\langle D_{1/2} \rangle$ (nm)	$\langle D_i \rangle$ (nm)	<Da> (nm)	<Dv> (nm)	Dv/Da	Fraction Pt Detected
GC1-1	13.8	10.0	7.3	10.0	1.37	0.21
GC1-2	15.8	10.5	7.8	11.4	1.46	0.42
GC1-3	16.5	11.7	9.4	12.5	1.34	0.59
GC1-4	17.7	13.9	10.1	13.5	1.33	0.40
GC1-5	17.7	14.4	10.6	13.6	1.29	0.48
GC1-6	17.0	12.6	8.3	12.2	1.47	0.69
GC1-7	17.3	14.4	8.8	12.5	1.42	0.75
GC1-8	16.9	13.7	9.1	12.4	1.37	0.72
GC1-9	20.3	15.9	10.8	14.4	1.33	0.46
GC1-10	20.8	17.5	11.6	14.8	1.28	0.26

Table 6.2 Average crystallite sizes for Catalyst GC2 (1.12 wt% Pt/γ-Al_2O_3)

Runs	$\langle D_{1/2} \rangle$ (nm)	$\langle D_i \rangle$ (nm)	<Da> (nm)	<Dv> (nm)	Dv/Da	Fraction Pt Detected
GC2-1	1.5	1.9	≃2.0	≃2.0	--	0.15
GC2-2	3.3	3.4	5.0	5.4	1.08	0.90
GC2-3	3.1	3.2	4.9	5.0	1.02	0.69
GC2-4	2.3	2.4	4.4	4.7	1.08	0.26
GC2-5	3.7	3.8	4.5	4.6	1.02	0.15
GC2-6	7.9	6.6	6.3	7.6	1.20	1.00
GC2-7	10.9	9.5	7.9	9.0	1.15	0.68
GC2-8	10.3	8.0	6.0	7.9	1.32	0.68
GC2-9	<2.0	<2.0	<2.0	<2.0	--	0.00
GC2-10	6.1	5.4	6.3	6.9	1.09	1.00
GC2-11	14.9	10.1	8.1	10.3	1.28	0.80
GC2-12	22.1	23.9	13.0	20.3	1.56	1.00
GC2-13	29.6	31.6	11.8	24.2	2.04	0.20

Table 6.3 Average crystallite sizes for Catalyst GC3 (5.06 wt% $Pt/\gamma-Al_2O_3$)

Runs	$<D_{1/2}>$ (nm)	$<D_i>$ (nm)	<Da> (nm)	<Dv> (nm)	Dv/Da	Fraction Pt Detected
GC3-1	2.9	3.4	4.4	4.8	1.08	0.37
GC3-2	2.9	2.9	5.0	5.4	1.08	0.63
GC3-3	9.5	9.8	9.1	10.4	1.14	0.93
GC3-4	11.5	10.1	8.8	10.1	1.15	0.89
GC3-5	12.8	10.6	9.4	11.0	1.17	0.46
GC3-6	13.0	11.3	9.8	11.3	1.16	0.64
GC3-7	13.8	11.0	9.7	11.7	1.20	0.59
GC3-8	2.3	2.5	4.7	5.3	1.13	0.19
GC3-9	16.0	12.7	10.0	12.6	1.26	1.00
GC3-10	6.3	4.6	5.8	7.0	1.21	0.32

Table 6.4 Average crystallite sizes for Catalyst GC4 (5.06 wt% $Pt/\gamma-Al_2O_3$)

Runs	$<D_{1/2}>$ (nm)	$<D_i>$ (nm)	<Da> (nm)	<Dv> (nm)	Dv/Da	Fraction Pt Detected
GC4-1	5.7	4.0	5.8	6.6	1.14	0.32
GC4-2	4.7	3.8	5.4	6.8	1.26	0.50
GC4-3	8.5	7.7	7.4	8.1	1.10	0.92
GC4-4	8.8	7.8	7.5	8.2	1.10	0.87
GC4-5	9.6	7.9	7.8	8.8	1.12	0.70
GC4-6	11.9	9.1	8.7	10.2	1.18	0.59

sizes, $\langle D_a \rangle$, and the volume average sizes, $\langle D_v \rangle$, obtained by Fourier analysis are also tabulated in these tables (see Equations 5.13 and 5.17).

The $\langle D_i \rangle$ values from the Scherrer equation are volume weighted average crystallite sizes (16); hence, the values of $\langle D_i \rangle$ and $\langle D_v \rangle$ should be approximately equal. Examination of the results in Tables 6.1 to 6.4 shows that the $\langle D_i \rangle$ and $\langle D_v \rangle$ values are about the same for average Pt crystallite sizes larger than about 8 nm. For these large average Pt sizes the $\langle D_i \rangle$ values tend to be slightly higher than the $\langle D_v \rangle$ values. However, for small average Pt sizes the $\langle D_i \rangle$ values are usually considerably lower than the $\langle D_v \rangle$ values. There are two main reasons for the differences among $\langle D_i \rangle$ and $\langle D_v \rangle$: one, the numerical differentiation of the Fourier coefficients introduces errors in $P_v(D)$ and hence, $\langle D_v \rangle$; and two, the Fourier analysis does not include Pt crystallite smaller than about 2.0 nm in diameter, but the $\langle D_i \rangle$ includes some of the smaller Pt crystallite. The first reason accounts for the differences among $\langle D_i \rangle$ and $\langle D_v \rangle$ for average sizes ≥8 nm, while the second reason is the cause for the disagreement at the small average Pt sizes.

The ratios of $\langle D_v \rangle$ to $\langle D_a \rangle$ reported in the tables are an indication of the breadth of the size distribution. A D_v/D_a ratio equal to unity means that all Pt crystallites detected have the same size. The larger the value of D_v/D_a, the broader the Pt crystallite size distribution. The shapes of the Pt crystallite size distributions will be discussed in Section 6.4.

The fractions of Pt detected in the Pt 111 lines are tabulated in the final columns of Tables 6.1 to 6.4. All the Pt in a sample scatters x-rays, but not all the scattered x-rays contribute to intensity of the diffraction lines. For example, small Pt clusters containing a few atoms (e.g. <10 atoms) do not have well developed crystalline planes and the scattered x-rays from these Pt atoms are equally distributed over all angles, i.e. these nonpreferentially scattered x-rays contribute to the background intensity and not the intensity of the diffraction lines.

The fraction of Pt which contributes to the intensity of the Pt 111 line is given by:

$$X = A_i / A_{MAX} \qquad [6.1]$$

A_i = the area under the Pt 111 line for a catalyst sample i

A_{MAX} = the area under the Pt 111 line for a catalyst of the same composition as sample i but in which all the Pt is detected by XRD

The values of A_i were obtained for each sample by integrating the fitted function $F_v(2\theta)$ (Equation 5.3) over a range of 8 °2θ, 4° on each side of the 2θ value at which the maximum intensity occurred. The values of A_{MAX} for each of the four catalysts was taken as the values of A_i for a heavily sintered sample of each catalyst. The values of A_{MAX} were 63.2, 63.7, 317.0, (c/s)·(°2θ) for catalysts GC1, GC2 and GC3, respectively. The value of A_{MAX} for catalysts GC4 was the same as that for catalyst GC3, since these two catalysts had the same Pt content and the same support.

The Fourier method of analysis used in the present work detects Pt crystallites down to about 2 nm in size. Hence, the fraction of Pt detected in the Pt what is present in Pt crystallites ≥2.0 nm. The fraction of Pt detected has to be known in order to compare XRD results with chemisorption results.

6.3 Comparison of XRD and Chemisorption Results

The Pt dispersion is obtained from chemisorption measurements (see section 2.3.1). The easiest way to compare XRD results with chemisorption results reported in Tables 4.2 to 4.5 is to convert the size information obtained by XRD into Pt dispersions. The relationship between Pt dispersion, Φ, and area average crystallite size is:

$$\Phi = 1.07/\langle D_a \rangle \qquad [6.2]$$

with $\langle D_a \rangle$ in nm.

Equation 6.2 is based on spherical Pt particles (or hemispherical Pt particles with the flat face in contact with the support surface) and an area of 0.084 nm² per surface Pt atom. The area of 0.084 nm^2 per surface Pt atom is the average area per Pt atom for Pt atoms located in the three low index planes, i.e. the Pt (111), (100) and (110) surfaces have areas per Pt atom of 0.0666, 0.0770 and 0.1088 nm^2, respectively. Equation 6.2 is valid for Pt particles ≥2.0 nm, since at smaller sizes the geometric considerations, e.g. spherical particles, become invalid. Hence, Equation 6.2 can be used to calculate the dispersion of the XRD detected Pt.

The Pt not detected by XRD is present in Pt crystallites smaller than 2 nm and this undetected Pt has a dispersion between 0.5 and 1.0. Hence, a range of Pt dispersions can be calculated from the XRD results. The lower limit of this range is obtained by assuming that the XRD undetected Pt has a dispersion of 0.5, i.e.:

$$\Phi_{low} = 0.5 - X[0.5 - 1.07/\langle D_a \rangle] \qquad [6.3]$$

The upper limit of the dispersion from the XRD results is calculated by assuming the XRD undetected Pt has a dispersion of 1.0, i.e.:

$$\Phi_{high} = 1.0 - X[1.0 - 1.07/\langle D_a \rangle] \qquad [6.4]$$

The results of hydrogen chemisorption and XRD are compared in Tables 6.5 to 6.8.

Table 6.5 Comparison of hydrogen chemisorption and XRD results for Catalyst GC1

Run	Hydrogen Uptakes (H/Pt)	Range of Pt Dispersions from XRD	Calculated Dispersion of Undetected Pt
GC1-1	0.44	0.43 - 0.82	0.52
GC1-2	0.42	0.35 - 0.64	0.62
GC1-3	0.53	0.27 - 0.48	1.13
GC1-4	0.47	0.34 - 0.64	0.71
GC1-5	0.55	0.31 - 0.57	0.96
GC1-6	0.41	0.24 - 0.40	1.03
GC1-7	0.35	0.22 - 0.34	1.04
GC1-8	0.25	0.23 - 0.37	0.59
GC1-9	0.58	0.32 - 0.59	0.99
GC1-10	0.82	0.39 - 0.76	1.08

Table 6.6 Comparison of hydrogen chemisorption and XRD results for Catalyst GC2

Run	Hydrogen Uptakes (H/Pt)	Range of Pt Dispersions from XRD	Calculated Dispersion of Undetected Pt
GC2-1	0.86	0.51 - 0.93	0.92
GC2-2	0.08	0.24 - 0.29	-1.13
GC2-3	0.41	0.30 - 0.46	0.84
GC2-4	0.76	0.43 - 0.80	0.94
GC2-5	0.74	0.46 - 0.89	0.83
GC2-6	0.19	0.17 - 0.17	--
GC2-7	0.20	0.25 - 0.41	0.34
GC2-8	n.m.	0.28 - 0.44	--
GC2-9	0.94	0.50 - 1.00	0.94
GC2-10	0.23	0.17 - 0.17	--
GC2-11	0.19	0.21 - 0.31	0.42
GC2-12	0.04	0.08 - 0.08	--
GC2-13	0.61	0.42 - 0.82	0.74

n.m. = not measured

Table 6.7 Comparison of hydrogen chemisorption and XRD results for Catalyst GC3

Run	Hydrogen Uptakes (H/Pt)	Range of Pt Dispersions from XRD	Calculated Dispersion of Undetected Pt
GC3-1	n.m.	0.40 - 0.72	--
GC3-2	0.49	0.32 - 0.51	0.96
GC3-3	0.15	0.14 - 0.18	0.58
GC3-4	0.18	0.16 - 0.22	0.65
GC3-5	0.37	0.23 - 0.38	0.97
GC3-6	0.40	0.25 - 0.43	0.92
GC3-7	0.52	0.27 - 0.48	1.11
GC3-8	0.94	0.45 - 0.85	1.11
GC3-9	0.11	0.11 - 0.11	--
GC3-10	0.95	0.40 - 0.74	1.31

Table 6.8 Comparison of hydrogen chemisorption and XRD results for Catalyst GC4

Run	Hydrogen Uptakes (H/Pt)	Range of Pt Dispersions from XRD	Calculated Dispersion of Undetected Pt
GC4-1	n.m.	0.40 - 0.74	--
GC4-2	0.53	0.35 - 0.60	0.86
GC4-3	0.17	0.17 - 0.21	0.46
GC4-4	0.22	0.19 - 0.25	0.73
GC4-5	0.42	0.25 - 0.40	1.08
GC4-6	0.54	0.28 - 0.48	1.14

n.m. = not measured

All the Pt was detected by XRD for four of the runs listed in Tables 6.5 to 6.8, (i.e. runs GC2-6, GC2-10, GC2-12 and GC3-9). For these four runs the values of Φ_{low} and Φ_{high} are the same since X=1.0. Comparison of the H/Pt ratio with the values of dispersion obtained by XRD shows that the maximum difference between the dispersions based on hydrogen chemisorption and XRD is 0.06. This maximum difference is well within the accuracy of the measurements. The reproducibility of H/Pt ratios is about ±0.03. The accuracy of the average Pt crystallite size is probably no better than ±10%, and the reliability of the fraction of Pt detected is ±0.05 at best. Hence, the agreement of XRD and chemisorption results for cases in which all Pt is detected by XRD is excellent. Comparison of the results for which not all the Pt was detected by XRD and for which H/Pt ratios were measured (32 runs), shows that the H/Pt ratio for 20 of the 32 runs fall within the ranges of dispersion calculated from XRD measurements. If one considers the above-mentioned errors in H/Pt, X and $<D_a>$, then agreement among XRD and chemisorption is obtained for all runs except Runs GC2-2, GC3-8 and GC3-10. The reason for the lack of agreement for Run GC2-2 (after treatment in the He at 800°C) is not known, but low H/Pt ratios have occasionally been observed after treatment in He at high temperatures (54). The H/Pt ratios for Runs GC3-8 and GC3-10 are probably too high since over four hydrogen pulses were adsorbed during the hydrogen uptake measurements. The dynamic pulses method overestimates the hydrogen uptake if several pulses of hydrogen are required to saturate the sample because desorption of hydrogen occurs between additions of pulses (21).

Another method of comparing the chemisorption and XRD results is to calculate the dispersion of the undetected Pt which is required to obtained on overall dispersion equal to the H/Pt ratio. The calculated dispersion of XRD undetected Pt, Φ_{undet}, is given by:

$$\Phi_{undet} = [(H/Pt) - 1.07\ X/\langle D_a \rangle]/[1 - X] \qquad [6.5]$$

The values of Φ_{undet} are listed in the last columns of Tables 6.5 to 6.8. Values of Φ_{undet} between about 0.3 and 1.2 are within the accuracy of the methods. The values of Φ_{undet} of Run GC2-2, and to a lesser degree for Run GC3-10, are the only values which show a significant disagreement between chemisorption and XRD results.

The Pt dispersions calculated from XRD results were based on $\langle D_a \rangle$, and $\langle D_a \rangle$ was obtained from the Pt crystallite size distribution. The good agreement obtained between XRD and chemisorption indicates that the Pt crystallite size distributions presented in the next section are reasonably accurate.

6.4 Pt Crystallite Size Distributions

The Pt crystallite size distributions, obtained by the Fourier method described in Chapter 5, are presented and discussed in this section. The crystallite size distributions for the series of treatments done on Catalysts GC1 are shown in Figure 6.1. The distributions shown in the figures are surface area weighted size distributions, i.e. $P_a(D)$ given by Equation 5.10. However, the distribution functions have been normalized so that the area under the curves is equal to the fraction of Pt detected by XRD, i.e.:

$$\Sigma P_a(D) \; dD = X \qquad [6.6]$$

Examination of the crystallite size distributions in Figure 6.1 leads to the following observations for the sequential treatments of Catalyst GC1 (see Table 4.2 for description of treatments):

1. Treatment at 510°C in an atmosphere containing CCl_4 resulted in an increase in the amount of Pt detected without significantly altering the Pt crystallite size distribution (cf. GC1-1 and GC1-2)
2. Treatment of GC1-2 in O_2 at 550°C further increased the fraction of Pt detected and changed the crystallite size distribution, i.e. Pt crystallites <5.0 nm essentially disappeared from the distribution (cf. GC1-2 and GC1-3).
3. Treatment of GC1-3 at 510°C in an atmosphere containing

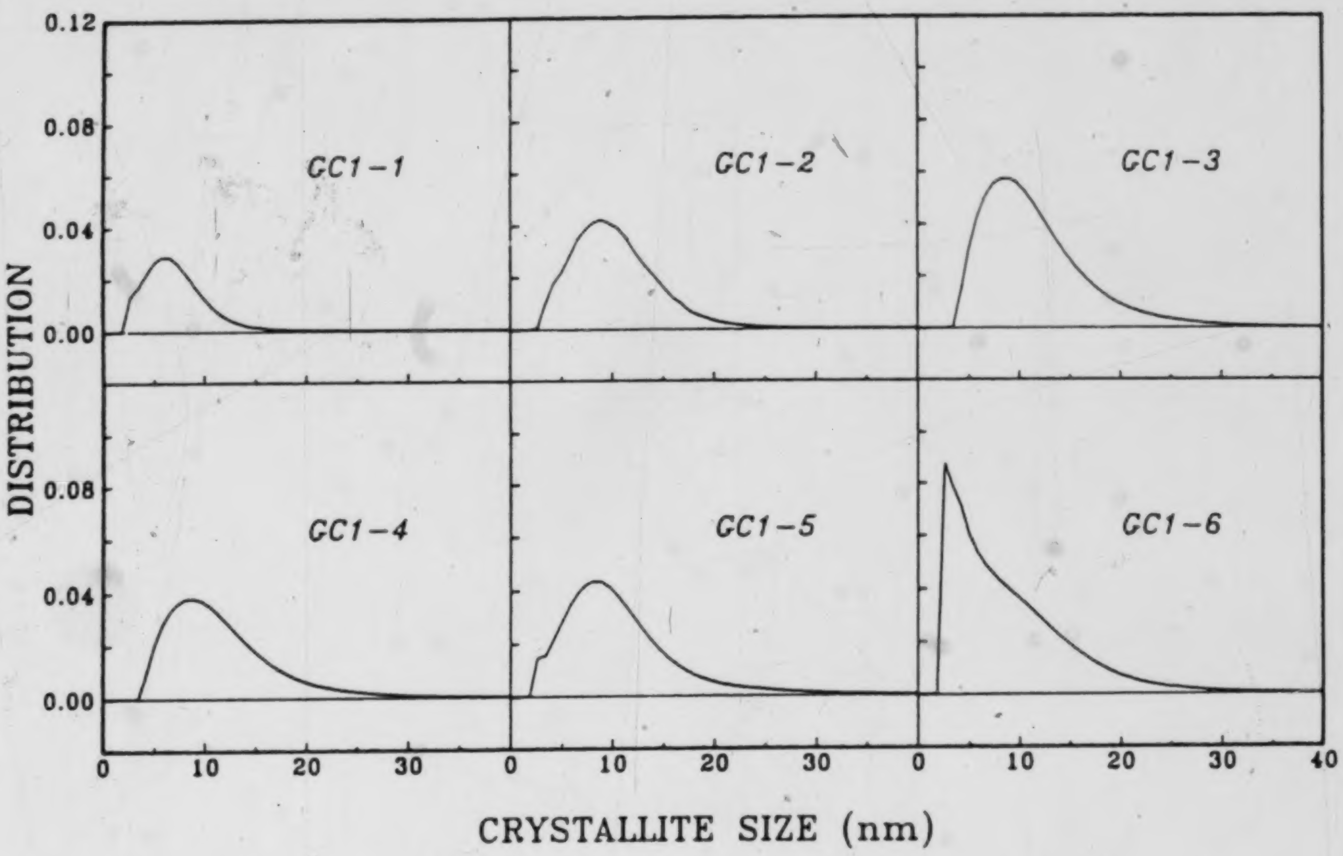

Figure 6.1 Crystallite Size Distribution for Catalyst GC1

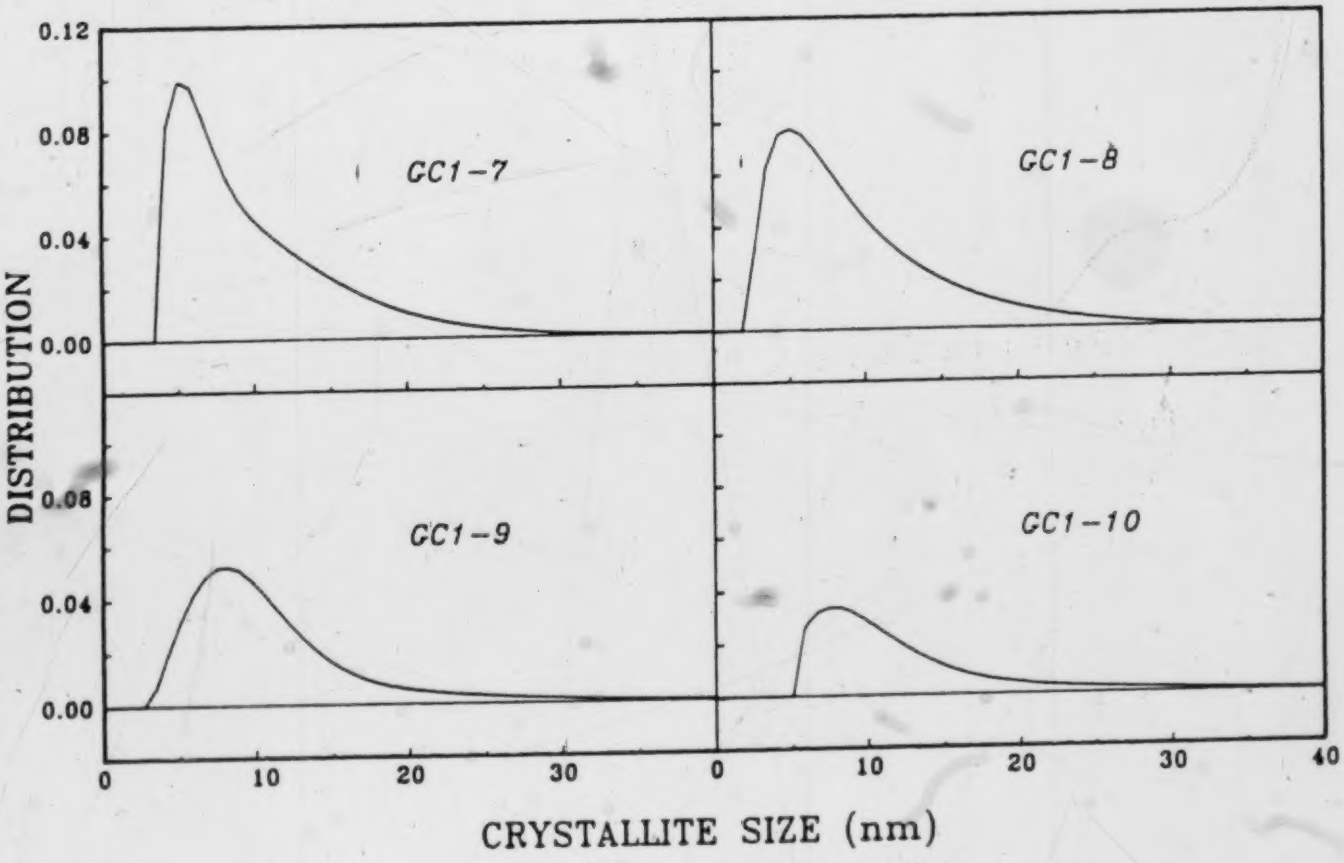

Figure 6.1 Crystallite Size Distribution for Catalyst GC1
(Continued)

C_2HCl_3 decreased the fraction of Pt detected but did not greatly alter the shape of the distribution (cf. GC1-3 and GC1-4).

4. Treatment of GC1-4 in O_2 at 550°C resulted in the formation of small, but XRD detected crystallites (cf. GC1-4 and GC1-5).
5. Treatment of GC1-5 in atmospheres containing HCl at low concentration (0.05 mol%) resulted in a significant increase in the amount of Pt detected. This additional XRD detected Pt was present as <5 nm crystallites (see GC1-6)
6. Treatment of GC1-6 in O_2 at 550°C resulted in the disappearance of the small Pt crystallites and a small increase in the amount of XRD detected Pt (cf. GC1-6 and GC1-7).
7. Treatment of GC1-7 in an O_2-N_2 mixture containing HCl (0.08 mol%) resulted in a shift of the distributions to smaller sizes (cf. GC1-7 and GC1-8).
8. Treatment of GC1-8 in an atmosphere contains higher concentration of HCl (0.4 mol%) caused the disappearance of the smaller Pt crystallites; these became so small that they were no longer detected by XRD (see GC1-8, GC1-9 and GC1-10).

The sequence of treatments for Catalyst GC2 resulted in the following changes in Pt crystallite size distributions ([illegible] figure 6.2 and table 4.3):

1. Treatment in the He at 800°C resulted in relatively

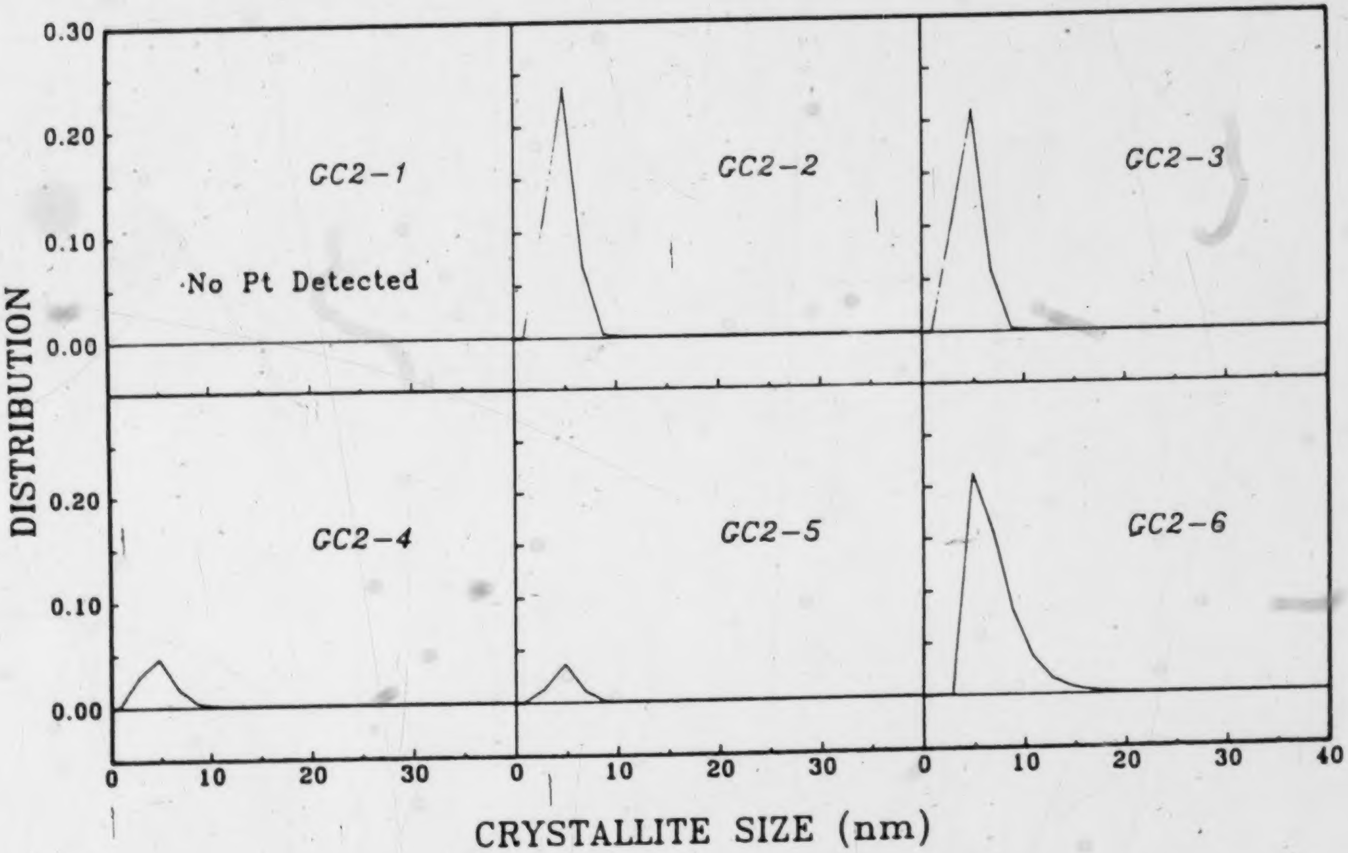

Figure 6.2 Crystallite Size Distribution for Catalyst GC2

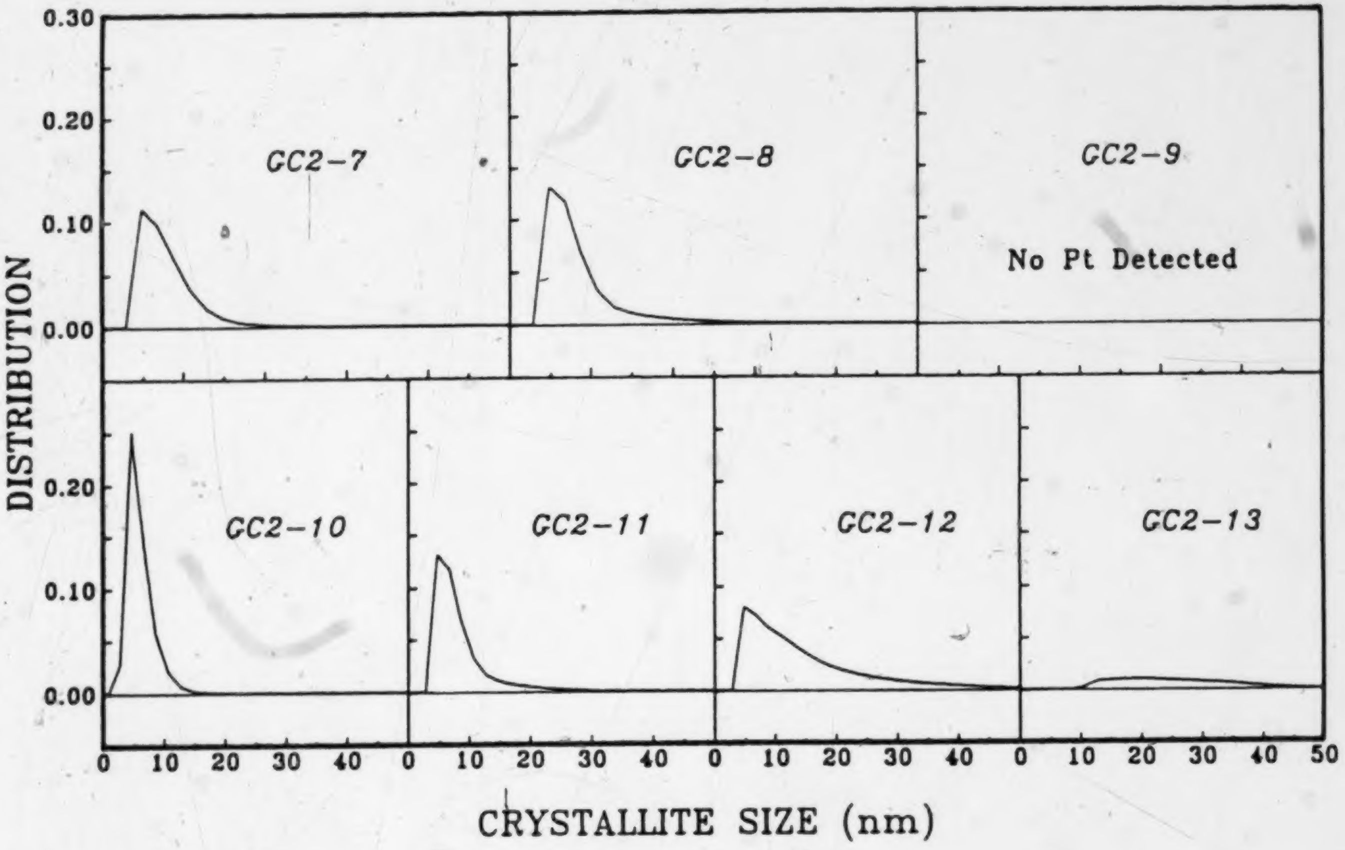

Figure 6.2 Crystallite Size Distribution for Catalyst GC2
(Continued)

narrow size distribution with low average sizes and most of the Pt was detected by XRD (see GC2-2, GC2-6 and GC2-10)

2. Treatment in O_2 at 700°C after treatment in He at 800°C resulted in a decrease in the amount of Pt detected and a slight broadening of the size distribution (see GC2-7 and GC2-11). Subsequent treatment in O_2 at 800°C resulted in further broadening of the size distribution (GC2-12).
3. Treatment in atmospheres containing 0.4% HCl resulted in decreases in the amount of Pt detected (for the case of GC2-9 no Pt was detected).
4. Treatment in Cl_2-containing atmosphere caused a large decrease in detected Pt and the disappearance of Pt crystallites smaller than 10 nm (see GC2-13).

The behavior of the 5 wt% Pt catalyst (GC3 and GC4) were similar to that of the 1% catalysts, i.e. treatment in O_2 at 700°C and 800°C resulted in broad size distributions (see Figure 6.3, GC3-3 and GC3-9), and treatment in He at 800°C resulted in relatively narrow size distributions (see Figure 6.4, GC4-3), and treatment in atmosphere containing 3.25 mol% Cl_2 resulted in decreases in the fractions of the Pt detected (see GC3-8 and GC3-10). Pt redispersion also occurred at lower Cl_2 concentrations (0.06 mol%), but the Pt redispersion was much slower (see GC3-6, GC3-7, GC4-4, GC4-5 and GC4-6).

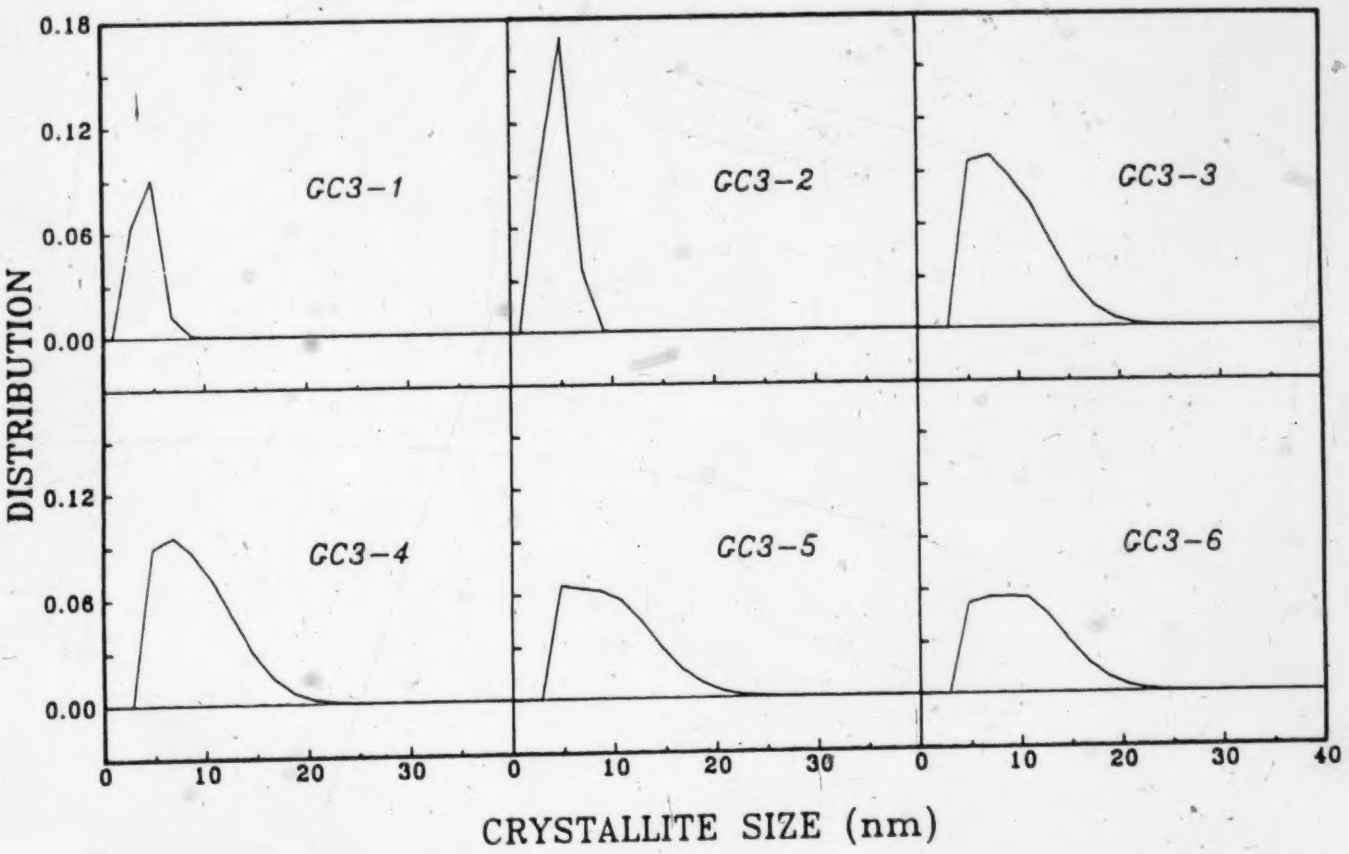

Figure 6.3 Crystallite Size Distribution for Catalyst GC3

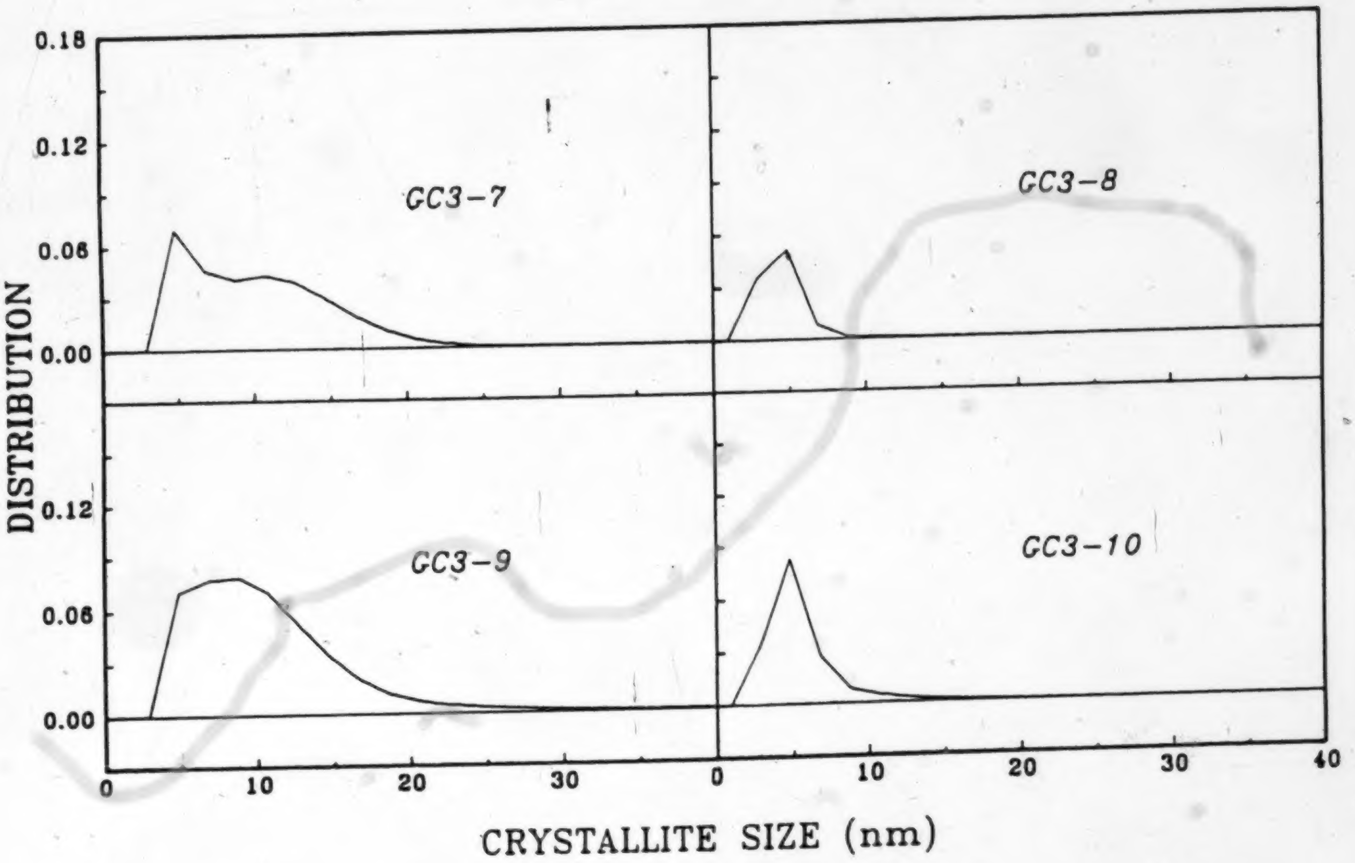

Figure 6.3 Crystallite Size Distribution for Catalyst GC3
(Continued)

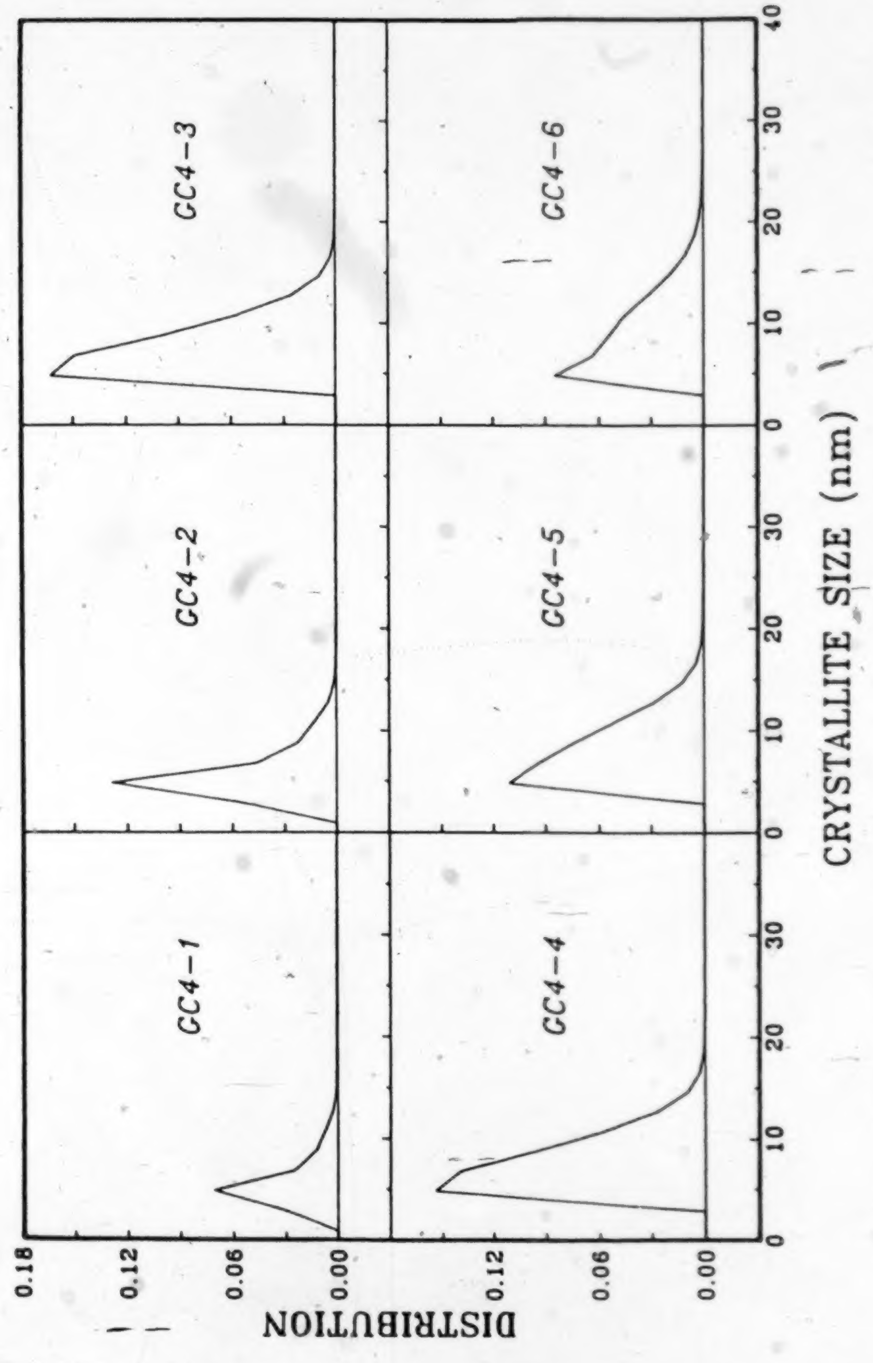

Figure 6.4 Crystallite Size Distribution for Catalyst GC4

The influence of 500°C treatment in hydrogen was different for the 1 and 5 wt% catalysts. Treatment of the 1% Pt catalysts in hydrogen did not affect the Pt average crystallite sizes, the size distribution or the fraction of Pt detected. However, treatment of the 5% Pt catalysts in hydrogen caused significant increases in the amount of Pt detected, but the average crystallite sizes and the shapes of the size distributions were not changed appreciably (see GC3-1 and GC3-2, Figure 6.3 and Table 6.3; GC4-1 and GC4-2, Figure 6.4 and Table 6.4). The observed changes in size distribution and fraction of Pt detected by XRD provide insight into the processes occurring during the sintering and redispersion of Pt/γ-Al_2O_3 catalysts.

6.5 Processes Occurring during Sintering and Redispersion

It is known that the composition of treatment atmosphere has a pronounced effect on the sintering and redispersion of supported metal catalysts (4,5,9,12). The results of this study are in agreement with this observation. However, the changes in the Pt crystallite size distribution further elucidate the processes occurring during sintering and redispersion. All the observed changes can be accounted for by an atomic (molecular) sintering and redispersion mechanism (9,55,56). The atomic (molecular) sintering mechanism consists of detachment of Pt containing species (Pt atoms in reducing and inert atmospheres and Pt-chlorine and Pt-oxygen species in chlorine and oxygen containing atmospheres) from metal crystallites and migration of these entities over the support surface. The migrating species may become immobilized at sites on the support surface which interact strongly with the migrating species (trap sites) or they may become incorporated into Pt crystallites upon collision with Pt crystallites. Sintering occurs when few or no trap sites are present, and redispersion occurs if trap sites are present. The observed behavior during the various treatments will be interpreted in terms of this atomic migration mechanism.

6.5.1 Treatments in Oxygen

It has frequently been reported that treatment of chlorine-containing Pt/γ-Al_2O_3 catalysts in oxygen at temperature <600°C results in increases in Pt dispersion (i.e. redispersion) (9). This observation was largely based on adsorption results. The H/Pt ratios for Runs GC1-3, GC1-5 (Table 4.2) are in agreement with this observation since H/Pt ratios increased as a result of O_2 treatments at 550°C. However, for Run GC1-7 treatment in O_2 at 550°C caused a decrease in the H/Pt ratio. The Pt crystallite size distributions shown in Figure 6.1 and the fractions of Pt detected, reported in Table 6.1, offer an explanation for this apparent discrepancy.

Treatment at 550°C for all three runs resulted in increases in the fraction of Pt detected by XRD and in increase of average Pt crystallite size. It is usually expected that increases in Pt crystallite sizes are accompanied by decreases in dispersion (see Equation 6.2) even if the fraction of Pt detected remains constant. However, the changes in the Pt crystallite size distribution (see Section 6.4 and Figure 6.1) indicate that treatments in O_2 at 550°C resulted in simultaneous sintering and redispersion. Prior to the O_2 treatment, the undetected Pt was present as small (<2 nm) Pt particles with dispersions of 0.6 to 0.7 for Catalysts GC1-2 and GC1-4 (see last column of Table 6.5). Treatment in O_2 at 550°C converted some of this Pt into atomically dispersed Pt (i.e. Pt immobilized at trap sites) while some of the other Pt became incorporated into Pt crystallites. This 'splitting' of the size distribution into a very bimodal distribution can result in increases in average sizes of XRD detected crystallites and increases in Pt dispersion. For treatments GC1-3 and GC1-5 the redispersion (i.e. formation of atomically dispersed Pt) dominated, while for Run GC1-7 sintering (i.e. incorporation of migrating species into larger crystallites) dominated.

The results for O_2 treatment at 700°C demonstrate the sensitive balance between sintering and redispersion. Treatments in O_2 at 700°C of catalysts sintered in He resulted in a decrease in the fraction of detected Pt, an increase in the average crystallite size of the XRD detected Pt, and relatively constant H/Pt ratios. The crystallite size distributions show that even at 700°C in O_2 redispersion occurs, but sintering is more pronounced. Treatment in

O_2 at 800°C only results in sintering.

6.5.2 Treatment in Chlorine-Containing Atmospheres

Chlorine-containing compounds are usually used in the regeneration of sintered Pt/γ-Al_2O_3 catalysts (57). The chlorine has two effects: one, it increases the rate of dissociation of Pt species (Pt chlorides or Pt oxychlorides) from the Pt crystallites, and two, it causes the formation of trap sites. The results reported above show that the nature of the chlorine compound and the concentration are important factors in the redispersion of sintered Pt/Al_2O_3 catalysts. The least effective of the compounds studied were CCl_4 and C_2HCl_3 (a subsequent O_2 treatment was required to increase Pt dispersion). HCl was a relatively effective redispersing agent at higher concentrations (0.4 mol.%). The most effective compound for redispersion was Cl_2. Redispersion occurred even in the absence of oxygen and at temperatures as low as 450°C (see Runs GC2-13, GC3-8 and GC3-10). The rate of redispersion in Cl_2 was dependent on the Cl_2 concentration; increases in Cl_2 concentrations resulted in increased redispersion rates.

The treatments in the HCl and chlorinated hydrocarbons showed behavior similar to that obtained during treatment in oxygen, i.e. both sintering and redispersion occurred simultaneously. The overall effect of a treatment, i.e. increases or decreases in Pt dispersion, was dependent on the concentration of the chlorine-containing compound.

Treatment in atmospheres containing Cl_2, on the other hand, always resulted in increases in Pt dispersion.

6.5.3 Treatment in Helium

Treatment in helium always resulted in sintering. Sintering in helium was much slower than sintering in oxygen because the dissociation of Pt atoms from Pt crystallites is much slower than the dissociation of Pt oxide species from Pt crystallites. No redispersion occurs in He since the migrating Pt species do not interact strongly with the support, i.e. there are no trap sites for migrating Pt atoms. This lack of trap sites results in relatively narrow Pt crystallites size distributions. The behaviour during treatment in He is typical of that reported for treatments in reducing and inert atmospheres (9).

6.5.4 Processes Occurring during the Reduction Step

All catalysts were reduced in hydrogen at 500°C after each treatment. This reduction is required prior to adsorption measurements since adsorption uptakes on unreduced catalysts do not correspond to the Pt dispersion. The results for Runs GC3-2 and GC4-2 (5% Pt catalysts) showed that sintering can occur during reduction at 500°C. The 500°C reduction of samples GC3-1 and GC4-1 resulted in increases in the fraction of Pt detected without significant changes in average Pt crystallite sizes and size distributions, i.e. undetected Pt becomes incorporated into larger Pt crystallites and new Pt crystallites are formed by nucleation of migrating species. These processes do not occur to a detectable extent in 1% Pt catalysts due to the lower concentration of small Pt crystallites and insufficient concentration of migrating species for nucleation of new Pt crystallites.

Reduction of catalysts after treatment in oxygen or chlorine containing atmospheres undoubtedly causes changes in the Pt dispersion. Pt complexes (oxide and/or chloride) are reduced to elemental Pt. The reduction of Pt located at trap sites eliminates the strong Pt-support interaction and it is possible that the resulting Pt atoms migrate over the support and nucleate into new crystallites or become incorporated into existing Pt crystallites. However, no studies were done on unreduced catalysts after oxygen and chlorine treatment. It is recommended that XRD patterns be measured before and after reduction in order to obtain information on the effect of reduction on Pt crystallite size distributions.

6.5.5 Summary of Sintering and Redispersion Processes

The XRD results have added greatly to our understanding of the sintering and redispersion processes. The most important conclusion from the XRD studies, which could not have made from chemisorption results alone, is the simultaneous sintering and redispersion which occurs during treatment of chlorine-containing $Pt/\gamma\text{-}Al_2O_3$ in oxygen. The formation of very bimodal Pt size distribution (i.e. atomically dispersed Pt and large Pt crystallites) which exists during treatments in O_2 illustrates the delicate balance between sintering and redispersion processes.

The Pt crystallite size distributions can also be used for testing the validity of proposed mechanistic models of sintering and redispersion. The XRD results presented in this study show that Pt dispersion alone is insufficient to characterize supported Pt catalysts since the same Pt dispersion can be obtained for many different Pt crystallite size distributions. Hence, sintering models which only use dispersion or average Pt particle size,(6,7,58) as a measure of the state of Pt cannot be used to represent the sintering and redispersion of supported Pt catalysts.

7. CONCLUSIONS AND RECOMMENDATIONS

The results presented in this thesis have demonstrated that wide-angle x-ray diffraction is a very useful tool for characterizing supported metal catalysts, even for crystalline supports which causes interference with the metal diffraction lines. It is concluded that the metal crystallite size information (average sizes and size distributions) obtained from XRD measurements by the methods described in Chapter 5 (support subtraction, smoothing and Fourier analysis) are reliable because good agreement is obtained with hydrogen chemisorption results. The size distributions obtained from XRD have aided in determining the processes which occur during sintering and redispersion. All the results obtained can be interpreted in terms of an atomic migration mechanism for sintering and redispersion.

It is recommended that detailed mathematical modelling of sintering and redispersion be done using the information on Pt crystallite size distribution obtained during this study. It is also recommended that improvements be made in the XRD data analysis methods. Possible improvements include: one, development of better methods for removing the support contribution from the catalyst XRD pattern with the objective of eliminating or reducing the need for baseline corrections; two, examination of alternate and better procedures for obtaining the second derivative of the Fourier coefficients especially in the low Fourier number range; and three, determination of more accurate integrated areas for samples in which all the Pt is detected by XRD in order to increase the accuracy of the fraction of Pt detected by XRD. Additional verification of absence of strain for catalysts treated in various atmospheres is also required.

8. REFERENCES

1. Sterba, M.J. and Haensel, V., Ind. Eng. Chem., Proc. Res. Dev., **15**, 2-16 (1976).

2. Pick, W.C.S., M.Sc. Thesis, University of Alberta, 1984.

3. Herrmann, R.A., Adler, S.F., Goldstein, M.S. and DeBaun, R.M., J. Phys. Chem., **65**, 2189-2194 (1961).

4. Wanke, S.E. and Flynn, P.C., Catal. Rev.-Sci. Eng., **12**, 93-135 (1975)

5. Wynblatt, P. and Gjostein, N.A., Prog. Solid State Chem., **9**, 21-58 (1975).

6. Ruckenstein, E. and Dadyburjor, D.B., Rev. Chem. Eng., **1**, 251-355 (1983).

7. Lee, H.H. and Ruckenstein, E., Catal. Rev.-Sci. Eng., **25**, 475-550 (1983).

8. Wanke, S.E., *in* "Sintering and Heterogeneous Catalysis", (G.C. Kuczynski, A.E. Miller, and G.A. Sargent, Eds.), Mat. Sci. Res., Vol. **16**, pp. 223-241, Plenum Press, New York, 1984.

9. Wanke, S.E., Szymura, J.A. and Yu, T.-T., *in* "Catalyst Deactivation", (E.E. Petersen and A.T. Bell, Eds.), pp. 65-95, Marcel Dekker, New York, 1987.

10. Boudart, M., Aldag, A.W., Ptak, L.D. and Benson, J.E., J. Catal., **11**, 35-45 (1968).

11. Lietz, G., Lieske, H., Spindler, H., Hanke, W., and Völter, J., J. Catal., **81**, 17-25 (1983).

12. Foger, K. and Jaeger, H., J. Catal., **92**, 64-87 (1985).

13. Foger, K., Hay, D. and Jaeger, H., J. Catal., **96**, 154-169 (1985).

14. Foger, K., Hay, D. and Jaeger, H., J. Catal., **96**, 170-181 (1985).

15. Yu, T.-T. Szymura, J.A. and Wanke, S.E., *in* "Preprints - 10th Canadian Symposium on Catalysis" (J. Downie, Ed.), pp. 536-545, Kingston, Ont., 1986.

16. Matyi, R.J., Schwartz, L.H. and Butt, J.B., Catal. Rev.-Sci. Eng., **29**, 41-99 (1987).

17. Flynn, P.C. and Wanke, S.E., Can. J. Chem. Eng., **53**, 636-640 (1975).

18. Foger, K., *in* "Catalysis, Science and Technology", (J.R. Anderson and M. Boudart, Eds.), Vol. **6**, pp. 227-305, Springer-Verlag, Berlin, 1984.

19. Gruber, H.L., J. Phys. Chem., **66**, 48-54 (1962).

20. Cormack, D. and Moss, R.L., J. Catal., **13**, 1-11 (1969).

21. Wanke, S.E., Lotochinski, B.K., and Sidwell, H.C., Can. J. Chem. Eng., **59**, 357-361 (1981).

22. Dautzenberg, F.M. and Wolters, H.B.M., J. Catal., **51**, 26-39 (1978).

23. Tauster, S.J. and Fung, S.C., J. Catal., **55**, 29-35 (1978).

24. Szymura, J.A. and Wanke, S.E., ACS Symp. Ser. **298**, 169-181 (1986).

25. Flynn, P.C. and Wanke, S.E., J. Catal., **33**, 233-248 (1974).

26. Freel, J., J. Catal., **25**, 139-148 (1972).

27. Adams, C.R., Benesi, H.A., Curtis, R.M. and Meisenheimer, R.G., J. Catal., **1**, 336-344 (1962).

28. Treacy, M.M.J. and Howie, A., J. Catal., **63**, 265-269 (1980).

29. Von Heimendahl, M., "Electron Microscopy of Materials", (Trans. by U.E. Wolff), p. 2, Academic Press, New York, 1980.

30. Gallezot, P., "Catalysis, Science and Technology", (J.R. Anderson, and M. Boudart, Eds.), **Vol.5**, pp. 221-273, Springer-Verlag, Berlin, 1984.

31. Cullity, B.D., "Elements of X-ray Diffraction", Addison-Wesley, Reading, Mass, 1978.

32. Pope, D., Smith, W.L., Eastlake, M.J., and Moss, R.L., J. Catal., **22**, 72-84 (1971).

33. Müller, J., Pure and Appl. Chem., **19**, 151-165 (1969).

34. Sashital, S.R., Cohen, J.B., Burwell, R.L., Jr., and Butt, J.B., J. Catal., 50, 479-493 (1977).

35. Klug, H.P., and Alexander, L.E., "X-ray Diffraction Procedures for Polycrystalline and Amorphous Materials", (2nd Edition), Chap. 9, John Wiley & Sons, New York, 1974.

36. Ganesan, P., Kuo, H.K., Saavedra, A., and De Angelis, R.J., J. Catal., 52, 310-320 (1978).

37. Moraweck, B., Renouprez, A.J. and Imelik, B., J. Chim. Phys. 70, 594-599 (1973).

38. Smith, W.L., J. Appl. Cryst., 5, 127-130 (1972).

39. Somorjai, G.A., *in* "X-ray and Electron Methods of Analysis", (H. van Olphen and W. Parrish, Eds.), pp. 101-126, Plenum, New York, 1968.

40. Renouprez, A., Hoang-Van, C. and Compagnon, P.A., J. Catal., 34, 411-422 (1974).

41. Gallezot, P., Alarcon-Diaz, A., Dalmon., J.-A., Renouprez, A.J. and Imelik, B., J. Catal., 39, 334-349 (1975).

42. Bumberger, H., Chang, Y.C., Phillips, M.G., Delaglio, F. and Goodisman, J., J. Catal., 97, 561-564 (1986).

43. Richardson, J.T. and Desai, P., J. Catal., 42, 294-302 (1976).

44. Warren, B.E., "X-Ray Diffraction", Addison-Wesley, Reading, Mass., 1969.

45. Cohen, J.B., "Diffraction Methods in Materials Science", Macmillan, New York, 1966.

46. Păuşescu, P., Mănăilă, R. and Popescu, M., J. Appl. Cryst., 7, 281-286 (1974).

47. Delhez, R., de Keijser, Th.H. and Mittemeijer, E.J., Fresenius Z. Anal. Chem., 312, 1-16 (1982).

48. Langford, J.I., National Bureau of Standards Special Publication 567, pp. 255-269, Washington, D.C., 1980.

49. Langford, J.I., J. Appl. Cryst., 11, 10-14 (1978).

50. Ruland, W., J. Appl. Cryst., 1, 90-101 (1968).

51. Adamiec, J., Fiedorow, R.M.J. and Wanke, S.E., J. Catal., **95**, 492-500 (1985).

52. Fiedorow, R.M.J. and Wanke, S.E., J. Catal., **43**, 32-42 (1976).

53. Kuester, J.L. and Mize, J.H., "Optimization Techniques with Fortran", pp. 240-250, McGraw-Hill, New York, 1973.

54. Yu, T.-T., private communication.

55. Flynn, P.C. and Wanke, S.E., J. Catal., **34**, 390-399 (1974).

56. Flynn, P.C. and Wanke, S.E., J. Catal., **34**, 400-410 (1974).

57. Franck, J.P. and Martino, G., *in* "Progress in Catalyst Deactivation", (J.L. Figueiredo, ed.), pp. 355-397, Martinus Nijhoff, The Hague, Holland, 1982.

58. Dadyburjor, D.B., Marsh, S.P. and Glicksman, M.E., J. Catal., **99**, 358-374 (1986).

9. Appendix A. Programs and Documentation

This appendix contains listings of the computer programs and associated subroutines used for the various calculations required to obtain Pt crystallite sizes and size distributions from XRD data. The programs are written in FORTRAN for use on HP-1000 computers under the RTE6-VM operating system. The HP-1000 computers in the DACS Centre of the Department of Chemical Engineering were used for all the calculations. Limited documentation is also provided for some of the programs. Additional documentation is given in the M.Sc. thesis by Pick (2).

The main programs and their functions are:

Program XRMD - used to subtract support XRD patterns from XRD patterns for supported catalysts.

Program YXFIT - used to fit subtracted XRD patterns with the function given by Equation 5.3.

Program YXPRO - used to compute the Fourier coefficients for measured, machine and pure profiles.

Program YXCOR - used to calculate the crystallite size distributions from the Fourier coeficients.

Program XPURE - used to generate a pure XRD profile from a specified crystallite size distibution.

9.1 Program XRMD

```
FTN4
      PRGRAM XRMD
      PRGRAM FOR CALCULATING THE X-RAY METAL DIFFRACTION
      INTEGER A,C,X
      DIMENSION IDCB1(144),IDCB2(144),IDCB3(144),NAME1(5),NAME2(5)
      DIMENSION NAME3(5),IBUF(10),ISIZE(2)
      DATA ISIZE/40,10/,C/0/,D/0./,NAME1/2HXR,2HAV,2H00,2HJU/
      DATA NAME2/2HXR,2HAV,2H00,2HJU/
      DATA NAME3/2HXP,2HTD,2H00,0,135/
C
C
      WRITE (1,10)
 10   FORMAT(/,'ENTER THE FILENM FOR INPUT FILE 1')
      READ(1,20) (NAME1(J),J=1,3)
 20   FORMAT(3A2)
      IF(OPEN(IDCB1,IERR,NAME1,0,NAME1(4),NAME1(5)).LT.0) GO TO 888
      WRITE(1,23)
 23   FORMAT(/,'ENTER THE SCALING FACTOR FOR FILE 1')
      READ(1,*)SCAL1
      WRITE(1,27)
   27 FORMAT('ENTER THE INTEGER ANGLE SHIFT FOR FILE 1',
     & /,5X,'DEGREES 2*THETA * 100')
      READ(1,*) IMV1
      WRITE(1,30)
 30   FORMAT(/,'ENTER THE FILENM FOR INPUT FILE 2')
      READ(1,20) (NAME2(J),J=1,3)
      WRITE(1,33)
 33   FORMAT(/,'ENTER THE SCALING FACTOR FOR FILE 2')
      READ(1,*) SCAL2
      WRITE(1,37)
   37 FORMAT('ENTER THE ANGLE SHIFT FOR FILE 2')
      READ(1,*) IMV2
      IF(OPEN(IDCB2,IERR,NAME2,0,NAME2(4),NAME2(5)).LT.0) GO TO 888
C
      WRITE(1,40)
 40   FORMAT(/,'ENTER THE # FOR THE XPTD FILE')
      READ(1,20) NAME3(3)
      WRITE(1,45)
   45  FORMAT('ENTER TWO POINTS FOR A LINEAR BASELINE AS...',
     &  /,5X,'IANG1,BASE1,IANG2,BASE2,')
      READ(1,*) IANG1,BASE1,IANG2,BASE2
C
C         BASEL=RK1*IANG +RK2
C
      RK1=(BASE2-BASE1)/FLOAT(IANG2-IANG1)
      RK2=BASE1-RK1*FLOAT(IANG1)
      WRITE(1,50)
   50  FORMAT('ENTER "0" TO ZERO ALL NEGATIVE RESULTS')
      READ(1,*) IZERO
      CALL CREAT(IDCB3,IERR,NAME3,ISIZE,3,NAME3(4),NAME3(5))
      IF(IERR.LT.O) GO TO 888
      IF(OPEN(IDCB3,IERR,NAME3,0,NAME3(4),NAME3(5)).LT.0) GO TO 888
C
C
 100   DO 110 I=1,10
 110   IBUF(I)=2H
```

```
      CALL READF(IDCB1,IERR,IBUF,10,LEN)
      IF(IERR.LT.0) GO TO 888
      IF(LEN.EQ.-1) GO TO 500
      CALL CODE
      READ(IBUF,*) A,B
      A=A+IMV1
      IF(A.EQ.C) GO TO 600
      IF(A.LT.C) GO TO 100
C
 200   DO 210 I=1,10
 210   IBUF(I)=2H
C
      CALL READF(IDCB2,IERR,IBUF,10,LEN)
      IF(IERR.LT.0) GO TO 888
      IF(LEN.EQ.-1) GO TO 500
      CALL CODE
      READ(IBUF,*) C,D
      C=C+IMV2
      IF(C.EQ.A) GO TO 600
      IF(C.LT.A) GO TO 200
      GO TO 100
C
 500   IEND=1
C
 600  X=A
      BASEL=RK1*X + RK2
      Y=B*SCAL1-D*SCAL2 - BASEL
      IF(IZERO.EQ.0.AND.Y.LT.0.0) Y=0.0
      DO 610 I=1,10
 610   IBUF(I)=2H
      CALL CODE
      WRITE(IBUF,620) X,Y
 620   FORMAT(I5,2X,F8.2)
      CALL WRITF(IDCB3,IERR,IBUF,10,LEN)
      IF(IERR.LT.0) GO TO 888
      IF(IEND.EQ.1) GO TO 777
      GO TO 100
C
 777   IF(CLOSE(IDCB1,IERR).LT.0) GO TO 888
      IF(CLOSE(IDCB2,IERR).LT.0) GO TO 888
      IF(CLOSE(IDCB3,IERR).LT.0) GO TO 888
      GO TO 999
C
 888   WRITE(1,890) IERR
 890   FORMAT(/5X,'TROUBLE IN FMP CALL. IERR= 'I5)
C
 999   STOP
      END
```

9.2 Program YXFIT

```
FTN4
$FILES 0,1
      PROGRAM YXFIT(4,200)
C
C        PROGRAM USED TO
C
C        1--- FIT THE RAW DATA TO THE MODIFIED VOIGT PROFILE
C        2--- DETERMINE:
C                        PEAK HEIGHT
C                        HALF WIDTH, IN RAD.
C                        AREA OF THE PEAK STUDIED
C        3--- CALCULATE:
C                        BETA(INT. BREADTH), IN RAD.
C                        PHI(HALF WIDTH/INT. BREADTH)
C        4--- STORE THE RESULTS TO 'OUT' IF DESIRED
C
C
C        SUBSCRIPT(K)---REFERS TO THE ANGLE OF TIME DOMAIN
C                       LOCATION
C        X(K)=ANGLE, DEG 2*THETA
C        IANG(K)=ANGLE, DEG 2*THETA*100
C        PARA(I)=PARAMETERS FOR MODIFIED VOIGT PROFILE
C
C
      DIMENSION IANG(500), RINT(500), RINTN(500)
      DIMENSION PARA(16),PARMN(16),PARMX(16)
      DIMENSION NAME1(9),IDCB1(144),IBUF(32)
      COMMON X(500)


      DATA NAME1/2H  ,2H  ,2HJU,135/
      NPAR=8
      IOUT1=1
      IANGN=0
C
C     **** SPECIFY INPUT ****
C
C     1. NAME
C     2. PEAK LOCATION
C     3. PEAK RANGE
C
      WRITE(1,10)
   10 FORMAT(/,'ENTER THE FILE LOCATION OF THE RAW DATA')
      READ(1,15) (NAME1(I),I=1,3)
   15 FORMAT(4A2)
C
      WRITE(1,20)
   20 FORMAT('ENTER THE APPROXIMATE PEAK LOCATION',
     & 'AND THE FIT RANGE')
      READ(1,*) PMAX,PRANG
C
      MINAN=IFIX((PMAX-PRANG/2.)*100.)
      MAXAN=IFIX((PMAX+PRANG/2.)*100.)
```

```
C
C     **** DEFINE OUTPUT ****
C
C     1. DEVICE
C     2. ID CODE
C     3. ANGLE RANGE
C     4. DATA POINTS
C
      WRITE(1,60)
   60 FORMAT(/,'ENTER DATA OUTPUT DEVICE (1=TERMINAL, 11=OUT)')
        OPEN(11,FILE='OUT::140')
      READ(1,*) IOUT
C
      WRITE(1,70)
   70 FORMAT('ENTER THE CATALYST IDENTIFICATION CODE')
      READ(1,15) (NAME1(I),I=6,9)
C
      WRITE(1,75)
   75 FORMAT('ENTER THE REGENERATION WIDTH, AND THE',
     & '(ODD) NUMBER OF DATA POINTS IN OUTPUT FILE')
      READ(1,*) WIDTH, IDIMR
C

      NFOR=(IDIMR-1)/2
      KCNTR=NFOR+1
C
C     **** READ INPUT PROFILE ****
C
      CALL NREAD(IDCB1,NAME1,MINAN,MAXAN,IDEL,IDIM,IANG,RINT)
      CALL DIST(IANG,RINT,IDIM)
C
C     **** ESTIMATE PARAMETERS FOR BEST FIT ****
C
      CALL  ESTB(RINT,IANG,IDIM,NPAR,PARA,PARMN,PARMX)
C
C     **** FITTING BY USING ROUTINE BSOLVE ****
C
      CALL  FIT(IDIM,NPAR,PARA,PARMN,PARMX,RINT,IOUT1)
C
C     **** GENERATE FITTING PROFILE ****
C
      CALL  NEWX(PARA,IDIMR,WIDTH)
      CALL NEWPK(PARA,NPAR,IDIMR,RINTN,IANG,RINT,IOUT)
C
C     **** CALCULATE ****
C
C     1. PEAK HEIGHT
C     2. HALF HEIGHT WIDTH
C     3. INTEGRAL AREA
C     4. INTEGRAL WIDTH
C
      CALL RPORT(PARA,IDIMR,WIDTH,KCNTR,NFOR,RINTN,NAME1,IOUT)
C
C
999   STOP
      END
```

```
C
C-----------------------------------------------------------------
C
      FUNCTION FPRIM(B,X1)
      DIMENSION B(8)
      U=B(8)
      IF (X1.GT.B(3)) U=1.
      DELX=X1-B(3)
      P1=B(1)*B(2)*B(4)/(1.+U*B(2)*DELX**2)**(B(4)+1.)
      P2=B(5)*B(6)*B(7)*(EXP(-U*B(6)*DELX**2))**B(7)
      FPRIM=-2.*U*DELX*(P1+P2)
      RETURN
      END
C
C-----------------------------------------------------------------
C
      SUBROUTINE RPORT(B,IDIMR,WIDTH,KCNTR,NFOR,RINTN,NAME1,IOUT)
      COMMON X(500)
      DIMENSION RINTN(IDIMR),NAME1(9),B(8)
      RAD=0.01745329
      HT=B(1)+B(5)
      HO2=HT/2.
C
C
C
C        NEWTON'S METHOD TO DETERMINE XHLO AND XHHI
C
C
      XHLO=B(3)-(B(1)*SQRT((2.**(1./B(4))-1.)/(B(8)*B(2)))+
     & B(5)*SQRT(-ALOG(0.5**(1./B(7)))/(B(8)*B(6))))/HT
      XHHI=B(3)+(B(1)*SQRT((2.**(1./B(4))-1.)/B(2))+
     & B(5)*SQRT(-ALOG(0.5**(1./B(7)))/B(6)))/HT
      DO 30 I=1,5
      XHLO=XHLO-(PK(B,XHLO)-HO2)/FPRIM(B,XHLO)
      XHHI=XHHI-(PK(B,XHHI)-HO2)/FPRIM(B,XHHI)
 30   CONTINUE
      WHAF=RAD*(XHHI-XHLO)
C
C
      CALL NALIN(PARA,IDIMR,WIDTH,KCNTR,NFOR,RINTN,AREA1)
      AREA1=AREA1/100.
      BETA=RAD*AREA1/HT
      PHI=WHAF/BETA
      WRITE(IOUT,60) (NAME1(I), I=6,8)
 60   FORMAT(//,10X,'REPORT FOR CATALYST: ',3A2)
      WRITE(IOUT,65) (NAME1(I),I=1,3)
 65   FORMAT(/,10X,'LOCATED IN FILE: ',3A2)
      WRITE(IOUT,70) (I,B(I),I=1,8)
 70   FORMAT(//,10X,'MODIFIED VOIGT PARAMETERS',/,14X,'I',7X,'B(I)'
     & /,8(/,10X,I5,5X,F10.5))
      WRITE(IOUT,75)
```

```
75    FORMAT(/,10X,'MODIFIED RESULTS:')
      WRITE(IOUT,80) HT,WHAF
80    FORMAT(/,10X,'REAK HEIGHT=',F10.5,/,10X,'HALF WIDTH=',1PE12.3,
     & 2X,'RADIANS')
      WRITE(IOUT,85)
85    FORMAT(/,10X,'CALCULATED PARAMETERS:')
      WRITE(IOUT,90) AREA1,BETA
90    FORMAT(/,10X,'INT.AREA=',F10.5,/,10X,'BETA=',1PE12.3,2X,'RADIANS')
      WRITE(IOUT,95) PHI
95    FORMAT(/,10X,'PHI=(HALF WIDTH/BETA)=',1PE12.3)
      RETURN
      END
```

9.2.1 Documentation for YXFIT

This program is used to fit subtracted XRD profiles to a Modified Voigt function with 8 adjustable parameters (B(i)).

(See Equation 5.3 for Voigt function)

```
Fv = Y + Z

 Y=B(1)/(1.+B(8)*B(2)*(X-B(3))**2)**B(4)

 Z=B(5)*(EXP(-B(8)*B(6)*(X-B(3))**2))**B(7)
```

The input is:

1. FILE LOCATION OF THE RAW DATA
   subtracted XRD profile
2. REGENERATION WIDTH
   the range of angle will output
3. NUMBER OF DATA POINTS
   points = fit range / step
4. OUTPUT DEVICE
   a temporary file OUT is used for storing output data
5. APPROXIMATE PEAK LOCATION
   Bragg angle of the peak will be studied
6. FIT RANGE
   angle range to be studied
7. PARAMETER TO BE CHANGED
   parameters fixed by user

An example of the use follows:

```
:RU,YXFIT

ENTER THE FILE LOCATION OF THE RAW DATA
TS208
ENTER THE REGENERATION WIDTH, AND THE (ODD) DATA POINTS
8.4,421

ENTER DATA OUTPUT DEVICE (1=TERMINAL, 11=OUT)
11
ENTER THE CATALYST IDENTIFICATION CODE
TS208

ENTER THE APPROXIMATE PEAK LOCATION AND THE FIT RANGE
39.8,7.6

ENTER THE SCALING FACTOR FOR FILE TS208
1
ENTER "1" TO APPLY ANGLE CORRECTION
0
INITIAL GUESSES ARE:
           GUESS          MIN          MAX
     1       8.51E+00       8.51E-02       4.26E+01
     2       2.50E-01       1.00E-03       1.00E+03
     3       3.97E+01       3.17E+01       4.76E+01
     4       1.00E+00       5.00E-01       2.00E+01
     5       8.51E+00       8.51E-02       4.26E+01
     6       1.73E-01       3.47E-03       8.66E+00
     7       1.00E+00       5.00E-01       2.00E+01
     8       1.00E+00       1.00E-01       1.50E+00
ENTER THE PARAMETER TO BE CHANGED
0
1          BSOLVE REGRESSION ALGORITHM


    INITIAL GUESSES     UPPER LIMITS    LOWER LIMITS
         .851E+01          .426E+02          .851E-01
         .250E+00          .100E+04          .100E-02
         .397E+02          .476E+02          .317E+02
         .100E+01          .200E+02          .500E+00
         .851E+01          .426E+02          .851E-01
         .173E+00          .866E+01          .347E-02
         .100E+01          .200E+02          .500E+00
         .100E+01          .150E+01          .100E+00

  ICON =  8    PH =   .10960344E+04    ITERATION NO. =   1

  ICON =  8    PH =   .37020593E+03    ITERATION NO. =   2

  ICON =  8    PH =   .35206238E+03    ITERATION NO. =   3
ICON =  8     PH =   .34830737E+03    ITERATION NO. =   4

ICON =  8     PH =   .34708130E+03    ITERATION NO. =   5

ICON =  8     PH =   .32874933E+03    ITERATION NO. =   6

ICON =  8     PH =   .32412946E+03    ITERATION NO. =   7

ICON =  8     PH =   .31918921E+03    ITERATION NO. =   8

ICON =  8     PH =   .31420776E+03    ITERATION NO. =   9

ICON =  8     PH =   .30974524E+03    ITERATION NO. =  10
     1 3.85270360E+00
     2 1.47134800E+00
     3 3.96054310E+01
     4 1.66275070E+00
     5 1.22833160E+01
     6 1.51525530E-01
     7 8.76850250E-01
     8 1.41629840E+00
ENTER "1" TO STOP ITERATIONS

0

  ICON =  8     PH =   .30651624E+03    ITERATION NO. =  11

  ICON =  8     PH =   .30481549E+03    ITERATION NO. =  12

  ICON =  8     PH =   .30417188E+03    ITERATION NO. =  13

  ICON =  8     PH =   .30392938E+03    ITERATION NO. =  14

  ICON =  8     PH =   .30380255E+03    ITERATION NO. =  15

  ICON =  7     PH =   .30371106E+03    ITERATION NO. =  16

  ICON =  7     PH =   .30363788E+03    ITERATION NO. =  17

  ICON =  7     PH =   .30357208E+03    ITERATION NO. =  18

  ICON =  7     PH =   .30351477E+03    ITERATION NO. =  19

  ICON =  7     PH =   .30346246E+03    ITERATION NO. =  20
       1 3.23819400E+00
       2 1.25901720E+00
       3 3.96203230E+01
       4 3.71274040E+00
       5 1.31652910E+01
       6 1.57846870E-01
       7 9.13295150E-01
       8 1.36125760E+00
  ENTER "1" TO STOP ITERATIONS
```

```
0

  ICON =  7    PH =   .30341656E+03    ITERATION NO. =  21

  ICON =  7    PH =   .30337628E+03    ITERATION NO. =  22

  ICON =  5    PH =   .30333966E+03    ITERATION NO. =  23

  ICON =  6    PH =   .30330554E+03    ITERATION NO. =  24

  ICON =  6    PH =   .30327679E+03    ITERATION NO. =  25

  ICON =  7    PH =   .30325421E+03    ITERATION NO. =  26

  ICON =  7    PH =   .30323108E+03    ITERATION NO. =  27

  ICON =  6    PH =   .30320795E+03    ITERATION NO. =  28

  ICON =  7    PH =   .30318866E+03    ITERATION NO. =  29

  ICON =  6    PH =   .30317035E+03    ITERATION NO. =  30
       1 3.18058680E+00
       2 7.24636550E-01
       3 3.96194460E+01
       4 5.87371440E+00
       5 1.31753520E+01
       6 1.57772990E-01
       7 9.13019060E-01
       8 1.36404560E+00
ENTER "1" TO STOP ITERATIONS

0

  ICON =  7    PH =   .30294135E+03    ITERATION NO. =  31

  ICON =  7    PH =   .30291229E+03    ITERATION NO. =  32

  ICON =  7    PH =   .30290027E+03    ITERATION NO. =  33

  ICON =  6    PH =   .30289050E+03    ITERATION NO. =  34

  ICON =  7    PH =   .30288104E+03    ITERATION NO. =  35

  ICON =  6    PH =   .30287933E+03    ITERATION NO. =  36

  ICON =  2    PH =   .30287915E+03    ITERATION NO. =  37

  ICON =  0    PH =   .30287909E+03    ITERATION NO. =  38
```

```
   SOLUTIONS OF THE EQUATIONS

   B( 1) =     .31149602E+01

   B( 2) =     .18781728E+00

   B( 3) =     .39618225E+02

   B( 4) =     .19883560E+02

   B( 5) =     .13175747E+02

   B( 6) =     .15772307E+00

   B( 7) =     .91157734E+00

   B( 8) =     .13680644E+01

THE LEAST SQUARES OBJECTIVE FUNCTION =       .302879E+03


     K-ALPHA BROADENING CORRECTED
ENTER "1" TO LIST THE VOIGHT FIT PEAK
1
:
```

9.3 Program YXPRO

```
FTN4
$FILES 0,1
      PROGRAM YXPRO(4,200)
C
C          PROGRAM USED FOR:
C
C             1---FORM THE FOURIER COEFFICIENTS (HR,HI) FROM DATA
C                 OF AN OBSERVED PROFILE
C             2---FORM THE FOURIER COEFFICIENTS (GR,GI) FROM 8 RAPA.
C                 OF AN 'INFINTELY' LARGE CRYSTALLITE PROFILE
C             3---CALCULATE THE FOURIER COEFFICIENTS (FR,FI) OF PURE
C                 X-RAY DIFFRACTION PROFILE
C             4---DETERMINE:
C                 THE AREA WEIGHTED SIZE DISTRIBUTION FUNCTION

C                 THE VOLUME WEIGHTED SIZE DISTRIBUTION FUNCTION
C             5---STORE ALDF AND VLDF IN 'OTPT' IF REQUIRED
C
C
      DOUBLE PRECISION FR(125),FI(125),HR(125),HI(125),GR(125),GI(125)
      DIMENSION IANG(500),RINT(500),RINTN(500)
      DIMENSION IANGB(500),RINTB(500),RINTNB(500)
      DIMENSION NAME1(5),IBUF(32)
      DIMENSION B(12)
      DIMENSION VDF(150),ADF(150),PS(150),VDF1(150),ADF1(150),PS1(150)
      COMMON X(500)
      DATA NAME1/2H  ,2H  ,2H  ,2HJU/
C
      IOUT=1
      RLAM=0.1542
      RAD=3.141593/180.
C
C     **** INITIAL SPECIFICATION ****
C
      CALL NINIT(NAME1,MINAN,MAXAN,NPAR,PMAX,WIDTH)
      CALL RREAD(IDCB,NAME1,MINAN,MAXAN,IDEL,IDIM,IANG,RINT)
      CALL CNTRD(NAME1,IDIM,IANG,RINT,MINAN,MAXAN,CNTR,IOUT,AREA1)
      CALL ALIGN(IANG,IDEL,CNTR,IDIM,KCNTR,NFOR,IOUT)
      CALL WIND1(RINT,KCNTR,NFOR,IDIM)
C
C     **** GENERATE HR AND HI ****
C
      CALL FOR(RINT,IDIM,KCNTR,NFOR,HR,HI,IOUT)
C
C     **** MACHINE PROFILE PARAMETERS ****
C
      B(1)=180.00
      B(2)=82.07
      B(3)=39.77
      B(4)=0.84
      B(5)=220.00
      B(6)=50.27
      B(7)=1.43
      B(8)=0.60
```

```
C
C     **** PERFORM MACHINE PROFILE ****
C
      CALL NEWX(B,IDIM,WIDTH)
      CALL NEWPK(B,NPAR,IDIM,RINTNB,IANGB,RINTB,IOUT)
      CALL ALINE(B,IDIM,WIDTH,KCNTR,NFOR,RINTNB,AREA2)
C
      DO 20 K=1,IDIM
      RINTNB(K)=RINTNB(K)*AREA1/AREA2
   20 CONTINUE
C
C     **** GENERATE GR AND GI ****
C
      CALL FOR(RINTNB,IDIM,KCNTR,NFOR,GR,GI,IOUT)
C
C     **** MODIFY GR AND GI ****
C
      IDEL1=2
      IDEL2=1
      CALL NNURN(GR,GI,IDEL1,IDEL2,NFOR,IOUT)
C
      WRITE(1,30)
   30 FORMAT(/,'ENTER "1" TO COUTINUE, "0" TO TEST PROGRAM')
      READ(1,*) NNN
      IF(NNN.GT.0) GOTO 40
C
C     **** PROGRAM TESTING ****
C
      DO 35 J=1, NFOR
       FR(J)=HR(J)
       FI(J)=HI(J)
   35 CONTINUE
C
      CALL MACHP(FR,FI,GR,GI,NFOR,HR,HI)
      CALL PROF(HR,HI,GR,GI,FR,FI,NFOR,IOUT)
C
      NADF=30
      NVDF=30
      ANMIN=RAD*FLOAT(IANG(KCNTR-NFOR))/(100.*2.)
      ANMAX=RAD*FLOAT(IANG(KCNTR+NFOR))/(100.*2.)
      A=(RLAM/2.)/(SIN(ANMAX)-SIN(ANMIN))
      JP1LO=3
C
      CALL MARAD(FR,NFOR,ADF1,PS1,NADF,AREA1,IOUT,A,JP1LO)
      CALL MVOLD(FR,NFOR,VDF1,PS1,NVDF,AREA1,IOUT,A,JP1LO)
C
      GOTO 100
C
C     **** CALCULATE FR AND FI ****
C
   40 CALL PROF(HR,HI,GR,GI,FR,FI,NFOR,IOUT)
C
C     **** SPECIFY OUTPUT DEVICE AND NUMBER OF POINTS ****
C
      WRITE(1,50)
   50  FORMAT(/,'ENTER OUTPUT DEVICE(1=TERMINAL, 10=OTPT)')
       OPEN(10, FILE='OTPT::135')
      READ(1,*) IOUT1
C
```

```
      WRITE(1,60)
  60   FORMAT(/,'ENTER THE NO. OF POINT OF DISTRIBUTION FUNCTION')
      READ(1,*) NMUL
      NADF=NMUL
      NVDF=NMUL
C
C     **** CALCULATE ADF AND VDF ****
C
      ANMIN=RAD*FLOAT(IANG(KCNTR-NFOR))/(100.*2.)
      ANMAX=RAD*FLOAT(IANG(KCNTR+NFOR))/(100.*2.)
      A=(RLAM/2.)/(SIN(ANMAX)-SIN(ANMIN))
      JP1LO=3
C
      CALL MARAD(FR,NFOR,ADF1,PS1,NADF,AREA1,IOUT1,A,JP1LO)
      CALL MVOLD(FR,NFOR,VDF1,PS1,NVDF,AREA1,IOUT1,A,JP1LO)
  100 STOP
      END
C
C-----------------------------------------------------------------
C
      SUBROUTINE NNURN(GR,GI,IDEL1,IDEL2,NFOR,IOUT)
      DOUBLE PRECISION GR(NFOR),GI(NFOR)
      DIMENSION DUMR(125),DUMI(125)
      IRATIO=IDEL1/IDEL2
      RATIO=FLOAT(IDEL1)/FLOAT(IDEL2)
      IF(ABS(FLOAT(IRATIO)-RATIO).GT.0.05) GO TO 90
C
      DO 20 JP1=1,NFOR
        J=JP1-1
        JPP1=J/IRATIO+1
        FRAC=FLOAT(J)/RATIO - J/IRATIO
        DUMR(JP1)=GR(JPP1)+FRAC*(GR(JPP1+1)-GR(JPP1))
        DUMI(JP1)=GI(JPP1)+FRAC*(GI(JPP1+1)-GI(JPP1))
   20 CONTINUE
C
      DO 30 JP1=1,NFOR
        J=JP1-1
        GR(JP1)=DUMR(JP1)/RATIO
        GI(JP1)=DUMI(JP1)/RATIO
   30 CONTINUE
      GO TO 100
   90 WRITE(1,95)
   95  FORMAT('ERROR-IDEL1 IS NOT AN EVEN MULTIPLE OF IDEL2-'
     & /,5X,'** DO NOT BELIEVE THE PURE PROFILE, FR, AND FI**')
  100 RETURN
      END
```

9.3.1 Documentation for YXPRO

This program is used :

A. To calculate the crystallite size broadening Fourier coefficients F from an observed profile H and XRD machine profile G.

F = H/G

Fr = (Hr*Gr+Hi*Gi)/(Gr**2+Gi**2)

Fi = (Hi*Gr+Hr*Gi)/(Gr**2+Gi**2)

B. To determine the average crystallite size and size distribution from Fourier coefficients Fr.

(SEE Equation 5.11 and 5.16)

The input is:

1. FILE LOCATION OF THE RAW DATA
   fitted XRD data
2. APPROXIMATE PEAK LOCATION
   Bragg angle
3. RANGE OF INTERESTING
   angle range to be studied
4. FOURIER NUMBER
   the number of Fourier coefficients
5. OUTPUT DEVICE
   a termporary file OTPT is used for storing output file
6. POINTS OF DISTRIBUTION FUNCTION
   output data points

An example of use follows:

```
:RU,YXPRO

ENTER THE FILE LOCATION OF THE RAW DATA
TF208

ENTER THE APPROXIMATE PEAK LOCATION AND THE RANGE OF INTEREST
39.8,8.0

 ENTER THE NUMBER OF PEAKS, NPEAK
1
ENTER THE CATALYST IDENTIFICATION CODE (EG PI16)
TF208

ENTER THE SCALING FACTOR FOR FILE TF208
1

          ** FILE: TF208  **
THE PEAK AREA IS:  58.582 C*DEG/S
THE CENTROID IS AT:   39.823 DEG 2*THETA

THERE ARE   401 DATA POINTS
THE CLOSEST TO THE CENTROID IS:   202
AT AN ANGLE OF:    39.83
  120 FOURIER COEFFICIENTS WILL BE USED
THE PEAKS WILL BE STUDIED FROM:    37.43 TO    42.23
ENTER "1" TO APPLY THE MODIFIED HANNING WINDOW
1
ENTER THE NO. OF TAPERED COEFS. IN THE WINDOW, M2M
     (TOTAL NO. OF POINTS= 241)
201
ENTER "1" TO LIST SPLIT COS BELL WINDOW FITTED SERIES
0

           FOURIER COEFFICIENTS
     J          A(J)          B(J)          AMP(J)


     0       1.277E+01      0.000E+00      1.277E+01
     1       7.565E+00     -3.030E-01      7.571E+00
     2       1.357E+00     -3.650E-01      1.405E+00
     3       3.223E-01     -2.554E-01      4.112E-01
     4       1.725E-01     -1.690E-01      2.415E-01
     5       3.999E-02     -9.421E-02      1.023E-01
     6       4.111E-03     -4.139E-02      4.159E-02
     7      -9.348E-03     -1.413E-02      1.694E-02
     8      -6.093E-03     -2.816E-03      6.713E-03
     9      -4.660E-03      4.714E-04      4.684E-03
    10      -1.883E-03      1.389E-03      2.340E-03
    11      -1.240E-03      1.095E-03      1.654E-03
    12      -2.844E-04      8.473E-04      8.938E-04
    13      -1.847E-05      6.837E-04      6.839E-04
```

```
     14       5.005E-04       4.582E-04        6.785E-04
     15       3.617E-04       3.430E-04        4.985E-04
     16       3.844E-04       3.166E-04        4.980E-04
     17       3.026E-04       6.990E-05        3.106E-04
     18       2.384E-04      -1.360E-04        2.745E-04
     19      -7.622E-05       2.696E-05        8.084E-05
     20      -1.286E-04       2.910E-04        3.182E-04
     21      -1.039E-05       1.997E-04        2.000E-04
     22       2.456E-04      -4.938E-05        2.505E-04
     23       1.133E-04      -1.834E-04        2.155E-04
     24       9.000E-06      -1.898E-04        1.900E-04
     25       2.233E-04      -2.398E-04        3.277E-04
     26       2.669E-04      -2.829E-04        3.889E-04
     27       1.094E-04      -5.529E-05        1.226E-04
     28       9.745E-05       3.571E-04        3.701E-04
     29       1.075E-04       4.132E-04        4.270E-04
     30       1.844E-04       1.832E-04        2.599E-04
     31       1.827E-04      -1.726E-05        1.836E-04
     32       1.148E-05      -7.607E-05        7.693E-05
     33      -6.868E-05      -7.613E-05        1.025E-04
     34       2.018E-04      -1.985E-04        2.831E-04
     35       2.872E-04      -3.408E-04        4.457E-04
     36       2.065E-04      -1.894E-04        2.802E-04
     37       2.241E-04      -2.379E-05        2.254E-04
     38       1.817E-04      -1.739E-04        2.515E-04
     39       3.999E-06      -2.134E-04        2.134E-04
     40      -1.074E-04      -9.442E-05        1.430E-04
ENTER "1" TO LIST THE CAUCHY FIT PEAK

              FOURIER COEFFICIENTS
      J          A(J)            B(J)           AMP(J)


      0       2.396E+01       0.000E+00        2.396E+01
      1       2.103E+01      -6.381E-01        2.104E+01
      2       1.817E+01      -5.504E-01        1.818E+01
      3       1.595E+01      -5.337E-01        1.596E+01
      4       1.392E+01      -4.101E-01        1.392E+01
      5       1.209E+01      -3.570E-01        1.209E+01
      6       1.039E+01      -2.546E-01        1.040E+01
      7       8.835E+00      -2.059E-01        8.838E+00
      8       7.418E+00      -1.261E-01        7.419E+00
      9       6.135E+00      -8.964E-02        6.135E+00
     10       5.005E+00      -3.216E-02        5.005E+00
     11       4.010E+00      -1.224E-02        4.010E+00
     12       3.168E+00       2.231E-02        3.169E+00
     13       2.450E+00       2.409E-02        2.451E+00
     14       1.872E+00       3.783E-02        1.872E+00
     15       1.393E+00       2.440E-02        1.393E+00
     16       1.027E+00       2.321E-02        1.028E+00
     17       7.314E-01       9.860E-04        7.314E-01
     18       5.210E-01      -7.433E-03        5.210E-01
```

```
   19       3.514E-01       -3.142E-02        3.528E-01
   20       2.421E-01       -4.035E-02        2.455E-01
   21       1.508E-01       -6.098E-02        1.627E-01
   22       1.012E-01       -6.644E-02        1.211E-01
   23       5.363E-02       -8.149E-02        9.756E-02
   24       3.575E-02       -8.232E-02        8.975E-02
   25       1.024E-02       -9.189E-02        9.246E-02
   26       7.641E-03       -8.878E-02        8.911E-02
   27      -7.814E-03       -9.420E-02        9.453E-02
   28      -3.737E-03       -8.854E-02        8.862E-02
   29      -1.506E-02       -9.133E-02        9.257E-02
   30      -8.305E-03       -8.441E-02        8.482E-02
   31      -1.809E-02       -8.579E-02        8.768E-02
   32      -1.032E-02       -7.851E-02        7.919E-02
   33      -1.959E-02       -7.924E-02        8.162E-02
   34      -1.146E-02       -7.211E-02        7.301E-02
   35      -2.058E-02       -7.259E-02        7.546E-02
   36      -1.232E-02       -6.584E-02        6.699E-02
   37      -2.145E-02       -6.630E-02        6.968E-02
   38      -1.317E-02       -6.001E-02        6.144E-02
   39      -2.235E-02       -6.053E-02        6.452E-02
   40      -1.408E-02       -5.474E-02        5.652E-02




ENTER OUTPUT DEVICE(1=TERMINAL, 10=OTPT)
10

ENTER THE NO. OF POINT OF DISTRIBUTION FUNCTION
30
ENTER "1" TO LIST THE AREA WEIGHTED DIST. FUNCTION
1
ENTER "1" TO LIST THE VOLUME WEIGHTED DISTR. FUNCTION
1
:
```

9.4 Program YXCOR

```
FTN4
$FILES 0,2
           PROGRAM YXCOR(4,200)
C
C
C          THE PROGRAM USED FOR
C
C          1. CORRECTING DISTR. FUNCTION FOR DETECTABILITY
C          2. CALCULATING MODIFIED DISPERSIONS
C
C
C      R-----CRYSTALLITE SIZE
C      P-----DISTRIBUTION FUNCTION
C      Y-----CORRECTED DISTRIBUTION FUNCTION
C      Z-----DISPERSION
C
C      FACT2 IS THE DETECTABLE FACTOR
C
          INTEGER A(100)
          DIMENSION R(100),P(100),S(100)
          DIMENSION Y(100),Z(100)
C
C
C      **** READ INPUT PROFILE ****
C                (NAME1)
C
      WRITE(1,50)
   50 FORMAT('ENTER NUMBER OF DATA POINTS')
      READ(1,*) NN
      OPEN(10,FILE='NAME1::135')
      DO 70 I=1,NN
      READ(10,*) A(I),R(I),P(I)
       IF (P(I).GT.0.) GOTO 20
       P(I)=0.00
   70 CONTINUE
      CLOSE(10)
C
C      **** SPECIFY OUTPUT DEVICE ****
C                (NAME3)
C
      OPEN(12,FILE='NAME3::135')
C
C       **** SUMMATION ****
C
      WRITE(1,85)
   85 FORMAT(/,5X,'SIZE',7X,'AREA')
      S(1)=0.
      DO 100 I=2,NN
      WRITE(1,95) R(I-1),S(I-1)
   95 FORMAT(2X,F8.4,5X,F6.4)
      S(I)=S(I-1)+(P(I)+P(I-1))/2.*(R(I)-R(I-1))
  100 CONTINUE
      WRITE(1,95) R(NN),S(NN)
C
```

```
C
C      **** CORRECTION FOR DETECTABILITY ****
C
       FACT1=1.0000/S(NN)
       WRITE(1,110)
 110   FORMAT('ENTER THE FRACTION Pt DETECTED')
       READ(1,*) FACT2
       DO 120 I=1,NN
       Y(I)=P(I)*FACT1*FACT2
 120   CONTINUE
C
C      **** CALCULATION OF DISPERSION ****
C
       W=0.
       DO 130 I=1,NN
       W=W+Y(I)
 130   CONTINUE
       FACT3=1.0000/W
C
       Z(1)=0.
       DO 135 I=2, NN
       Z(I)=Z(I-1)+FACT3*Y(I)/R(I)
C
C
       Z(I)=1.02*Z(I)
 135   CONTINUE
C
C      **** PRINT OUT ****
C
       WRITE(12,140)
 140   FORMAT(3X,'CORRECTED DISTRIBUTION PROFILE'
      & /,/,2X,'J',2X,' SIZE ',2X,'DISTR.FUNC.'2X,'D.P.')
       DO 160 I=1,NN
       WRITE(12,150) A(I),R(I),Y(I),Z(I)
 150   FORMAT(I3,2X,F8.3,2X,F9.7,2X,F8.4)
 160   CONTINUE
C
999    STOP
       END
```

9.5 Program XPURE

```
FTN4
      PROGRAM XPURE(4,200)
      DIMENSION IDCB(144),NAME(5),IBUF(10),ISIZE(2)
      DIMENSION DP(50),VFRAC(50)
      DATA NAME/2HXP,2HUR,2H  ,2HJU,135/,ISIZE/40,10/
C        DP(I)=LENGTH OF PARTICLE SIDE
C        VFRAC(I)=VOLUME FRACTION OF PARTICLES SIZE DP(I)
C
C        EPSILON IN RADIANS OF THETA
C
C        ASSUME RLAM=0.1542 NM
      WRITE(1,3)
    3 FORMAT('ENTER THE NUMBER OF PARTICLE SIZES IN THE PSDF')
      READ(1,*) NPS
      WRITE(1,4)
    4  FORMAT('ENTER PROFILE STEP SIZE, DEG 2*THETA')
      READ(1,*) DELTH
      WRITE(1,7)
    7  FORMAT('ENTER CONTROL DIGIT, ICON:',/,
     & 5X,'1=USE GAUSSIAN (NORMAL) LENGTH DISTRIBUTION',/,
     & 5X,'2=USE ONE SIZE SPHERICAL PARTICLES',/,
     & 5X,'3=LOG-NORMAL LENGTH DISTRIBUTION',/,
     & 5X,'4=USER ENTERED LENGTH DISTRIBUTION FUNCTION')
      READ(1,*) ICON
      IF(ICON.GT.3) GO TO 14
      IF(ICON.GT.2) GO TO 12
      IF(ICON.GT.1) GO TO 10
      CALL NLDF(DP,VFRAC,NPS)
      GO TO 19
   10 CALL SLDF(DP,VFRAC,NPS)
      GO TO 19
   12 CALL LNLDF(DP,VFRAC,NPS)
      GO TO 19
   14 CALL ULDF(DP,VFRAC,NPS)
   19 CALL LAVG(DP,VFRAC,NPS)
      WRITE(1,20)
   20  FORMAT('ENTER THE "XPURnn" FILE NUMBER')
      READ(1,25) NAME(3)
   25  FORMAT(3A2)
      WRITE(1,27)
   27  FORMAT('ENTER "1" TO LIST THE VOL WEIGHTED LENGTH DISTRI.')
      READ(1,*) ILDF
      IF(ILDF.NE.1) GO TO 29
      CALL LDF(DP,VFRAC,NPS)
   29 WRITE(1,30)
   30  FORMAT('ENTER THE BRAGG ANGLE AND RANGE OF INTEREST, ',
     & 'DEG 2*THETA')
      READ(1,*) ANG,WIDTH
C
      PI=3.1415926
      RAD=0.017453
      RLAM=0.1542
      THETB=RAD*ANG/2.
      DS=RLAM/(2.*SIN(THETB))
      ILAST=IFIX(WIDTH/DELTH)+1
      IANMN=IFIX((ANG-WIDTH/2.)*100.)
```

```
C
C
      CALL CREAT(IDCB,IERR,NAME,ISIZE,3,NAME(4),NAME(5))
      IF(IERR.LT.0) GO TO 90
      CALL OPEN(IDCB,IERR,NAME,0,NAME(4),NAME(5))
      IF(IERR.LT.0) GO TO 90
C
C
C
C
      DO 70 K=1,ILAST
        IANG=IANMN+IFIX(DELTH*100.)*(K-1)
        SUM=0.
        THETA=RAD*FLOAT(IANG)/200.
        S=2.*DS*SIN(THETA)/RLAM-1.
        IF(ABS(S).LT.1.E-4) GO TO 52
         RINT=1./(SIN(PI*S)**2)
         DO 50 I=1,NPS
          ARG=PI*S*DP(I)/DS
          SUM=SUM+SIN(ARG)*SIN(ARG)*VFRAC(I)/DP(I)
   50    CONTINUE
         RINT=RINT*SUM
         GO TO 55
   52   DO 54 I=1,NPS
   54   SUM=SUM+((DP(I)/DS)**2)*VFRAC(I)/DP(I)
        RINT=SUM
   55   DO 57 J=1,10
   57   IBUF(J)=2H
       CALL CODE
       WRITE(IBUF,60) IANG,RINT
   60   FORMAT(1X,I5,3X,F9.3)
       CALL WRITF(IDCB,IERR,IBUF,10)
       IF(IERR.LT.0) GO TO 90
   70 CONTINUE
      CALL CLOSE(IDCB,IERR)
      IF(IERR.LT.0) GO TO 90
      GO TO 100
C
C
   90 WRITE(1,91) IERR
   91 FORMAT(/,2X,'ERROR IN FMP CALL. IERR= ',I3)
  100 STOP
      END
C
C------------------------------------------------------------
C
      SUBROUTINE ULDF(DP,VFRAC,NL)
      DIMENSION DP(NL),VFRAC(NL)
    5 DO 20 J=1,NL
      WRITE(1,10) J
   10  FORMAT(/,5X,'ENTER THE PARTICLE SIZE, NM',/
     &  'AND THE MASS FRACTION FOR SIZE NO. ',I3)
      READ(1,*) DP(J),VFRAC(J)
   20 CONTINUE
      WRITE(1,30)
   30  FORMAT('LENGTH DISTRIBUTION FUNCTION',/,10X,'DP',10X,'VFRAC')
```

```
      DO 40 J=1,NL
       WRITE(1,35) DP(J),VFRAC(J)
   35   FORMAT(2(5X,F10.5))
   40 CONTINUE
      WRITE(1,50)
   50  FORMAT('ENTER "1" TO RE-ENTER THE LDF')
      READ(1,*) IREAD
      IF(IREAD.EQ.1) GO TO 5
      RETURN
      END
C
C-----------------------------------------------------------------
C
      SUBROUTINE NLDF(DP,VFRAC,NL)
      DIMENSION DP(NL),VFRAC(NL)
      WRITE(1,10)
   10  FORMAT('ENTER THE AVERAGE LENGTH, RLAV (NM)')
      READ(1,*) RLAV
      SIGMAX=RLAV/2.71523
      WRITE(1,20) SIGMAX
   20  FORMAT('ENTER THE STD. DEV. OF LDF, MAX. REALISTIC=',F8.3)
      READ(1,*) SIG
      XLO=RLAV-2.71523*SIG
      DELX=SIG*2.71523*2./FLOAT(NL-1)
      SUM1=0.
      SUM2=0.
      DO 30 J=1,NL
        DP(J)=XLO + FLOAT(J-1)*DELX
        Z=(DP(J)-RLAV)/SIG
        VFRAC(J)=0.3989*EXP(-Z*Z/2.)
        SUM1=SUM1+VFRAC(J)
   30 CONTINUE
      WRITE(1,40)
   40  FORMAT(/,10X,'NORMALIZED PARTICLE SIZE DIST. FUNCTION',/,
     & 10X,'DP',10X,'VFRAC')
      DO 50 J=1,NL
        VFRAC(J)=VFRAC(J)/SUM1
        PV=VFRAC(J)/DELX
        WRITE(1,45) DP(J),PV
   45   FORMAT(2(5X,F10.4))
   50 CONTINUE
      RETURN
      END
C
C-------------------------------------------------------------------
C
      SUBROUTINE SLDF(DP,VFRAC,NPS)
      DIMENSION DP(NPS),VFRAC(NPS)
    5 WRITE(1,10)
   10  FORMAT('ENTER THE PARTICLE DIAMETER')
      READ(1,*)DIA
      RLAVG=0.75*DIA
      WRITE(1,20)RLAVG
   20  FORMAT(/,2X,'WEIGHT AVERAGE LENGTH IS: ',F10.3,' NM',
     &  /,'ENTER "1" TO RE-ENTER')
      READ(1,*) ICON
      IF(ICON.EQ.1) GO TO 5
      DELX=DIA/FLOAT(NPS)
      SUM1=0.
      DO 30 J=1,NPS
        DP(J)=DELX/2. + DELX*FLOAT(J-1)
        VFRAC(J)=3.*(DP(J)/DIA)**2
        SUM1=SUM1+VFRAC(J)
   30 CONTINUE
C
      WRITE(1,40)
   40 FORMAT('NORMALIZED VOLUME WEIGHTED LENGTH DISTRIBUTION FUNC. ',
     & 10X,'DP',10X,'VFRAC')
      DO 50 J=1,NPS
        VFRAC(J)=VFRAC(J)/SUM1
        PV=VFRAC(J)/DELX
        WRITE(1,45) DP(J),PV
   45    FORMAT(2(5X,F10[illegible]))
   50 CONTINUE
      RETURN
      END
C
C-----------------------------------------------------------------
C
      SUBROUTINE LNLDF(DP,VFRAC,NL)
      DIMENSION DP(NL),VFRAC(NL)
    5 WRITE(1,10)
   10  FORMAT('ENTER THE THREE PARAMETERS R, T, AND U')
      READ(1,*)R,T,U
      RK=R/(T*U)
      PVMAX=RK**(R/T)*EXP(-U*RK)
      XMAX=RK**(1./T)
C
C
      XP=2.*XMAX
      XN=XP
      DO 30 J=1,30
        FUN=(XP**R)*EXP(-U*(XP**T))- PVMAX/50.
        DFUN=EXP(-U*(XP**T))*(R*XP**(R-1.) - T*U*(XP**(R+T-1.)))
        XN=XP- FUN/DFUN
        IF(ABS(XN-XP).LT.1.E-3) GO TO 40
        XP=XN
   30 CONTINUE
   40 DELX=XN/FLOAT(NL)
      SUM1=0.
      DO 50 J=1,NL
        DP(J)=DELX*(FLOAT(J)-0.5)
        VFRAC(J)=DP(J)**R*EXP(-U*(DP(J)**T))
        SUM1=SUM1+VFRAC(J)
   50 CONTINUE
C
      WRITE(1,60) R,T,U
   60   FORMAT(/,10X,'NORMALIZED LENGTH DISTRIBUTION FUNCTION',//
     &5X,'FOR LOG-NORMAL DISTRIBUTION: R= ',F8.4,' T= ',F8.4,
     & //,10X,'DP',10X,'VFRAC')
C
      DO 80 J=1,NL
        VFRAC(J)=VFRAC(J)/SUM1
        PV=VFRAC(J)/DELX
        WRITE(1,70) DP(J),PV
   70    FORMAT(2(5X,F10.4))
   80 CONTINUE
      RETURN
      END
```

```
C
C-----------------------------------------------------------------------
C
      SUBROUTINE LAVG(DP,VFRAC,NPS)
      DIMENSION DP(NPS),VFRAC(NPS)
      REAL NAVG
C
      SUMV=0.
      SUMA=0.
      SUMN1=0.
      SUMN2=0.
C
      DO 20 J=1,NPS
        SUMV=SUMV+VFRAC(J)*DP(J)
        SUMA=SUMA+VFRAC(J)/DP(J)
        SUMN1=SUMN1+VFRAC(J)/(DP(J)*DP(J))
        SUMN2=SUMN2+VFRAC(J)/(DP(J)**3)
   20 CONTINUE
C
      VAVG=SUMV
      AAVG=1./SUMA
      NAVG=SUMN1/SUMN2
      VOA=VAVG/AAVG
      WRITE(1,30) VAVG,AAVG,VOA,NAVG
   30  FORMAT(//,5X,'THE VOLUME AVERAGE LENGTH IS: ',F6.2,' NM',
     & /,5X,'THE AREA AVERAGE LENGTH IS:   ',F6.2,' NM',
     & /,5X,'THE RATIO <Lv>/<La> IS:       ',F6.3,
     & /,5X,'THE NUMBER AVERAGE LENGTH IS: ',F6.2,' NM')
      RETURN
      END
C
C-----------------------------------------------------------------------
C
      SUBROUTINE LDF(DP,VFRAC,NPS)
      DIMENSION DP(NPS),VFRAC(NPS)
C
      DELDP=DP(2)-DP(1)
C
      WRITE(1,10)
   10  FORMAT(2X,'ENTER LU FOR OUTPUT (TERMINAL=1):')
      READ (1,*) LUW
C
C
      DO 30 J=1,NPS
        VLDFJ=VFRAC(J)/DELDP
        WRITE(LUW,20) DP(J),VLDFJ
   20     FORMAT(3X,F10.4,5X,F10.4)
   30 CONTINUE
C
      RETURN
      END
```

9.6 Subroutine ALIGN

```
FTN4
      SUBROUTINE ALIGN(IANG,IDEL,CNTR,IDIM,KCNTR,NFOR,IOUT)
      DIMENSION IANG(IDIM)
      TEST1=1.E6
      TEST2=TEST1
      DO 20 K=1,IDIM
       TEST1=ABS(FLOAT(IANG(K))/100.-CNTR)
       IF(TEST1.LT.TEST2) KCNTR=K
       TEST2=AMIN1(TEST2,TEST1)
   20 CONTINUE
C
      IF(IDIM.GT.20) GO TO 40
      WRITE(1,30)
   30  FORMAT(/,10X,'** ERROR ** RANGE ((MAXAN-MINAN/IDEL) IS TOO',
     & 'SMALL')
      GO TO 99
C
   40 NDUM=MIN0((KCNTR-1),(IDIM-1-KCNTR))
      IF(NDUM.GT.10)NFOR=10
      IF(NDUM.GT.20)NFOR=20
      IF(NDUM.GT.30)NFOR=30
      IF(NDUM.GT.40)NFOR=40
      IF(NDUM.GT.60)NFOR=60
      IF(NDUM.GT.80)NFOR=80
      IF(NDUM.GT.100) NFOR=100
      IF(NDUM.GT.120) NFOR=120
      CANG=FLOAT(IANG(KCNTR))/100.
      WRITE(IOUT,50)IDIM,KCNTR,CANG,NFOR
   50  FORMAT(/,'THERE ARE ',I5,' DATA POINTS',
     & /,'THE CLOSEST TO THE CENTROID IS: ',I5,
     & /,'AT AN ANGLE OF: ',F8.2,
     & /,I5,' FOURIER COEFFICIENTS WILL BE USED')
      ANGLO=FLOAT(IANG(KCNTR-NFOR))/100.
      ANGHI=FLOAT(IANG(KCNTR+NFOR))/100.
      WRITE(IOUT,60) ANGLO,ANGHI
   60 FORMAT('THE PEAKS WILL BE STUDIED FROM: ',F8.2,' TO ',F8.2)
   99 RETURN
      END
```

9.7 Subroutine ALINE

```
FTN4
      SUBROUTINE ALINE(B,IDIM,WIDTH,KCNTR,NFOR,RINTN,AREA1,AREA2,AREA3,
     1                 CHOICE)
      DIMENSION B(8),RINTN(IDIM)
      INTEGER CHOICE
      COMMON X(500)
      RAD=0.0174533
      W2=WIDTH/2.
      WA=0.555556
      WB=0.888889
      T1=0.774597
      IDMM2=IDIM-2
      AREA1=0.
      AREA2=0.
      AREA3=0.
C
C       SIMPSON'S RULE TO DETERMINE AREA UNDER PEAK, AREA1
C
      DO 20 K=1,IDMM2,2
       AREA1=AREA1 + 2.*RINTN(K) + 4.*RINTN(K+1)
   20 CONTINUE
      AREA1=(AREA1-RINTN(1)+RINTN(IDIM))*(X(2)-X(1))/3.
C
      IF(CHOICE .EQ. 1 .OR. CHAOICE .EQ. 0) GO TO 70
C      GAUSSIAN QUADRATURE TO DETERMINE THE AREA FROM MEASURED TO THE
C      ENDS OF THE PEAK (AT S=-0.5, S=0.5)
      HTFRC=100.*PK(B,X(KCNTR)-W2)/(B(1)+B(5))
      A=1./SIN(X(KCNTR)*RAD/2.)
      XLO=2.*ATAN(1./SQRT(4*A*A-1.))/RAD
      X1=((X(1)-XLO)*(-T1) + X(1) + XLO)/2.
      X2=(X(1)+XLO)/2.
      X3=((X(1)-XLO)*T1 + X(1) + XLO)/2.
      AREA2=(WA*(PK(B,X1)+PK(B,X3)) +WB*PK(B,X2))*(X(1)-XLO)/2.
C
      IF(CHOICE .EQ. 2) GO TO 70
      XHI=2.*ATAN(SQRT(4.*A*A-9.))/RAD
      X1=((X(IDIM)-XHI)*(-T1)+X(IDIM)+XHI)/2.
      X2=(X(IDIM)+XHI)/2.
      X3=((XHI-X(IDIM))*T1+X(IDIM)+XHI)/2.
      AREA3=(WA*(PK(B,X1)+PK(B,X3))+WB*PK(B,X2))*(XHI-X(IDIM))/2.
C
      ARFRC=AREA1/(AREA1+AREA2+AREA3)
      HITE=B(1)+B(5)
      WRITE(1,50) HITE,HTFRC
 50    FORMAT(2X,'THE MAX. PEAK HT. IS: ',F8.2,
      &/,2X,'THE EDGE IS AT: ',F8.2,' % OF THE PEAK MAX HT')
       WRITE(1,60) AREA1, ARFRC
 60    FORMAT(2X,'THE AREA STUDIED: 'F8.3,' DEG 2THETA*C/S',
      &/,2X,'WHICH IS: 'F8.2,' % OF THE TOTAL AREA')
 C
 70    RETURN
       END
```

9.8 Subroutine CNTRD

```
FTN4
      SUBROUTINE CNTRD(NAME,IDIM,IANG,RINT,MINAN,MAXAN,CNTR,IOUT,AREA)
      DIMENSION IANG(1000),RINT(1000),NAME(5)
      IDEL=IANG(3)-IANG(2)
      DELAN=FLOAT(IDEL)/100.
      SUM1=0.
      SUM2=0.
C
C      SET NPONT (THE NUMBER OF INTEGRATING POINTS) TO AN ODD NUMBER
C
      NPONT=IDIM
      TEST1=FLOAT(NPONT/2)
      TEST2=FLOAT(NPONT)/2.
      IF((TEST2-TEST1).LT.0.1) NPONT=NPONT-1
C
      DO 20 I=1,NPONT,2
       XFI=RINT(I)*FLOAT(IANG(I))
       XFIP1=RINT(I+1)*FLOAT(IANG(I+1))
       SUM1=SUM1 + XFI*2. + XFIP1*4.
       SUM2=SUM2 + RINT(I)*2. + RINT(I+1)*4.
  20  CONTINUE
      XF1=RINT(1)*FLOAT(IANG(1))
      XFN=RINT(NPONT)*FLOAT(IANG(NPONT))
      SUM1=SUM1-XF1-XFN
      SUM2=SUM2-RINT(1)-RINT(NPONT)
      AREA=DELAN*SUM2/3.
      CNTR=SUM1/(SUM2*100.)
      WRITE(IOUT,25) (NAME(I),I=1,3)
  25  FORMAT(/,10X,'** FILE: ',3A2,' **')
      WRITE(IOUT,30) AREA,CNTR
  30  FORMAT('THE PEAK AREA IS:',F8.3,' C*DEG/S',
     & /,'THE CENTROID IS AT: ',F8.3,' DEG 2*THETA')
      RETURN
      END
```

9.9 Subroutine DIST

```
FTN4
      SUBROUTINE DIST(IANG,RINT,IDIM)
C
C        CHANGE ANGLE TO INTERPLANAR DISTANCE BY:
C         X=1/D=2*SIN(THETA)/LAMBDA
C            LAMBDA=1.5418 ANGSTROM
C            IANG=100*2*THETA
C        THIS ROUTINE ALSO PERFORMS APPROXIMATE ANGULAR CORRECTIONS
C        ON THE INTENSITY OF SUBTRACTED PROFILES
C
C        LET APPARENT INTENSITY=PURE INTENSITY*K(THETA)
C        WHERE K(THETA)=LORENZ-POLARIZATION *TEMP *SCATTERING FACTORS
C
C
C
C          X(K)=ANGLE (in Degrees 2*Theta)
C
      DIMENSION IANG(IDIM),RINT(IDIM)
      COMMON X(500)
      RLAM=1.5418
      RINMX=0.0
      XINMX=0.0
      XHAF=0.0
      WRITE(1,10)
   10 FORMAT('ENTER "1" TO APPLY ANGLE CORRECTION')
      READ(1,*) ICOR
      IF(ICOR.NE.1) GO TO 75
C
C     CORRECT INTENSITY
C
C        CALCULATE THE TEMPERATURE FACTOR CONSTANTS
C        ASSUMING CUBIC CRYSTALS OF PT-IR ALLOY
C        VALUES OF PHI FROM LINEAR APPROXIMATION OF
C        Cullity, Appendix 15.
C
      ITEMP=0
      TDEBY=257.5
      TEMP=293.
      X1=TDEBY/TEMP
      IF(X1.LT.0.7.OR.X1.GT.1.0) GO TO 15
      PHI=0.839-(X1-0.7)*0.203
      A=77.5
      RM1=1.15E4*TEMP/(TDEBY*TDEBY*A)*(PHI+X1/4.)
      GO TO 20
   15 WRITE(1,16)
   16 FORMAT('**ERROR-TEMPERATURE EXCEEDS RANGE FOR TEMPERATURE'
     1 ,' FACTOR INTERPOLATION-- TEMP FACTOR SET=1.0')
      ITEMP=1
      RM1=0.
   20 DO 50 K=1,IDIM
        TWOTH=(3.141592/180.)*FLOAT(IANG(K))/100.
        THETA=TWOTH/2.
C
C        CALCULATE THE RECIPROCAL INTERPLANAR DISTANCES,X
C
        X(K)=2.*SIN(THETA)/RLAM
```

```
C
C       CALCULATE THE LORENZ-POLARIZATION FACTOR
C
       RLPF=(1.0+(COS(TWOTH))**2)/(SIN(THETA)*SIN(THETA)*COS(THETA))
C
C       CALCULATE THE TEMPERATURE FACTOR
C
       TF=EXP(-2.*RM1*(X(K)/2.)**2)
       IF(ITEMP.EQ.1) TF=1.0
       RINT(K)=RINT(K)/(RLPF*TF)
C
C       CALCULATE THE SCATTERING FACTOR
C
       F=77.01-34.8*X(K)
       IF(X(K).GE.0.38.AND.X(K).LE.1.0) GO TO 40
   30  WRITE(1,31)
   31  FORMAT('**WARNING-RECIPROCAL LATTICE SPACING OUT OF'
     1  ,' RANGE-')
   40  RINT(K)=RINT(K)/(F*F)
C

C       RESCALE THE PEAK (ARBITRARILY BY 50000*)
C
       RINT(K)=RINT(K)*5.E4
C      RINMX=AMAX1(RINMX,RINT(K))
C      IF(RINMX.EQ.RINT(K)) XINMX=X(K)
C      RIHAF=RINMX/2.
C      IF(RINT(K).LE.RIHAF.AND.RINT(K-1).GE.RIHAF)
C    1  XHAF=X(K)
       X(K)=FLOAT(IANG(K))/100.
   50 CONTINUE
C
C      LIST THE CORRECTED PEAK IF DESIRED
C
      WRITE(1,60)
   60 FORMAT('ENTER "1" FOR A LIST OF THE CORRECTED PEAK')
      READ(1,*) ILIST
      IF(ILIST.NE.1) GO TO 81
      DO 70 K=1,IDIM
       WRITE(1,65) IANG(K),RINT(K)
   65  FORMAT(2X,I5,2X,F8.4)
   70 CONTINUE
      GO TO 81
C
C       GENERATE THE RECIPROCAL SPACINGS IF NO CORRECTION IS REQUESTED
C
   75 DO 80 K=1,IDIM
       THETA=(3.141592/180.)*FLOAT(IANG(K))/(100.*2.)
C      X(K)=2.*SIN(THETA)/RLAM
       X(K)=FLOAT(IANG(K))/100.
C      RINMX=AMAX1(RINMX,RINT(K))
C      IF(RINMX.EQ.RINT(K)) XINMX=X(K)
C      RIHAF=RINMX/2.
C      IF(RINT(K).LE.RIHAF.AND.RINT(K-1).GE.RIHAF)
C    1  XHAF=X(K)
   80 CONTINUE
   81 CONTINUE
```

```
C  81 IF(XHAF.GT.1.E-6) GO TO 82
C     XHAF=(X(1)+XINMX)/2.
C  82 WRITE(1,83) RINMX,XINMX,XHAF
C  83 FORMAT(2X,'THE MAXIMUM PEAK HEIGHT IS: ',F8.2,
C    1 /,'AT RECIPROCAL SPACING: ',F8.4,' ANGSTROM**-1',
C    2 /,'THE HALF HEIGHT OF THE PEAK OCCURS AT: ',F8.4)
  100 RETURN
      END
```

9.10 Subroutine ESTB

```
FTN4
      SUBROUTINE ESTB(RINT,IANG,IDIM,NPAR,PARA,PARMN,PARMX)
C
C     ESTIMATE THE PARAMETERS FOR THE BEST FIT CAUCHY CURVE
C
       DIMENSION PARA(NPAR),PARMN(NPAR),PARMX(NPAR)
       DIMENSION RINT(1),IANG(1)
       DIMENSION IPAR(2)
       COMMON X(500)
C
C       Estimate the parameters for the best fit Modified Cauchy
C               F = F1 + F2
C         where
C               F1=PARA(1)/(1 + PARA(2)*U*(ANG-PARA(3))**2)**PARA(4)
C               F2=PARA(5)*EXP(-PARA(6)*U*(ANG-PARA(3))**2)**PARA(7)
C                U=1.0 if X<PARA(3)
C                U=PARA(8) if X>PARA(3)
C         ASSUME:
C               PARA(1)=PARA(5)=(PEAK HT)/2.
C               PARA(4)=PARA(7)=PARA(8)=1.0
C
      IANHF=0
      IANMX=0
      NPEAK=NPAR/8
      DO 10 I=1,NPAR
       PARA(I)=1.
   10 CONTINUE
      IF(NPAR.GT.8) GO TO 30
      DO 20 K=1,IDIM
       PARA(1)=AMAX1(PARA(1),RINT(K))
       IF(PARA(1).EQ.RINT(K)) IANMX=IANG(K)
       RIHAF=PARA(1)/2.
       IF(RINT(K).LE.RIHAF.AND.RINT(K-1).GE.RIHAF) IANHF=IANG(K)
   20 CONTINUE
      IF(IANHF.GT.0) GO TO 22
      IANHF=(IANG(1)+IANMX)/2
   22 PARA(1)=PARA(1)/2.
      PARA(2)=ABS((FLOAT(IANMX-IANHF))/100.)**(-2)
      PARA(3)=FLOAT(IANMX)/100.
      PARA(5)=PARA(1)
      PARA(6)=0.6931/(FLOAT(IANHF-IANMX)/100.)**2
      GO TO 110
   30 WRITE(1,35) NPEAK
   35 FORMAT(/,2X,'THE PROGRAM WILL ATTEMPT TO FIND ',I5,' PEAKS',
     & /,5X,'ENTER THE INITIAL GUESSES FOR PEAK LOCATION',
     & /,10X,'1 - The (111) Peaks of Pt and Ir '
     & /,10X,'2 - The (200) Peaks of Pt and Ir '
     & /,10X,'3 - Enter the initial guesses, deg 2*theta')
      READ(1,*) IGESS
      IF(IGESS.LT.1.OR.IGESS.GT.3) GO TO 30
      IF(IGESS.GT.2) GO TO 50
      IF(IGESS.GT.1) GO TO 40
      PARA(3)=39.79
      PARA(11)=40.71
      IF(NPEAK.LT.3) GO TO 60
      PARA(11)=40.25
      GO TO 60
   40 PARA(3)=46.27
      PARA(11)=47.36
      GO TO 60
   50 READ(1,*)(PARA(I),I=3,NPAR,8)
C
   60 DO 80 I=1,NPEAK
        IPAR(I)=IFIX(PARA(3+8*(I-1))*100.)
        DO 70 K=1,IDIM
          IF(IPAR(I).GE.IANG(K).AND.IPAR(I).LE.IANG(K+1))
     &     PARA(1+8*(I-1))=RINT(K)/2.
   70   CONTINUE
      PARA(5+8*(I-1))=PARA(1+8*(I-1))
   80 CONTINUE
C
  110 DO 120 I=1,NPAR,8
        PARMN(I)=PARA(I)/100.
        PARMX(I)=PARA(I)*5.0
        PARMN(I+1)=0.001
        PARMX(I+1)=1000.
        PARMN(I+2)=PARA(I+2)*0.8
        PARMX(I+2)=PARA(I+2)*1.2
        PARMN(I+3)=0.5
        PARMX(I+3)=20.0
        PARMN(I+4)=PARMN(I)
        PARMX(I+4)=PARMX(I)
        PARMN(I+5)=PARA(I+5)/50.
        PARMX(I+5)=PARA(I+5)*50.
        PARMN(I+6)=0.5
        PARMX(I+6)=20.
        PARMN(I+7)=0.1
        PARMX(I+7)=1.5
  120 CONTINUE
C
  200 WRITE(1,220)
  220  FORMAT('INITIAL GUESSES ARE:'/,12X,'GUESS',10X,'MIN',10X,'MAX')
      DO 240 I=1,NPAR
        WRITE(1,230) I,PARA(I),PARMN(I),PARMX(I)
  230  FORMAT(3X,I4,3(5X,1PE10.2))
  240 CONTINUE
  245 WRITE(1,250)
  250 FORMAT('ENTER THE PARAMETER TO BE CHANGED')
      READ(1,*) JPAR
      IF(JPAR.LT.1) GO TO 999
      WRITE(1,260) JPAR
  260 FORMAT('ENTER THE NEW PARAMETER, MIN, AND MAX FOR NO. ',I5)
      READ(1,*) PARA(JPAR),PARMN(JPAR),PARMX(JPAR)
      GO TO 200
  999 RETURN
        END
```

9.11 Subroutine FIT

```
FTN4
      SUBROUTINE FIT(IDIM,NPAR,B,BMIN,BMAX,Y,IOUT)
C     MAIN LINE PROGRAM FOR SUBROUTINE BSOLVE
C     WRITTEN BY W.BALL MODIFIED FOR XPROF BY W.C.S. PICK
C
C     DESCRIPTION OF USER PARAMETERS
C
C    NN = NUMBER OF DATA POINTS OR NUMBER OF EQUATIONS
C    KK = NUMBER OF UNKNOWN COEFFICIENTS
C     B = VECTOR OF UNKNOWN COEFFICIENTS
C  BMIN = VECTOR OF MINIMUM VALUES OF B
C  BMAX = VECTOR OF MAXIMUM VALUES OF B
C     X = VECTOR OF THE INDEPENDENT VARIABLE DATA POINTS(1)
C     Y = VECTOR OF DEPENDENT VARIABLE
C    PH = LEAST SQUARES OBJECTIVE FUNCTION
C     Z = COMPUTED VALUES OF DEPENDENT VARIABLE
C    BV = CODE VECTOR: 1.0 FOR NUMERICAL DERIVITAVES
C
C (1) THIS PROGRAM IS CURRENTLY SET UP FOR ONE INDEPENDENT VARIABLE
C
C     DESCRIPTION OF OUTPUT PARAMETERS
C
C  ICON = THE NUMBER OF COEFFICIENTS NOT SATISFYING THE CONVERGENCE
C         CRITERION
C     B = THE FINAL VALUE OF THE REGRESSION COEFFICIENTS
C  YCAL = THE VALUE OF THE DEPENDENT CALCULATED FROM THE REGRESSION
C         COEFFICIENTS
C
      DIMENSION P(2000),A(16,18),AC(16,18),FV(16),DV(16)
      DIMENSION B(16),Z(250),Y(IDIM),BV(16),BMIN(16),BMAX(16)
      COMMON X(500)
C     EXTERNAL FUNC
      NI = 1
      NO = 1
C     READ IN NUMBER OF DATA POINTS, UNKNOWNS.
C     READ (NI,*) NN, KK
      NN=IDIM
      KK=NPAR
C011  FORMAT (8I10)
C     READ IN INITIAL GUESSES.
C     READ (NI,*) (B(J), J=1,KK)
C12   FORMAT(8E10.3)
C     READ IN LIMITS ON VARIABLES.
C     READ (NI,*) (BMIN(J), J=1,KK)
C     READ (NI,*) (BMAX(J), J=1,KK)
C     READ IN INDEPENDENT VARIABLES.
C     READ IN DEPENDENT VARIABLES.
C     READ (NI,*) (X(I), I=1,NN)
C     READ(NI,*) (Y(I),I=1,NN)
C 847 FORMAT(10F8.6)
C 851 FORMAT(10F8.4)
      FNU=0.0
      FLA=0.0
      TAU=0.0
      EPS=0.0
      PHMIN=0.0
      I=0
      KD=KK
      FV(1)=0.0
      DO 100 J=1,KK
      BV(J)=1
 100  CONTINUE
      ICON=KK
      ITER = 0
      WRITE (IOUT,015)
 015  FORMAT (1H1,10X,27HBSOLVE REGRESSION ALGORITHM )
C     WRITE(NO,018)
C18   FORMAT(' ',//,'  RAW DATA  ',//,12X,'X',14X,'  Y ')
C     DO 701 J=1,NN
C701  WRITE(NO,017)X(J),Y(J)
      WRITE(NO,016)
  016 FORMAT(' ',//,'    INITIAL GUESSES    UPPER LIMITS    LOWER
     1')
      DO 700 J=1,KK
 700  WRITE(NO,~~017)B(J)~~,BMAX(J),BMIN(J)
 017  FORMAT(3E17.3)
 1050 DO 1099 ICONT=1,10
 200  CALL BSOLVE(KK,B,NN,Z,Y,PH,FNU,FLA,TAU,EPS,PHMIN,I,ICON,FV,DV,BV,
     1BMIN,BMAX,P,DERIV,KD,A,AC,GAMM)
      ITER=ITER+1
      WRITE (NO,001) ICON, PH, ITER
 001  FORMAT (/,2X,6HICON = ,I3,4X, 5HPH = ,E15.8,4X, 16HITERATION
     1 ,I3)
      IF (ICON) 10, 300, 1099
 10   IF (ICON+1)   20, 60, 1099
 20   IF (ICON+2)   30, 70, 1099
 30   IF (ICON+3)   40, 80, 1099
 40   IF (ICON+4)   50, 90, 1099
 50   GO TO 95
 1099 CONTINUE
      DO 1100 J=1,KK
 1100 WRITE(1,018)J, B(J)
  018  FORMAT(2X,I5,1PE15.8)
      WRITE(1,1110)
 1110  FORMAT('ENTER "1" TO STOP ITERATIONS')
      READ(1,*) ISTOP
      IF(ISTOP.EQ.1) GO TO 1000
      GO TO 1050
 60   WRITE (NO,004)
 004  FORMAT (//,2X,32HNO FUNCTION IMPROVEMENT POSSIBLE )
      GO TO 300
 70   WRITE (NO,005)
 005  FORMAT (//,2X, 28HMORE UNKNOWNS THAN FUNCTIONS)
      GO TO 300
 80   WRITE (NO,006)
 006  FORMAT (//,2X, 24HTOTAL VARIABLES ARE ZERO)
      GO TO 300
 90   WRITE (NO,007)
 007  FORMAT (//,2X,79HCORRECTIONS SATISFY CONVERGENCE REQUIREMENTS
     1LAMDA FACTOR (FLA) STILL LARGE)
      GO TO 300
 95   WRITE (NO,008)
 008  FORMAT (//,2X, 20HTHIS IS NOT POSSIBLE)
```

```
      GO TO 300
  300 WRITE (IOUT,002)
  002 FORMAT (//,2X, 26HSOLUTIONS OF THE EQUATIONS)
      DO 400 J=1,KK
      WRITE (IOUT,003) J, B(J)
  003 FORMAT (/,2X, 2HB(,I2,4H) = ,E16.8)
  400 CONTINUE
C     WRITE(NO,65)
C65   FORMAT(//,9X,'      X           Y          YCAL'/)
      SUM2=0.0
      DO 63 IE=1,NN
      SUM2=SUM2+(Y(IE)-Z(IE))**2
C     WRITE(NO,66) IE,X(IE),Y(IE),Z(IE)
C66   FORMAT(5X,I2,3E12.4)
   63 CONTINUE
      WRITE(NO,67)SUM2
   67 FORMAT(//,'THE LEAST SQUARES OBJECTIVE FUNCTION = ',E16.6,//)
 1000 RETURN
      END
```

9.12 Subroutine FOR

```
FTN4
      SUBROUTINE FOR(Y,IDIM,KCNTR,NFOR,A,B,IOUT)
      DIMENSION Y(IDIM)
      DOUBLE PRECISION A(NFOR),B(NFOR)
      DOUBLE PRECISION ARG,PI,ASUM,BSUM
      PI=3.1415926535898
      N=2*NFOR+1
      NM1=N-1
      DO 50 JP1=1,NFOR
       J=JP1-1
       ASUM=0.
       BSUM=0.
       DO 25 KPNT=1,N
        K=KPNT-1-NFOR
        KINDX=KCNTR+K
        ARG=2.*PI*FLOAT(J*K)/FLOAT(NM1)
        ASUM=ASUM + Y(KINDX)*DCOS(ARG)
        BSUM=BSUM + Y(KINDX)*DSIN(ARG)
   25  CONTINUE
       A(JP1)=2.*ASUM/FLOAT(NM1)
       B(JP1)=2.*BSUM/(FLOAT(NM1))
   50 CONTINUE
      WRITE(IOUT,70)
   70 FORMAT(/,12X,'FOURIER COEFFICIENTS',/,5X,'J',9X,'A(J)',9X,
     & 'B(J)',8X,'AMP(J)',//)
      NFORO=AMINO(41,NFOR)
      DO 90 JP1=1,NFORO
       J=JP1-1
       AMP=(A(JP1)*A(JP1) + B(JP1)*B(JP1))**0.5
       WRITE(IOUT,80) J,A(JP1),B(JP1),AMP
   80   FORMAT(3X,I3,3(5X,1PE10.3))
   90 CONTINUE
      RETURN
      END
```

9.13 Subroutine MACHP

```
FTN4
      SUBROUTINE MACHP(FR,FI,GR,GI,NFOR,HR,HI)
C
C     ROUTINE TO FOLD TWO PEAKS TOGETHER
C         H = F*G
C
      DOUBLE PRECISION FR(NFOR),FI(NFOR),GR(NFOR),GI(NFOR)
      DOUBLE PRECISION HR(NFOR),HI(NFOR)
      DO 30 JP1=1,NFOR
       HR(JP1)=(FR(JP1)*GR(JP1)-FI(JP1)*GI(JP1))/GR(1)
       HI(JP1)=(FR(JP1)*GI(GP1)+FI(JP1)*GR(JP1))/GR(1)
   30 CONTINUE
      RETURN
      END
```

9.14 Subroutine MARAD

```
FTN4
      SUBROUTINE MARAD(FR,NFOR,ADF,PS,NADF,AREA1,IOUT,A,JP1LO)
      DOUBLE PRECISION FR(NFOR),SUM1,SUM2
      DIMENSION ADF(400),PS(400)
C
C      ROUTINE TO DETERMINE THE AREA WEIGHTED LENGTH DISTRIBUTION
C     FUNCTION FROM THE REAL FOURIER COEFFICIENTS, FR(JP1)
C
C     KEY VARIABLES:
C         A=The Fourier distance, nm
C         PS(JP1)= A length given by: PS(JP1)=(JP1-1.5)*A
C         ADF(JP1)= The area weighted distribution function
C                   normalized to sum(ADF)=1.0
C
C
      WRITE(1,10)
   10  FORMAT('ENTER "1" TO LIST THE AREA WEIGHTED DIST. FUNCTION')
      READ(1,*) ILIST
      IF(ILIST.NE.1) GO TO 100
C
      RLAM=0.1542
      RAD=3.1415926/180.
      WRITE(IOUT,20)
   20  FORMAT(/,5X,'AREA WEIGHTED DISTRIBUTION FUNCTION'/,2X,
     & 'FOURIER FREQUENCY   LENGTH         DISTRIBUTION FUNCTION',/,
     & '                    (NM)    ')
C
      SUM1=0.
      SUM2=0.

      DO 30 I=1,NADF
        PS(I)=0.
        ADF(I)=0.
   30 CONTINUE
      DO 35 JP1=2,JP1LO
        PS(JP1)=(FLOAT(JP1-1)-0.5)*A
   35 CONTINUE
C
      DO 38 JP1=JP1LO,JP1LO+2
        J=JP1-1
        PS(JP1)=(FLOAT(J)-0.5)*A
        ADF(JP1)=(FR(JP1-2)-FR(JP1-1)-FR(JP1)+FR(JP1+1))/2.
      IF(ADF(JP1).GT.0.0) GOTO 39
      ADF(JP1)=0.0
 39   SUM1=SUM1+PS(JP1)*ADF(JP1)
      SUM2=SUM2+ADF(JP1)
 38   CONTINUE
 C
      DO 40 JP1=JP1LO+2,NADF
        J=JP1-1
        PS(JP1)=(FLOAT(J)-0.5)*A
        ADF(JP1)=(FR(JP1-2)-FR(JP1-1)-FR(JP1)+FR(JP1+1))/2.
        SUM1=SUM1+PS(JP1)*ADF(JP1)
        SUM2=SUM2+ADF(JP1)
   40 CONTINUE
```

```
C
      PSAV=SUM1/SUM2
C
      DO 60 JP1=1,NADF
        J=JP1-1
        ADF(JP1)=ADF(JP1)/(SUM2*A)
        WRITE(IOUT,50) J,PS(JP1),ADF(JP1)
   50     FORMAT(5X,I5,10X,F10.3,5X,F10.7)
   60 CONTINUE
  65  WRITE(IOUT,70) PSAV
   70  FORMAT(//,2X,'THE AREA AVERAGE LENGTH IS: ',F10.2,' NM')
  100 RETURN
      END
```

9.15 Subroutine MVOLD

```
FTN4
      SUBROUTINE MVOLD(FR,NFOR,VDF,PS,NVDF,AREA1,IOUT,A,JP1LO)
      DOUBLE PRECISION FR(NFOR),SUM1,SUM2
      DIMENSION VDF(400),PS(400)
C
      WRITE(1,10)
10    FORMAT('ENTER "1" TO LIST THE VOLUME WEIGHTED DISTR. FUNCTION')
      READ(1,*) ILIST
      IF(ILIST.NE.1) GO TO 100
C
      RLAM=0.1542
      RAD=3.1415926/180.
C
      WRITE(IOUT,20)
20    FORMAT(/,5X,'VOLUME WEIGHTED DISTRIBUTION FUNCTION'/,2X
     & 'FOURIER FREQUENCY   LENGTH        DISTRIBUTION FUNCTION',/,2X
     & '                     (NM)    ')
C
      SUM1=0.
      SUM2=0.

      DO 30 I=1, NVDF
        PS(I)=0.
        VDF(I)=0.
30    CONTINUE
      DO 35 JP1=2,JP1LO
        PS(JP1)=(FLOAT(JP1-1)-0.5)*A
35    CONTINUE
C
      DO 38 JP1=JP1LO,JP1LO+2
        J=JP1-1
        FACT=(FLOAT(J)-0.5)
        PS(JP1)=(FLOAT(J)-0.5)*A
        VDF(JP1)=(FR(JP1-2)-FR(JP1-1)-FR(JP1)+FR(JP1+1))*FACT/2.

      IF(VDF(JP1).GT.0.0) GOTO 39
      VDF(JP1)=0.0
39    SUM1=SUM1+PS(JP1)*VDF(JP1)
      SUM2=SUM2+VDF(JP1)
38    CONTINUE
C
      DO 40 JP1=JP1LO+2,NVDF
        J=JP1-1
        FACT=(FLOAT(J)-0.5)
        PS(JP1)=(FLOAT(J)-0.5 )*A
        VDF(JP1)=(FR(JP1-2)-FR(JP1-1)-FR(JP1)+FR(JP1+1))*FACT/2.
        SUM1=SUM1+PS(JP1)*VDF(JP1)
        SUM2=SUM2+VDF(JP1)
40    CONTINUE
C
      PSAV=SUM1/SUM2
C
```

```
      DO 60 JP1=1,NVDF
        J=JP1-1
        VDF(JP1)=VDF(JP1)/(SUM2*A)
        WRITE(IOUT,50) J,PS(JP1),VDF(JP1)
50    FORMAT(5X,I5,10X,F10.3,5X,F10.7)
60    CONTINUE
65    WRITE(IOUT,70) PSAV
70    FORMAT(//,2X,'THE AVERAGE PARATICLE SIZE IS: ',F10.2,'NM')
100   RETURN
      END
```

9.16 Subroutine NEWPK

```
FTN4
      SUBROUTINE NEWPK(B,NPAR,IDIMR,RINTN,IANG,RINT,IOUT)
      DIMENSION B(12),RINTN(IDIMR),IANG(IDIMR),RINT(IDIMR)
      COMMON X(500)
      CALL FUNC(NPAR,B,IDIMR,RINTN,FV)
C
      WRITE(1,40)
   40 FORMAT('ENTER "1" TO LIST THE VOIGT FIT PEAK')
      READ(1,*) ILIST
      IF(ILIST.NE.1) GO TO 100
      WRITE(IOUT,50)
  50  FORMAT(//,'PEAK COMPARISON'/,5X,'ANGLE',3X,'OLD PEAK',
     & 3X,'NEW ANGLE',3X,'NEW PEAK')
      DO 70 K=1,IDIM
       ANG=FLOAT(IANG(K))/100.
       WRITE(IOUT,60) ANG,RINT(K),X(K),RINTN(K)
  60  FORMAT(3X,4(5X,F8.2))
   70 CONTINUE
  100 RETURN
      END
```

9.17 Subroutine NEWX

```
FTN4
      SUBROUTINE NEWX(B,IDIM,WIDTH)
      DIMENSION B(6)
      COMMON X(500)
      X(1)=B(3)-WIDTH/2.
      XDEL=WIDTH/FLOAT(IDIM-1)
      DO 20 K=2,IDIM
       X(K)=X(K-1)+XDEL
   20 CONTINUE
      RETURN
      END
```

9.18 Subroutine NINIT

```
FTN4
      SUBROUTINE NINIT(NAME1,MINAN,MAXAN,NPEAK,PMAX,PRANG)
      DIMENSION NAME1(5),CATID(2)
C
      WRITE(1,10)
   10  FORMAT(/,'ENTER THE FILE LOCATION OF THE RAW DATA ')
      READ(1,15) (NAME1(I),I=1,3)
   15  FORMAT(3A2)
C
      WRITE(1,40)
   40  FORMAT(/,'ENTER THE APPROXIMATE PEAK LOCATION AND THE RANGE',
     & ' OF INTEREST')
      READ(1,*)PMAX,PRANG
      MINAN=IFIX((PMAX-PRANG/2.)*100.)
      MAXAN=IFIX((PMAX+PRANG/2.)*100.)
      WRITE(1,50)
   50 FORMAT(/,' ENTER THE NUMBER OF PEAKS, NPEAK')
      READ(1,*) NPEAK
      WRITE(1,70)
   70  FORMAT('ENTER THE CATALYST IDENTIFICATION CODE (EG PI16)')
      READ(1,15) (CATID(I),I=1,2)
      WRITE(IOUT,80) (CATID(I),I=1,2)
   80  FORMAT(//,10X,'FOURIER ANALYSIS OF PEAKS IN CATALYST: ',2A2)
      RETURN
      END
```

9.19 Subroutine NNNPK

```
FTN4
      SUBROUTINE NNNPK(B,NPAR,IDIMR,RINTN,IANG,RINT,IOUT)
      DIMENSION B(12),RINTN(IDIMR),IANG(IDIMR),RINT(IDIMR)
      COMMON X(500)
      CALL FUNC(NPAR,B,IDIMR,RINTN,FV)
C
      WRITE(1,40)
   40 FORMAT('ENTER "1" TO LIST THE VOIGT FIT PEAK')
      READ(1,*) ILIST
      IF(ILIST.NE.1) GO TO 100
      DO 70 K=1,IDIMR
      X(K)=IFIX(X(K)*100.)
       WRITE(IOUT,60) X(K),RINTN(K)
   60  FORMAT(4X,I5,4X,F8.3)
   70 CONTINUE
  100 RETURN
      END
```

9.20 Subroutine NREAD

```
FTN4
      SUBROUTINE NREAD(IDCB,NAME,MINAN,MAXAN,IDEL,IDIM,IANG,RINT)
      DIMENSION NAME(5),IDCB(144),IBUF(10),IANG(1000),RINT(1000)
      CALL OPEN (IDCB,IERR,NAME,0,NAME(4),NAME(5))
      IF(IERR.LT.0) GO TO 100
      KK=0
      WRITE(1,5) (NAME(I),I=1,3)
    5 FORMAT(/,'ENTER THE SCALING FACTOR FOR FILE ',3A2)
      READ(1,*) SCAL1
      DO 50 K=1,10000
       DO 10 I=1,10
         IBUF(I)=2H
   10  CONTINUE
       KK=KK+1
       CALL READF(IDCB,IERR,IBUF,10,LEN)
       IF(IERR.LT.0) GO TO 80
       IF(LEN.EQ.-1) GO TO 100
       CALL CODE
       READ(IBUF,*) IANG(KK),RINT(KK)
       RINT(KK)=RINT(KK)*SCAL1
       IF(IANG(KK).GT.MAXAN) GO TO 55
       IF(IANG(KK).LT.MINAN) KK=0
   50 CONTINUE
   55 CONTINUE
      IDEL=2*(IANG(3)-IANG(2))


      IDIM=(KK-1)/2+1
      DO 77 I=1,IDIM
      II=I*2-1
      IANG(I)=IANG(II)
      RINT(I)=RINT(II)
 77    CONTINUE
      GO TO 100
   80 WRITE(1,90) IERR
   90 FORMAT(/,5X,'TROUBLE IN FMP CALL, ROUTINE RREAD. IERR= ',I5)
  100 RETURN
      END
```

9.21 Subroutine PROF

```
FTN4
      SUBROUTINE PROF(HR,HI,GR,GI,FR,FI,NFOR,IOUT)
      DOUBLE PRECISION HR(NFOR),HI(NFOR),GR(NFOR),GI(NFOR)
      DOUBLE PRECISION DEN,FR(NFOR),FI(NFOR)
C
      F0=H0/G0
C
      DO 20 JP1=1,NFOR
       DEN=GR(JP1)*GR(JP1) + GI(JP1)*GI(JP1)
       FR(JP1)=(HR(JP1)*GR(JP1) +HI(JP1)*GI(JP1))/DEN
       FI(JP1)=(HI(JP1)*GR(JP1) - HR(JP1)*GI(JP1))/DEN
   20 CONTINUE
C
      WRITE(IOUT,30)
   30   FORMAT(/,20X,'** PURE PROFILE FOURIER COEFFICIENTS **',
     & /,10X,'J',8X,'FR',8X,'FI',7X,'AMP',/)
      DO 50 JP1=1,NFOR
       J=JP1-1
       AMP=(FR(JP1)*FR(JP1) + FI(JP1)*FI(JP1))**0.5
       WRITE(IOUT,40) J,FR(JP1),FI(JP1),AMP
   40   FORMAT(6X,I5,3(2X,F8.3))
   50 CONTINUE
      RETURN
      END
```

9.22 Subroutine RREAD

```
FTN4
      SUBROUTINE RREAD(IDCB,NAME,MINAN,MAXAN,IDEL,IDIM,IANG,RINT)
      DIMENSION NAME(5),IDCB(144),IBUF(10),IANG(1000),RINT(1000)
      CALL OPEN (IDCB,IERR,NAME,0,NAME(4),NAME(5))
      IF(IERR.LT.0) GO TO 100
      KK=0
      WRITE(1,5) (NAME(I),I=1,3)
    5 FORMAT(/,'ENTER THE SCALING FACTOR FOR FILE ',3A2)
      READ(1,*) SCAL1
      DO 50 K=1,10000
       DO 10 I=1,10
         IBUF(I)=2H
   10  CONTINUE
       KK=KK+1
       CALL READF(IDCB,IERR,IBUF,10,LEN)
       IF(IERR.LT.0) GO TO 80
       IF(LEN.EQ.-1) GO TO 100
       CALL CODE
       READ(IBUF,*) IANG(KK),RINT(KK)
       RINT(KK)=RINT(KK)*SCAL1
       IF(IANG(KK).GT.MAXAN) GO TO 55
       IF(IANG(KK).LT.MINAN) KK=0
   50 CONTINUE
   55 CONTINUE
      IDEL=IANG(3)-IANG(2)
      IDIM=KK
      GO TO 100
   80 WRITE(1,90) IERR
   90 FORMAT(/,5X,'TROUBLE IN FMP CALL, ROUTINE RREAD. IERR= ',I5)
  100 RETURN
      END
```

9.23 Subroutine WIND1

```
FTN4
      SUBROUTINE WIND1(RINT,KCNTR,NFOR,IDIM)
      DIMENSION RINT(IDIM)
      COMMON X(500)
      N=NFOR*2+1
      PI=3.1415926535
      WRITE(1,10)
   10  FORMAT('ENTER "1" TO APPLY THE MODIFIED HANNING WINDOW')
      READ(1,*)IWIN
      IF(IWIN.NE.1) GO TO 100
      WRITE(1,20) N
   20 FORMAT('ENTER THE NO. OF TAPERED COEFS. IN THE WINDOW, M2M',
     & /,5X,'(TOTAL NO. OF POINTS=',I4,')')
      READ(1,*)M2M
      M=M2M/2
      DO 60 K=1,N
        KINDX=KCNTR-NFOR-1+K
        IF(K.GT.M) GO TO 30
        ARG=PI*(FLOAT(K)-1.5)/FLOAT(M)
        WIN=0.5*(1.-COS(ARG))
        GO TO 50
   30   IF(K.GT.N-M) GO TO 40
        WIN=1.
        GO TO 50
   40   ARG=PI*(FLOAT(N-K)+0.5)/FLOAT(M)
        WIN=0.5*(1.-COS(ARG))
   50   RINT(KINDX)=RINT(KINDX)*WIN
   60 CONTINUE
C
      WRITE(1,70)
   70  FORMAT('ENTER "1" TO LIST SPLIT COS BELL WINDOW FITTED SERIES')
      READ(1,*) ILIST
      IF(ILIST.NE.1) GO TO 100
      DO 90 K=1,N
        KINDX=KCNTR-NFOR-1+K
        WRITE(1,80) X(KINDX),RINT(KINDX)
   80    FORMAT(2(5X,F10.2))
   90 CONTINUE
  100 RETURN
      END
```

10. Appendix B. Tabulation of Results

Data sheets for each of the runs are located in this appendix. The names of the x-ray diffraction files in the HP-1000 computer and the parameters used in obtaining the subtracted diffraction patterns are presented. The parameters in the function used to fit the subtracted patterns (Eq. 5.3), the fraction of Pt detected, and the various average Pt crystallite sizes are also presented for each run.

DATA AND RESULTS SHEET FOR XRD PATTERNS

XRD Data Files:

Catalyst: XRYU15 Support: XRYU04

Catalyst Identification: GC1-1
Platinum Loading: 1.05 wt%

Parameters for Subtraction of Support Pattern

Scaling Factor for Catalyst = 1.0
Scaling Factor for Support = 0.95
Baseline Correction Parameters:
angle (° 2θ) 36.0, 44.0
magnitude(c/s) 13.0, 2.0

Results of Fitting Subtracted Pattern

Centre of Fit = 39.694 °2θ
Range of Angle Fit = ±4 °2θ
Fraction of Pt Detected by XRD = 0.21

Parameter Values in Fitting Function:
B1=8.110 B2=128.434 B3=39.694 B4=0.500
B5=6.036 B6=4.205 B7=1.034 B8=0.559

Number of Iterations = 173; Fit Converged: Yes
Residual Sum of Errors Squared = 138 $(c/s)^2$
Maximum Intensity of Fitted Peak = 14.15 c/s

Integrated Area = 13.25 (c/s * °2θ)
Width at Half-height = 0.0107 radians
Integral Width = 0.0163 radians

Calculated Pt Crystallite Sizes

$D_{1/2}$ (Based on Half-width) = 13.82 nm
D_i (Based on Int. width) = 10.04 nm
<Da> (Fourier Analysis) = 7.26 nm
<Dv> (Fourier Analysis) = 9.98 nm

DATA AND RESULTS SHEET FOR XRD PATTERNS

XRD Data Files:

Catalyst: XRYU16 Support: XRYU04

Catalyst Identification: GC1-2
Platinum Loading: 1.05 wt%

Parameters for Subtraction of Support Pattern

Scaling Factor for Catalyst = 1.0
Scaling Factor for Support = 0.95
Baseline Correction Parameters:
angle (° 2θ) 36.0, 44.0
magnitude(c/s) 10.0, -1.0

Results of Fitting Subtracted Pattern

Centre of Fit = 39.69 °2θ
Range of Angle Fit = ±4 °2θ
Fraction of Pt Detected by XRD = 0.42

Parameter Values in Fitting Function:
B1=18.602 B2=92.052 B3=39.692 B4=0.500
B5=11.135 B6=8.331 B7=0.928 B8=0.608

Number of Iterations = 286; Fit Converged: Yes
Residual Sum of Errors Squared = 152 $(c/s)^2$
Maximum Intensity of Fitted Peak = 29.74 c/s

Integrated Area = 26.68 (c/s *°2θ)
Width at Half-height = 0.00932 radians
Integral Width = 0.0157 radians

Calculated Pt Crystallite Sizes

$D_{1/2}$ (Based on Half-width) = 15.84 nm
D_i (Based on Int. width) = 10.45 nm
<Da> (Fourier Analysis) = 7.80 nm
<Dv> (Fourier Analysis) = 11.37 nm

DATA AND RESULTS SHEET FOR XRD PATTERNS

XRD Data Files:

Catalyst: XRYU17 Support: XRYU04

Catalyst Identification: GC1-3
Platinum Loading: 1.05 wt%

Parameters for Subtraction of Support Pattern

Scaling Factor for Catalyst = 1.0
Scaling Factor for Support = 0.95
Baseline Correction Parameters:
angle (° 2θ) 36.0, 44.0
magnitude(c/s) 11.0, -2.0

Results of Fitting Subtracted Pattern

Centre of Fit = 39.69 °2θ
Range of Angle Fit = ±4 °2θ
Fraction of Pt Detected by XRD = 0.59

Parameter Values in Fitting Function:
B1=27.913 B2=75.302 B3=39.694 B4=0.572
B5=17.937 B6=75.910 B7=1.263 B8 =0.557

Number of Iterations = 19; Fit Converged: Yes
Residual Sum of Errors Squared = 142 $(c/s)^2$
Maximum Intensity of Fitted Peak = 45.85 c/s

Integrated Area = 37.15 (c/s *°2θ)
Width at Half-height = 0.00896 radians
Integral Width = 0.01414 radians

Calculated Pt Crystallite Sizes

$D_{1/2}$ (Based on Half-width) = 16.47 nm
D_i (Based on Int. width) = 11.66 nm
<Da> (Fourier Analysis) = 9.35 nm
<Dv> (Fourier Analysis) = 12.50 nm

DATA AND RESULTS SHEET FOR XRD PATTERNS

XRD Data Files:

Catalyst: XRY26 Support: XRYU04

Catalyst Identification: GC1-4
Platinum Loading: 1.05 wt%

Parameters for Subtraction of Support Pattern

Scaling Factor for Catalyst = 1.0
Scaling Factor for Support = 0.95
Baseline Correction Parameters:
angle (° 2θ) 36.0, 44.0
magnitude(c/s) 11.0, -1.0

Results of Fitting Subtracted Pattern

Centre of Fit = 39.685 °2θ
Range of Angle Fit = ±4 °2θ
Fraction of Pt Detected by XRD = 0.40

Parameter Values in Fitting Function:
B1=16.860 B2=93.434 B3=39.685 B4=0.567
B5=20.258 B6=6.119 B7=1.552 B8=0.836

Number of Iterations = 23; Fit Converged: Yes
Residual Sum of Errors Squared = 69 $(c/s)^2$
Maximum Intensity of Fitted Peak = 37.12 c/s

Integrated Area = 25.07 (c/s *°2θ)
Width at Half-height = 0.00832 radians
Integral Width = 0.01179 radians

Calculated Pt Crystallite Sizes

$D_{1/2}$ (Based on Half-width) = 17.74 nm
D_i (Based on Int. width) = 13.91 nm
<Da> (Fourier Analysis) = 10.14 nm
<Dv> (Fourier Analysis) = 13.48 nm

DATA AND RESULTS SHEET FOR XRD PATTERNS

XRD Data Files:

Catalyst: XRYU30 Support: XRYU04

Catalyst Identification: GC1-5
Platinum Loading: 1.05 wt%

Parameters for Subtraction of Support Pattern

Scaling Factor for Catalyst = 1.0
Scaling Factor for Support = 0.95
Baseline Correction Parameters:
angle (° 2θ) 36.0, 44.0
magnitude(c/s) 10.0, -2.0

Results of Fitting Subtracted Pattern

Centre of Fit = 39.77 °2θ
Range of Angle Fit = ±4 °2θ
Fraction of Pt Detected by XRD = 0.48

Parameter Values in Fitting Function:
B1=18.064 B2=85.234 B3=39.772 B4=0.867
B5=18.271 B6=50.023 B7=34.020 B8=0.682

Number of Iterations = 234; Fit Converged: no
Residual Sum of Errors Squared = 305 $(c/s)^2$
Maximum Intensity of Fitted Peak = 46.63 c/s

Integrated Area = 30.46 (c/s *°2θ)
Width at Half-height = 0.00834 radians
Integral Width = 0.0114 radians

Calculated Pt Crystallite Sizes

$D_{1/2}$ (Based on Half-width) = 17.69 nm
D_i (Based on Int. width) = 14.36 nm
<Da> (Fourier Analysis) = 10.57 nm
<Dv> (Fourier Analysis) = 13.59 nm

DATA AND RESULTS SHEET FOR XRD PATTERNS

XRD Data Files:

Catalyst: XRYU31 Support: XRYU04

Catalyst Identification: GC1-6
Platinum Loading: 1.05 wt%

Parameters for Subtraction of Support Pattern

Scaling Factor for Catalyst = 1.0
Scaling Factor for Support = 0.95
Baseline Correction Parameters:
angle (° 2θ) 36.0, 44.0
magnitude(c/s) 10.0, -3.0

Results of Fitting Subtracted Pattern

Centre of Fit = 39.687 °2θ
Range of Angle Fit = ±4 °2θ
Fraction of Pt Detected by XRD = 0.69

Parameter Values in Fitting Function:
B1=46.501 B2=27.924 B3=39.687 B8=0.839
B5=12.140 B6=11.989 B7=0.981 B8=0.653

Number of Iterations = 19; Fit Converged: Yes
Residual Sum of Errors Squared = 178 $(c/s)^2$
Maximum Intensity of Fitted Peak = 58.64 c/s

Integrated Area = 43.89 (c/s * °2θ)
Width at Half-height = 0.00866 radians
Integral Width = 0.0130 radians

Calculated Pt Crystallite Sizes

$D_{1/2}$ (Based on Half-width) = 17.04 nm
D_i (Based on Int. width) = 12.56 nm
<Da> (Fourier Analysis) = 8.28 nm
<Dv> (Fourier Analysis) = 12.17 nm

DATA AND RESULTS SHEET FOR XRD PATTERNS

XRD Data Files:

Catalyst: XRYU32 Support: XRYU04

Catalyst Identification: GC1-7
Platinum Loading: 1.05 wt%

Parameters for Subtraction of Support Pattern

Scaling Factor for Catalyst = 1.0
Scaling Factor for Support = 0.95
Baseline Correction Parameters:
angle (° 2θ) 36.0, 44.0
magnitude(c/s) 11.0, -2.0

Results of Fitting Subtracted Pattern

Centre of Fit = 39.694 °2θ
Range of Angle Fit = ±4 °2θ
Fraction of Pt Detected by XRD = 0.75

Parameter Values in Fitting Function:
B1=65.51 B2=13.303 B3=39.694 B4=1.377
B5=0.353 B6=3.676 B7=0.746 B8=0.697

Number of Iterations = 13; Fit Converged: Yes
Residual Sum of Errors Squared = 119 $(c/s)^2$
Maximum Intensity of Fitted Peak = 64.86 c/s

Integrated Area = 42.32 (c/s * °2θ)
Width at Half-height = 0.00854 radians
Integral Width = 0.0114 radians

Calculated Pt Crystallite Sizes

$D_{1/2}$ (Based on Half-width) = 17.34 nm
D_i (Based on Int. width) = 14.40 nm
<Da> (Fourier Analysis) = 8.80 nm
<Dv> (Fourier Analysis) = 12.52 nm

DATA AND RESULTS SHEET FOR XRD PATTERNS

XRD Data Files:

Catalyst: XRYU33 Support: XRYU04

Catalyst Identification: GC1-8
Platinum Loading: 1.05 wt%

Parameters for Subtraction of Support Pattern

Scaling Factor for Catalyst = 1.0
Scaling Factor for Support = 0.95
Baseline Correction Parameters:
angle (° 2θ) 36.0, 44.0
magnitude(c/s) 9.0, -3.0

Results of Fitting Subtracted Pattern

Centre of Fit = 39.687 °2θ
Range of Angle Fit = ±4 °2θ
Fraction of Pt Detected by XRD = 0.72

Parameter Values in Fitting Function:
B1=63.135 B2=12.798 B3=39.687 B4=1.285
B5=3.530 B6=15.581 B7=2.355 B8=0.704

Number of Iterations = 67; Fit Converged: Yes
Residual Sum of Errors Squared = 161 $(c/s)^2$
Maximum Intensity of Fitted Peak = 66.60 c/s

Integrated Area = 45.65 (c/s * °2θ)
Width at Half-height = 0.00871 radians
Integral Width = 0.0120 radians

Calculated Pt Crystallite Sizes

$D_{1/2}$ (Based on Half-width) = 16.88 nm
D_i (Based on Int. width) = 13.66 nm
<Da> (Fourier Analysis) = 9.06 nm
<Dv> (Fourier Analysis) = 12.40 nm

DATA AND RESULTS SHEET FOR XRD PATTERNS

XRD Data Files:

Catalyst: XRY130 Support: XRYU04

Catalyst Identification: GC1-9
Platinum Loading: 1.05 wt%

Parameters for Subtraction of Support Pattern

Scaling Factor for Catalyst = 1.0
Scaling Factor for Support = 0.95
Baseline Correction Parameters:
angle (° 2θ) 36.0, 44.0
magnitude(c/s) 3.0, 3.0

Results of Fitting Subtracted Pattern

Centre of Fit = 39.659 °2θ
Range of Angle Fit = ±4 °2θ
Fraction of Pt Detected by XRD = 0.46

Parameter Values in Fitting Function:
B1=36.801 B2=47.932 B3=39.659 B4=0.971
B5=12.511 B6=0.491 B7=14.377 B8=0.587

Number of Iterations = 31; Fit Converged: Yes
Residual Sum of Errors Squared = 210 $(c/s)^2$
Maximum Intensity of Fitted Peak = 49.31 c/s

Integrated Area = 29.06 (c/s * °2θ)
Width at Half-height = 0.0073 radians
Integral Width = 0.0103 radians

Calculated Pt Crystallite Sizes

$D_{1/2}$ (Based on Half-width) = 20.25 nm
D_i (Based on Int. width) = 16.94 nm
<Da> (Fourier Analysis) = 10.79 nm
<Dv> (Fourier Analysis) = 14.40 nm

DATA AND RESULTS SHEET FOR XRD PATTERNS

XRD Data Files:

Catalyst: XRY134 Support: XRYU04

Catalyst Identification: GC1-10
Platinum Loading: 1.05 wt%

Parameters for Subtraction of Support Pattern

Scaling Factor for Catalyst = 1.0
Scaling Factor for Support = 0.95
Baseline Correction Parameters:
  angle (° 2θ) 36.0, 44.0
  magnitude(c/s) 5.0, -4.0

Results of Fitting Subtracted Pattern

Centre of Fit = 39.670 °2θ
Range of Angle Fit = ±4 °2θ
Fraction of Pt Detected by XRD = 0.26

Parameter Values in Fitting Function:
B1=24.876 B2=18.824 B3=39.670 B4=2.138
B5=5.273 B6=7.873 B7=0.549 B8=0.454

Number of Iterations = 35; Fit Converged: Yes
Residual Sum of Errors Squared = 292 $(c/s)^2$
Maximum Intensity of Fitted Peak = 30.15 c/s

Integrated Area = 16.22 (c/s * °2θ)
Width at Half-height = 0.00711 radians
Integral Width = 0.00939 radians

Calculated Pt Crystallite Sizes

$D_{1/2}$ (Based on Half-width) = 20.76 nm
D_i (Based on Int. width) = 17.46 nm
<Da> (Fourier Analysis) = 11.64 nm
<Dv> (Fourier Analysis) = 14.81 nm

DATA AND RESULTS SHEET FOR XRD PATTERNS

XRD Data Files:

Catalyst: XRYU46 Support: XRYU67

Catalyst Identification: GC2-1
Platinum Loading: 1.12 wt%

Parameters for Subtraction of Support Pattern

Scaling Factor for Catalyst = 1.0
Scaling Factor for Support = 0.95
Baseline Correction Parameters:
angle (° 2θ) 38.0, 42.0
magnitude(c/s) 4.0, 7.0

Results of Fitting Subtracted Pattern

Centre of Fit = 39.890 °2θ
Range of Angle Fit = ±4 °2θ
Fraction of Pt Detected by XRD = 0.15

Parameter Values in Fitting Function:
B1=1.980 B2=0.005 B3=39.891 B4=20.000
B5=0.032 B6=3.653 B7=20.00 B8=1.500

Number of Iterations = 310; Fit Converged: Yes
Residual Sum of Errors Squared = 152 $(c/s)^2$
Maximum Intensity of Fitted Peak = 2.01 c/s

Integrated Area = 9.74 (c/s * °2θ)
Width at Half-height = 0.0974 radians
Integral Width = 0.0847 radians

Calculated Pt Crystallite Sizes

$D_{1/2}$ (Based on Half-width) = 1.52 nm
D_i (Based on Int. width) = 1.94 nm
<Da> (Fourier Analysis) < 2.00 nm
<Dv> (Fourier Analysis) < 2.00 nm

DATA AND RESULTS SHEET FOR XRD PATTERNS

XRD Data Files:

Catalyst: XRY106   Support: XRYU87

Catalyst Identification: GC2-2
Platinum Loading: 1.12 wt%

Parameters for Subtraction of Support Pattern

Scaling Factor for Catalyst = 1.0
Scaling Factor for Support = 0.95
Baseline Correction Parameters:
angle (° 2θ) 36.0, 44.0
magnitude(c/s) 1.0, 4.0

Results of Fitting Subtracted Pattern

Centre of Fit = 39.752 °2θ
Range of Angle Fit = ±4 °2θ
Fraction of Pt Detected by XRD = 0.90

Parameter Values in Fitting Function:
B1=7.869 B2=0.190 B3=39.752 B4=2.412
B5=12.438 B6=0.439 B7=0.853 B8=1.242

Number of Iterations = 100; Fit Converged: Yes
Residual Sum of Errors Squared = 210 $(c/s)^2$
Maximum Intensity of Fitted Peak = 20.31 c/s

Integrated Area = 56.94 (c/s * °2θ)
Width at Half-height = 0.0445 radians
Integral Width = 0.0489 radians

Calculated Pt Crystallite Sizes

$D_{1/2}$ (Based on Half-width) = 3.32 nm
D_i (Based on Int. width) = 3.35 nm
<Da> (Fourier Analysis) = 4.99 nm
<Dv> (Fourier Analysis) = 5.37 nm

DATA AND RESULTS SHEET FOR XRD PATTERNS

XRD Data Files:

Catalyst: XRY107 Support: XRYU87

Catalyst Identification: GC2-3
Platinum Loading: 1.12 wt%

Parameters for Subtraction of Support Pattern

Scaling Factor for Catalyst = 1.0
Scaling Factor for Support = 0.95
Baseline Correction Parameters:
angle (°, 2θ) 36.0, 44.0
magnitude(c/s) 1.0, 2.0

Results of Fitting Subtracted Pattern

Centre of Fit = 39.752 °2θ
Range of Angle Fit = ±4 °2θ
Fraction of Pt Detected by XRD = 0.69

Parameter Values in Fitting Function:
B1=4.819 B2=0.101 B3=39.752 B4=3.894
B5=9.953 B6=0.412 B7=0.932 B8=0.959

Number of Iterations = 271; Fit Converged: Yes
Residual Sum of Errors Squared = 210 $(c/s)^2$
Maximum Intensity of Fitted Peak = 14.77 c/s

Integrated Area = 43.84 (c/s * °2θ)
Width at Half-height = 0.0478 radians
Integral Width = 0.0518 radians

Calculated Pt Crystallite Sizes

$D_{1/2}$ (Based on Half-width) = 3.09 nm
D_i (Based on Int. width) = 3.17 nm
<Da> (Fourier Analysis) = 4.94 nm
<Dv> (Fourier Analysis) = 5.03 nm

DATA AND RESULTS SHEET FOR XRD PATTERNS

XRD Data Files:

Catalyst: XRY109 Support: XRYU87

Catalyst Identification: GC2-4
Platinum Loading: 1.12 wt%

Parameters for Subtraction of Support Pattern

Scaling Factor for Catalyst = 1.0
Scaling Factor for Support = 0.95
Baseline Correction Parameters:
angle (° 2θ) 36.0, 44.0
magnitude(c/s) 4.0, 3.0

Results of Fitting Subtracted Pattern

Centre of Fit = 39.667 °2θ
Range of Angle Fit = ±4 °2θ
Fraction of Pt Detected by XRD = 0.26

Parameter Values in Fitting Function:
B1=2.204 B2=0.017 B3=39.667 B4=11.188
B5=2.238 B6=0.112 B7=1.403 B8=1.500

Number of Iterations = 61; Fit Converged: Yes
Residual Sum of Errors Squared = 180 $(c/s)^2$
Maximum Intensity of Fitted Peak = 4.26 c/s

Integrated Area = 16.49 (c/s * °2θ)
Width at Half-height = 0.0639 radians
Integral Width = 0.0675 radians

Calculated Pt Crystallite Sizes

$D_{1/2}$ (Based on Half-width) = 2.31 nm
D_i (Based on Int. width) = 2.43 nm
<Da> (Fourier Analysis) = 4.39 nm
<Dv> (Fourier Analysis) = 4,74 nm

DATA AND RESULTS SHEET FOR XRD PATTERNS

XRD Data Files:

Catalyst: XRY116 Support: XRYU87

Catalyst Identification: GC2-5
Platinum Loading: 1.12 wt%

Parameters for Subtraction of Support Pattern

Scaling Factor for Catalyst = 1.0
Scaling Factor for Support = 0.95
Baseline Correction Parameters:
angle (° 2θ) 36.0, 44.0
magnitude(c/s) 4.0, 3.0

Results of Fitting Subtracted Pattern

Centre of Fit = 39.854 °2θ
Range of Angle Fit = ±4 °2θ
Fraction of Pt Detected by XRD = 0.15

Parameter Values in Fitting Function:
B1=0.715 B2=12.776 B3=39.854 B4=0.759
B5=3.061 B6=0.395 B7=1.128 B8=0.864

Number of Iterations = 31; Fit Converged: Yes
Residual Sum of Errors Squared = 290 $(c/s)^2$
Maximum Intensity of Fitted Peak = 3.73 c/s

Integrated Area = 9.29 (c/s * °2θ)
Width at Half-height = 0.0395 radians
Integral Width = 0.0429 radians

Calculated Pt Crystallite Sizes

$D_{1/2}$ (Based on Half-width) = 3.74 nm
D_i (Based on Int. width) = 3.82 nm
<Da> (Fourier Analysis) = 4.49 nm
<Dv> (Fourier Analysis) = 4.57 nm

DATA AND RESULTS SHEET FOR XRD PATTERNS

XRD Data Files:

Catalyst: XRY142 Support: XRYU87

Catalyst Identification: GC2-6
Platinum Loading: 1.12 wt%

Parameters for Subtraction of Support Pattern

Scaling Factor for Catalyst = 1.0
Scaling Factor for Support = 0.95
Baseline Correction Parameters:
  angle (° 2θ) 38.0, 42.0
  magnitude(c/s) 1.0, 1.0

Results of Fitting Subtracted Pattern

Centre of Fit = 39.719 °2θ
Range of Angle Fit = ±4 °2θ
Fraction of Pt Detected by XRD = 1.00

Parameter Values in Fitting Function:
B1=29.801 B2=5.381 B3=39.719 B4=0.903
B5=15.016 B6=1.831 B7=1.001 B8=0.862

Number of Iterations = 33; Fit Converged: Yes
Residual Sum of Errors Squared = 90 $(c/s)^2$
Maximum Intensity of Fitted Peak = 44.82 c/s

Integrated Area = 63.48 (c/s * °2θ)
Width at Half-height = 0.0188 radians
Integral Width = 0.0247 radians

Calculated Pt Crystallite Sizes

$D_{1/2}$ (Based on Half-width) = 7.85 nm
D_i (Based on Int. width) = 6.64 nm
<Da> (Fourier Analysis) = 6.29 nm
<Dv> (Fourier Analysis) = 7.57 nm

DATA AND RESULTS SHEET FOR XRD PATTERNS

XRD Data Files:

Catalyst: XRY146 Support: XRYU87

Catalyst Identification: GC2-7
Platinum Loading: 1.12 wt%

Parameters for Subtraction of Support Pattern

Scaling Factor for Catalyst = 1.0
Scaling Factor for Support = 0.95
Baseline Correction Parameters:
angle (° 2θ) 38.0, 42.0
magnitude(c/s) 5.0, -1.0

Results of Fitting Subtracted Pattern

Centre of Fit = 39.688 °2θ
Range of Angle Fit = ±4 °2θ
Fraction of Pt Detected by XRD = 0.68

Parameter Values in Fitting Function:
B1=32.888 B2=3.822 B3=39.688 B4=1.975
B5=10.917 B6=2.547 B7=0.500 B8=1.065

Number of Iterations = 26; Fit Converged: Yes
Residual Sum of Errors Squared = 140 $(c/s)^2$
Maximum Intensity of Fitted Peak = 43.81 c/s

Integrated Area = 43.14 (c/s * °2θ)
Width at Half-height = 0.0136 radians
Integral Width = 0.0172 radians

Calculated Pt Crystallite Sizes

$D_{1/2}$ (Based on Half-width) = 10.87 nm
D_i (Based on Int. width) = 9.53 nm
<Da> (Fourier Analysis) = 7.87 nm
<Dv> (Fourier Analysis) = 9.02 nm

DATA AND RESULTS SHEET FOR XRD PATTERNS

XRD Data Files:

Catalyst: XRY148 Support: XRYU87

Catalyst Identification: GC2-8
Platinum Loading: 1.12 wt%

Parameters for Subtraction of Support Pattern

Scaling Factor for Catalyst = 1.0
Scaling Factor for Support = 0.95
Baseline Correction Parameters:
angle (° 2θ) 36.0, 44.0
magnitude(c/s) 5.0, -3.0

Results of Fitting Subtracted Pattern

Centre of Fit = 39.688 °2θ
Range of Angle Fit = ±4 °2θ
Fraction of Pt Detected by XRD = 0.68

Parameter Values in Fitting Function:
B1=24.563 B2=2.619 B3=39.688 B4=1.231
B5=12.382 B6=7.112 B7=1.363 B8=0.928

Number of Iterations = 119; Fit Converged: Yes
Residual Sum of Errors Squared = 158 $(c/s)^2$
Maximum Intensity of Fitted Peak = 36.945 c/s

Integrated Area = 43.46 (c/s * °2θ)
Width at Half-height = 0.0143 radians
Integral Width = 0.0205 radians

Calculated Pt Crystallite Sizes

$D_{1/2}$ (Based on Half-width) = 10.32 nm
D_i (Based on Int. width) = 8.00 nm
<Da> (Fourier Analysis) = 5.96 nm
<Dv> (Fourier Analysis) = 7.87 nm

DATA AND RESULTS SHEET FOR XRD PATTERNS

XRD Data Files:

Catalyst: XRY151 Support: XRYU87

Catalyst Identification: GC2-9
Platinum Loading: 1.12 wt%

Parameters for Subtraction of Support Pattern

Scaling Factor for Catalyst = 1.0
Scaling Factor for Support = 0.95
Baseline Correction Parameters:
angle (° 2θ) 36.0, 44.0
magnitude(c/s) 3.0, -2.0

Results of Fitting Subtracted Pattern

Centre of Fit = 39.441 °2θ
Range of Angle Fit = ±4 °2θ
Fraction of Pt Detected by XRD = 0.00

Parameter Values in Fitting Function:
no Pt detected - no fitting possible

Number of Iterations = 80; Fit Converged: No

Integrated Area = 0.00
Width at Half-height = ****** radians
Integral Width = ****** radians

Calculated Pt Crystallite Sizes

$D_{1/2}$ (Based on Half-width) < 2.00 nm
D_i (Based on Int. width) < 2.00 nm
<Da> (Fourier Analysis) < 2.00 nm
<Dv> (Fourier Analysis) < 2.00 nm

DATA AND RESULTS SHEET FOR XRD PATTERNS

XRD Data Files:

Catalyst: XRY153 Support: XRYU87

Catalyst Identification: GC2-10
Platinum Loading: 1.12 wt%

Parameters for Subtraction of Support Pattern

Scaling Factor for Catalyst = 1.0
Scaling Factor for Support = 0.95
Baseline Correction Parameters:
angle (° 2θ) 36.0, 44.0
magnitude(c/s) 3.0, -3.0

Results of Fitting Subtracted Pattern

Centre of Fit = 39.695 °2θ
Range of Angle Fit = ±4 °2θ
Fraction of Pt Detected by XRD = 1.00

Parameter Values in Fitting Function:
B1=16.798 B2=8.560 B3=39.695 B4=0.630
B5=19.476 B6=1.121 B7=0.868 B8=0.982

Number of Iterations = 47; Fit Converged: Yes
Residual Sum of Errors Squared = 180 $(c/s)^2$
Maximum Intensity of Fitted Peak = 36.27 c/s

Integrated Area = 63.60 (c/s * °2θ)
Width at Half-height = 0.0244 radians
Integral Width = 0.0306 radians

Calculated Pt Crystallite Sizes

$D_{1/2}$ (Based on Half-width) = 6.06 nm
D_i (Based on Int. width) = 5.36 nm
<Da> (Fourier Analysis) = 6.31 nm
<Dv> (Fourier Analysis) = 6.85 nm

DATA AND RESULTS SHEET FOR XRD PATTERNS

XRD Data Files:

Catalyst: XRY155 Support: XRYU87

Catalyst Identification: GC2-11
Platinum Loading: 1.12 wt%

Parameters for Subtraction of Support Pattern

Scaling Factor for Catalyst = 1.0
Scaling Factor for Support = 0.95
Baseline Correction Parameters:
angle (° 2θ) 36.0, 44.0
magnitude(c/s) 6.0, -4.0

Results of Fitting Subtracted Pattern

Centre of Fit = 39.671 °2θ
Range of Angle Fit = ±4 °2θ
Fraction of Pt Detected by XRD = 0.80

Parameter Values in Fitting Function:
B1=39.954 B2=41.135 B3=39.671 B4=0.644
B5=14.883 B6=0.791 B7=2.488 B8=1.180

Number of Iterations = 21; Fit Converged: Yes
Residual Sum of Errors Squared = 211 $(c/s)^2$
Maximum Intensity of Fitted Peak = 54.83 c/s

Integrated Area = 51.20 (c/s * °2θ)
Width at Half-height = 0.00991 radians
Integral Width = 0.0163 radians

Calculated Pt Crystallite Sizes

$D_{1/2}$ (Based on Half-width) = 14.90 nm
D_i (Based on Int. width) = 10.06 nm
<Da> (Fourier Analysis) = 8.07 nm
<Dv> (Fourier Analysis) = 10.31 nm

DATA AND RESULTS SHEET FOR XRD PATTERNS

XRD Data Files:

Catalyst: XRY157 Support: XRYU87

Catalyst Identification: GC2-12
Platinum Loading: 1.12 wt%

Parameters for Subtraction of Support Pattern

Scaling Factor for Catalyst = 1.0
Scaling Factor for Support = 0.95
Baseline Correction Parameters:
angle (° 2θ) 36.0, 44.0
magnitude(c/s) 4.0, -6.0

Results of Fitting Subtracted Pattern

Centre of Fit = 39.678 °2θ
Range of Angle Fit = ±4 °2θ
Fraction of Pt Detected by XRD = 1.00

Parameter Values in Fitting Function:
B1=155.862 B2=96.732 B3=39.678 B4=0.859
B5=6.328 B6=16.447 B7=0.500 B8=1.009

Number of Iterations = 17; Fit Converged: Yes
Residual Sum of Errors Squared = 208 $(c/s)^2$
Maximum Intensity of Fitted Peak = 162.19 c/s

Integrated Area = 63.66 (c/s * °2θ)
Width at Half-height = 0.00668 radians
Integral Width = 0.00685 radians

Calculated Pt Crystallite Sizes

$D_{1/2}$ (Based on Half-width) = 22.09 nm
D_i (Based on Int. width) = 23.94 nm
<Da> (Fourier Analysis) = 13.00 nm
<Dv> (Fourier Analysis) = 20.28 nm

DATA AND RESULTS SHEET FOR XRD PATTERNS

XRD Data Files:

Catalyst: XRY165 Support: XRYU87

Catalyst Identification: GC2-13
Platinum Loading: 1.12 wt%

Parameters for Subtraction of Support Pattern

Scaling Factor for Catalyst = 1.0
Scaling Factor for Support = 0.95
Baseline Correction Parameters:
angle (° 2θ) 36.0, 44.0
magnitude(c/s) 6.0, 1.0

Results of Fitting Subtracted Pattern

Centre of Fit = 39.694 °2θ
Range of Angle Fit = ±4 °2θ
Fraction of Pt Detected by XRD = 0.20

Parameter Values in Fitting Function:
B1=8.389 B2=148.308 B3=39.694 B4=0.509
B5=33.520 B6=91.483 B7=1.733 B8=0.523

Number of Iterations = 330; Fit Converged: Yes
Residual Sum of Errors Squared = 342 $(c/s)^2$
Maximum Intensity of Fitted Peak = 41.91 c/s

Integrated Area = 12.46 (c/s * °2θ)
Width at Half-height = 0.00499 radians
Integral Width = 0.00519 radians

Calculated Pt Crystallite Sizes

$D_{1/2}$ (Based on Half-width) = 29.56 nm
D_i (Based on Int. width) = 31.59 nm
<Da> (Fourier Analysis) = 11.84 nm
<Dv> (Fourier Analysis) = 24.19 nm

DATA AND RESULTS SHEET FOR XRD PATTERNS

XRD Data Files:

Catalyst: XRY211 Support: XRY196

Catalyst Identification: GC3-1
Platinum Loading: 5.06 wt%

Parameters for Subtraction of Support Pattern

Scaling Factor for Catalyst = 1.0
Scaling Factor for Support = 0.90
Baseline Correction Parameters :
  angle (° 2θ) 36.0, 44.0
  magnitude(c/s) -2.0, -6.0

Results of Fitting Subtracted Pattern

Centre of Fit = 39.697 °2θ
Range of Angle Fit = ±4 °2θ
Fraction of Pt Detected by XRD = 0.37

Parameter Values in Fitting Function:
B1=23.087 B2=0.123 B3=39.682 B4=1.670
B5=20.013 B6=3.214 B7=1.127 B8=0.921

Number of Iterations = 50; Fit Converged : Yes
Residual Sum of Errors Squared = 340 $(c/s)^2$
Maximum Intensity of Fitted Peak = 43.10 c/s

Integrated Area = 118.30 (c/s *°2θ)
Width at Half-height = 0.0503 radians
Integral Width = 0.00582 radians

Calculated Pt Crystallite Sizes

$D_{1/2}$ (Based on Half-width) = 2.93 nm
D_i (Based on Int. width) = 3.42 nm
<Da> (Fourier Analysis) = 4.44 nm
<Dv> (Fourier Analysis) = 4.81 nm

DATA AND RESULTS SHEET FOR XRD PATTERNS

XRD Data Files:

Catalyst: XRY204 Support: XRY196

Catalyst Identification: GC3-2
Platinum Loading: 5.06 wt%

Parameters for Subtraction of Support Pattern

Scaling Factor for Catalyst = 1.0
Scaling Factor for Support = 0.90
Baseline Correction Parameters :
angle ($^\circ 2\theta$) 36.0, 44.0
magnitude(c/s) 3.0, 4.0

Results of Fitting Subtracted Pattern

Centre of Fit = 39.643 $^\circ 2\theta$
Range of Angle Fit = ±4 $^\circ 2\theta$
Fraction of Pt Detected by XRD = 0.63

Parameter Values in Fitting Function:
B1=6.506 B2=0.079 B3=39.643 B4=2.970
B5=54.689 B6=0.361 B7=0.866 B8=1.187

Number of Iterations = 60; Fit Converged : No
Residual Sum of Errors Squared = 300 $(c/s)^2$
Maximum Intensity of Fitted Peak = 61.19 c/s

Integrated Area = 200.83 ($c/s * ^\circ 2\theta$)
Width at Half-height = 0.0508 radians
Integral Width = 0.0573 radians

Calculated Pt Crystallite Sizes

$D_{1/2}$ (Based on Half-width) = 2.91 nm
D_i (Based on Int. width) = 2.86 nm
<Da> (Fourier Analysis) = 4.99 nm
<Dv> (Fourier Analysis) = 5.40 nm

DATA AND RESULTS SHEET FOR XRD PATTERNS

XRD Data Files:

Catalyst: XRY207 Support: XRY196

Catalyst Identification: GC3-3
Platinum Loading: 5.06 wt%

Parameters for Subtraction of Support Pattern

Scaling Factor for Catalyst = 1.0
Scaling Factor for Support = 0.90
Baseline Correction Parameters :
angle (° 2θ) 36.0, 44.0
magnitude(c/s) -2.0, -6.0

Results of Fitting Subtracted Pattern

Centre of Fit = 39.724 °2θ
Range of Angle Fit = ±4 °2θ
Fraction of Pt Detected by XRD = 1.00

Parameter Values in Fitting Function:
B1=58.462 B2=0.286 B3=39.723 B4=3.055
B5=178.503 B6=3.133 B7=1.207 B8=0.986

Number of Iterations = 54; Fit Converged : No
Residual Sum of Errors Squared = 111 $(c/s)^2$
Maximum Intensity of Fitted Peak = 305.39 c/s

Integrated Area = 293.69 (c/s *°2θ)
Width at Half-height = 0.0173 radians
Integral Width = 0.0168 radians

Calculated Pt Crystallite Sizes

$D_{1/2}$ (Based on Half-width) = 9.48 nm
D_i (Based on Int. width) = 9.77 nm
<Da> (Fourier Analysis) = 9.07 nm
<Dv> (Fourier Analysis) = 10.35 nm

DATA AND RESULTS SHEET FOR XRD PATTERNS

XRD Data Files:

Catalyst: XRY217 Support: XRY196

Catalyst Identification: GC3-4
Platinum Loading: 5.06 wt%

Parameters for Subtraction of Support Pattern

Scaling Factor for Catalyst = 1.0
Scaling Factor for Support = 0.90
Baseline Correction Parameters :
angle (° 2θ) 36.0, 44.0
magnitude(c/s) -2.0, -7.0

Results of Fitting Subtracted Pattern

Centre of Fit = 39.716 °2θ
Range of Angle Fit = ±4 °2θ
Fraction of Pt Detected by XRD = 0.89

Parameter Values in Fitting Function:
B1=65.470 B2=1.001 B3=39.717 B4=1.684
B5=238.287 B6=5.224 B7=1.263 B8=0.994

Number of Iterations = 24; Fit Converged : Yes
Residual Sum of Errors Squared = 320 $(c/s)^2$
Maximum Intensity of Fitted Peak = 303.75 c/s

Integrated Area = 281.04 (c/s *°2θ)
Width at Half-height = 0.0128 radians
Integral Width = 0.0162 radians

Calculated Pt Crystallite Sizes

$D_{1/2}$ (Based on Half-width) = 11.53 nm
D_i (Based on Int. width) = 10.16 nm
<Da> (Fourier Analysis) = 8.79 nm
<Dv> (Fourier Analysis) = 10.14 nm

DATA AND RESULTS SHEET FOR XRD PATTERNS

XRD Data Files:

Catalyst: XRY222 Support: XRY196

Catalyst Identification: GC3-5
Platinum Loading: 5.06 wt%

Parameters for Subtraction of Support Pattern

Scaling Factor for Catalyst = 1.0
Scaling Factor for Support = 0.90
Baseline Correction Parameters :
angle (° 2θ) 36.0, 44.0
magnitude(c/s) 1.0, -6.0

Results of Fitting Subtracted Pattern

Centre of Fit = 39.732 °2θ
Range of Angle Fit = ±4 °2θ
Fraction of Pt Detected by XRD = 0.70

Parameter Values in Fitting Function:
B1=73.791 B2=5.779 B3=39.716 B4=0.826
B5=177.174 B6=8.421 B7=0.937 B8=0.972

Number of Iterations = 17; Fit Converged : Yes
Residual Sum of Errors Squared = 290 $(c/s)^2$
Maximum Intensity of Fitted Peak = 251.06 c/s

Integrated Area = 223.25 (c/s *°2θ)
Width at Half-height = 0.00115 radians
Integral Width = 0.00155 radians

Calculated Pt Crystallite Sizes

$D_{1/2}$ (Based on Half-width) = 12.81 nm
D_i (Based on Int. width) = 10.58 nm
<Da> (Fourier Analysis) = 9.43 nm
<Dv> (Fourier Analysis) = 11.04 nm

DATA AND RESULTS SHEET FOR XRD PATTERNS

XRD Data Files:

Catalyst: XRY234 Support: XRY196

Catalyst Identification: GC3-6
Platinum Loading: 5.06 wt%

Parameters for Subtraction of Support Pattern

Scaling Factor for Catalyst = 1.0
Scaling Factor for Support = 0.90
Baseline Correction Parameters :
angle (° 2θ) 36.0, 44.0
magnitude(c/s) 4.0, -6.0

Results of Fitting Subtracted Pattern

Centre of Fit = 39.732 °2θ
Range of Angle Fit = ±4 °2θ
Fraction of Pt Detected by XRD = 0.64

Parameter Values in Fitting Function:
B1=33.228 B2=0.772 B3=39.732 B4=1.625
B5=272.507 B6=0.500 B7=1.206 B8=0.877

Number of Iterations = 17; Fit Converged : Yes
Residual Sum of Errors Squared = 410 $(c/s)^2$
Maximum Intensity of Fitted Peak = 245.736 c/s

Integrated Area = 204.164 (c/s *°2θ)
Width at Half-height = 0.0113 radians
Integral Width = 0.0145 radians

Calculated Pt Crystallite Sizes

$D_{1/2}$ (Based on Half-width) = 13.00 nm
D_i (Based on Int. width) = 11.31 nm
<Da> (Fourier Analysis) = 9.76 nm
<Dv> (Fourier Analysis) = 11.29 nm

DATA AND RESULTS SHEET FOR XRD PATTERNS

XRD Data Files:

Catalyst: XRY237   Support: XRY196

Catalyst Identification: GC3-7
Platinum Loading: 5.06 wt%

Parameters for Subtraction of Support Pattern

Scaling Factor for Catalyst = 1.0
Scaling Factor for Support = 0.90
Baseline Correction Parameters :
angle (° 2θ) 36.0, 44.0
magnitude(c/s) 4.0, -3.0

Results of Fitting Subtracted Pattern

Centre of Fit = 39.742 °2θ
Range of Angle Fit = ±4 °2θ
Fraction of Pt Detected by XRD = 0.59

Parameter Values in Fitting Function:
B1=30.967 B2=0.615 B3=39.741 B4=1.521
B5=187.124 B6=7.808 B7=1.176 B8=0.939

Number of Iterations = 21; Fit Converged : Yes
Residual Sum of Errors Squared = 360 $(c/s)^2$
Maximum Intensity of Fitted Peak = 218.08 c/s

Integrated Area = 186.876 (c/s *°2θ)
Width at Half-height = 0.0107 radians
Integral Width = 0.0149 radians

Calculated Pt Crystallite Sizes

$D_{1/2}$ (Based on Half-width) = 13.79 nm
D_i (Based on Int. width) = 10.97 nm
<Da> (Fourier Analysis) = 9.71 nm
<Dv> (Fourier Analysis) = 11.65 nm

DATA AND RESULTS SHEET FOR XRD PATTERNS

XRD Data Files:

Catalyst: XRY208 Support: XRY196

Catalyst Identification: GC3-8
Platinum Loading: 5.06 %wt

Parameters for Subtraction of Support Pattern

Scaling Factor for Catalyst = 1.0
Scaling Factor for Support = 0.90
Baseline Correction Parameters :
angle (° 2θ) 36.0, 44.0
magnitude(c/s) 16.0 7.0

Results of Fitting Subtracted Pattern

Centre of Fit = 39.665 °2θ
Range of Angle Fit = ±4 °2θ
Fraction of Pt Detected by XRD = 0.19

Parameter Values in Fitting Function:
B1=6.782 B2=5.019 B3=39.664 B4=0.500
B5=9.610 B6=0.189 B7=0.690 B8=1.142

Number of Iterations = 23; Fit Converged : Yes
Residual Sum of Errors Squared = 170 $(c/s)^2$
Maximum Intensity of Fitted Peak = 16.392 c/s

Integrated Area = 61.13 (c/s *°2θ)
Width at Half-height = 0.0584 radians
Integral Width = 0.0651 radians

Calculated Pt Crystallite Sizes

$D_{1/2}$ (Based on Half-width) = 2.53 nm
D_i (Based on Int. width) = 2.52 nm
<Da> (Fourier Analysis) = 4.69 nm
<Dv> (Fourier Analysis) = 5.30 nm

DATA AND RESULTS SHEET FOR XRD PATTERNS

XRD Data Files:

Catalyst: XRY210 Support: XRY196

Catalyst Identification: GC3-9
Platinum Loading: 5.06 %wt

Parameters for Subtraction of Support Pattern

Scaling Factor for Catalyst = 1.0
Scaling Factor for Support = 0.90
Baseline Correction Parameters :
angle (° 2θ) 36.0, 44.0
magnitude(c/s) 4.0, 6.0

Results of Fitting Subtracted Pattern

Centre of Fit = 39.691 °2θ
Range of Angle Fit = ±4 °2θ
Fraction of Pt Detected by XRD = 1.00

Parameter Values in Fitting Function:
B1=254.040 B2=35.743 B3=39.691 B4=0.729
B5=172.356 B6=7.132 B7=0.928 B8=0.962

Number of Iterations = 17; Fit Converged : Yes
Residual Sum of Errors Squared = 210 $((c/s)^2$
Maximum Intensity of Fitted Peak = 426.396 c/s

Integrated Area = 316.965 (c/s *°2θ)
Width at Half-height = 0.00919 radians
Integral Width = 0.0129 radians

Calculated Pt Crystallite Sizes

$D_{1/2}$ (Based on Half-width) = 16.04 nm
D_i (Based on Int. width) = 12.71 nm
<Da> (Fourier Analysis) = 10.02 nm
<Dv> (Fourier Analysis) = 12.59 nm

DATA AND RESULTS SHEET FOR XRD PATTERNS

XRD Data Files:

Catalyst: XRY213 Support: XRY196

Catalyst Identification: GC3-10
Platinum Loading: 5.06 %wt

Parameters for Subtraction of Support Pattern

Scaling Factor for Catalyst = 0.322
Scaling Factor for Support = 0.90
Baseline Correction Parameters :
angle (° 2θ) 36.0, 44.0
magnitude(c/s) 8.0, 8.0

Results of Fitting Subtracted Pattern

Centre of Fit = 39.688 °2θ
Range of Angle Fit = ±4 °2θ
Fraction of Pt Detected by XRD = 0.32

Parameter Values in Fitting Function:
B1=35.928 B2=1.046 B3=39.688 B4=0.988
B5=13.383 B6=21.384 B7=0.670 B8=0.983

Number of Iterations = 47; Fit Converged : Yes
Residual Sum of Errors Squared = 213 ($(c/s)^2$
Maximum Intensity of Fitted Peak = 49.312 c/s

Integrated Area = 100.971 (c/s *°2θ)
Width at Half-height = 0.0233 radians
Integral Width = 0.0357 radians

Calculated Pt Crystallite Sizes

$D_{1/2}$ (Based on Half-width) = 6.31 nm
D_i (Based on Int. width) = 4.59 nm
<Da> (Fourier Analysis) = 5.80 nm
<Dv> (Fourier Analysis) = 7.00 nm

DATA AND RESULTS SHEET FOR XRD PATTERNS

XRD Data Files:

Catalyst: XRY212 Support: XRY196

Catalyst Identification: GC4-1
Platinum Loading: 5.06 wt%

Parameters for Subtraction of Support Pattern

Scaling Factor for Catalyst = 1.0
Scaling Factor for Support = 0.90
Baseline Correction Parameters:
angle (° 2θ) 36.0, 44.0
magnitude(c/s) 10.0, 6.0

Results of Fitting Subtracted Pattern

Centre of Fit = 39.709 °2θ
Range of Angle Fit = ±4 °2θ
Fraction of Pt Detected by XRD = 0.32

Parameter Values in Fitting Function:
B1=38.424 B2=2.514 B3=39.709 B4=0.652
B5=4.604 B6=26.538 B7=0.500 B8=1.112

Number of Iterations = 80; Fit Converged: Yes
Residual Sum of Errors Squared = 190 $(c/s)^2$
Maximum Intensity of Fitted Peak = 43.03 c/s

Integrated Area = 100.28 (c/s *°2θ)
Width at Half-height = 0.0257 radians
Integral Width = 0.0406 radians

Calculated Pt Crystallite Sizes

$D_{1/2}$ (Based on Half-width) = 5.74 nm
D_i (Based on Int. width) = 4.04 nm
<Da> (Fourier Analysis) = 5.81 nm
<Dv> (Fourier Analysis) = 6.61 nm

DATA AND RESULTS SHEET FOR XRD PATTERNS

XRD Data Files:

Catalyst: XRY206 Support: XRY196

Catalyst Identification: GC4-2
Platinum Loading: 5.06 wt%

Parameters for Subtraction of Support Pattern

Scaling Factor for Catalyst = 1.0
Scaling Factor for Support = 0.90
Baseline Correction Parameters:
angle (° 2θ) 36.0, 44.0
magnitude(c/s) 1.0, 4.0

Results of Fitting Subtracted Pattern

Centre of Fit = 39.671 °2θ
Range of Angle Fit = ±4 °2θ
Fraction of Pt Detected by XRD = 0.50

Parameter Values in Fitting Function:
B1=34.798 B2=1.779 B3=39.671 B4=1.690
B5=29.032 B6=0.314 B5=0.604 B8=1.109

Number of Iterations = 37; Fit Converged: Yes
Residual Sum of Errors Squared = 240 $(c/s)^2$
Maximum Intensity of Fitted Peak = 63.834 c/s

Integrated Area = 159.369 (c/s *°2θ)
Width at Half-height = 0.0316 radians
Integral Width = 0.0436 radians

Calculated Pt Crystallite Sizes

$D_{1/2}$ (Based on Half-width) = 4.67 nm
D_i (Based on Int. width) = 3.76 nm
<Da> (Fourier Analysis) = 5.40 nm
<Dv> (Fourier Analysis) = 6.81 nm

DATA AND RESULTS SHEET FOR XRD PATTERNS

XRD Data Files:

Catalyst: XRY221 Support: XRY219

Catalyst Identification: GC4-3
Platinum Loading: 5.06 wt%

Parameters for Subtraction of Support Pattern

Scaling Factor for Catalyst = 1.0
Scaling Factor for Support = 0.90
Baseline Correction Parameters :
angle (° 2θ) 36.0, 44.0
magnitude(c/s) -10.0, -1.0

Results of Fitting Subtracted Pattern

Centre of Fit = 39.722 °2θ
Range of Angle Fit = ±4 °2θ
Fraction of Pt Detected by XRD = 0.92

Parameter Values in Fitting Function:
B1=58.462 B2=0.286 B3=39.722 B4=3.055
B5=128.504 B6=3.132 B7=1.207 B8=0.986

Number of Iterations = 54; Fit Converged : Yes
Residual Sum of Errors Squared = 210 $(c/s)^2$
Maximum Intensity of Fitted Peak = 236.97 c/s

Integrated Area = 290.42 (c/s *°2θ)
Width at Half-height = 0.0173 radians
Integral Width = 0.0214 radians

Calculated Pt Crystallite Sizes

$D_{1/2}$ (Based on Half-width) = 8.53 nm
D_i (Based on Int. width) = 7.67 nm
<Da> (Fourier Analysis) = 7.40 nm
<Dv> (Fourier Analysis) = 8.12 nm

DATA AND RESULTS SHEET FOR XRD PATTERNS

XRD Data Files:

Catalyst: XRY224 Support: XRY196

Catalyst Identification: GC4-4
Platinum Loading: 5.06 wt%

Parameters for Subtraction of Support Pattern

Scaling Factor for Catalyst = 1.0
Scaling Factor for Support = 0.90
Baseline Correction Parameters:
  angle (° 2θ) 36.0, 44.0
  magnitude(c/s) -3.0, -1.0

Results of Fitting Subtracted Pattern

Centre of Fit = 39.746 °2θ
Range of Angle Fit = ±4 °2θ
Fraction of Pt Detected by XRD = 0.87

Parameter Values in Fitting Function:
B1=120.651 B2=2.241 B3=39.746 B4=1.302
B5=107.934 B6=3.876 B7=1.003 B8=0.995

Number of Iterations = 7; Fit Converged: Yes
Residual Sum of Errors Squared = 271 $(c/s)^2$
Maximum Intensity of Fitted Peak = 228.59 c/s

Integrated Area = 276.75 (c/s *°2θ)
Width at Half-height = 0.0167 radians
Integral Width = 0.0211 radians

Calculated Pt Crystallite Sizes

$D_{1/2}$ (Based on Half-width) = 8.84 nm
D_i (Based on Int. width) = 7.77 nm
<Da> (Fourier Analysis) = 7.46 nm
<Dv> (Fourier Analysis) = 8.21 nm

DATA AND RESULTS SHEET FOR XRD PATTERNS

XRD Data Files:

Catalyst: XRY231 Support: XRY205

Catalyst Identification: GC4-5
Platinum Loading: 5.06 wt%

Parameters for Subtraction of Support Pattern

Scaling Factor for Catalyst = 1.0
Scaling Factor for Support = 0.90
Baseline Correction Parameters :
angle (° 2θ) 36.0, 44.0
magnitude(c/s) -1.0, 10.0

Results of Fitting Subtracted Pattern

Centre of Fit = 39.763 °2θ
Range of Angle Fit = ±4 °2θ
Fraction of Pt Detected by XRD = 0.70

Parameter Values in Fitting Function:
B1=38.015 B2=0.644 B3=39.763 B4=1.348
B5=147.299 B6=9.088 B7=0.505 B8=0.995

Number of Iterations = 17; Fit Converged : Yes
Residual Sum of Errors Squared = 280 $(c/s)^2$
Maximum Intensity of Fitted Peak = 185.314 c/s

Integrated Area = 220.423 (c/s *°2θ)
Width at Half-height = 0.0154 radians
Integral Width = 0.0208 radians

Calculated Pt Crystallite Sizes

$D_{1/2}$ (Based on Half-width) = 9.57 nm
D_i (Based on Int. width) = 7.90 nm
<Da> (Fourier Analysis) = 7.83 nm
<Dv> (Fourier Analysis) = 8.78 nm

DATA AND RESULTS SHEET FOR XRD PATTERNS

XRD Data Files:

Catalyst: XRY236 Support: XRY205

Catalyst Identification: GC4-6
Platinum Loading: 5.06 wt%

Parameters for Subtraction of Support Pattern

Scaling Factor for Catalyst = 1.0
Scaling Factor for Support = 0.90
Baseline Correction Parameters :
angle (° 2θ) 36.0, 44.0
magnitude(c/s) -1.0, 0.0

Results of Fitting Subtracted Pattern

Centre of Fit = 39.748 °2θ
Range of Angle Fit = ±4 °2θ
Fraction of Pt Detected by XRD = 0.59

Parameter Values in Fitting Function:
B1=75.387 B2=7.576 B3=39.748 B4=0.713
B5=106.461 B6=5.903 B7=1.156 B8=1.110

Number of Iterations = 15; Fit Converged : Yes
Residual Sum of Errors Squared = 270 $(c/s)^2$
Maximum Intensity of Fitted Peak = 181.85 c/s

Integrated Area = 188.32 (c/s *°2θ)
Width at Half-height = 0.0124 radians
Integral Width = 0.0181 radians

Calculated Pt Crystallite Sizes

$D_{1/2}$ (Based on Half-width) = 11.87 nm
D_i (Based on Int. width) = 9.08 nm
<Da> (Fourier Analysis) = 8.66 nm
<Dv> (Fourier Analysis) = 10.19 nm